Evaluating Off-the-shelf Hardware for Indoor Positioning

YAQIN CHEN
MASTER´S THESIS
DEPARTMENT OF ELECTRICAL AND INFORMATION TECHNOLOGY |
FACULTY OF ENGINEERING | LTH | LUND UNIVERSITY

Evaluating Off-the-shelf Hardware for Indoor Positioning

Yaqin Chen

Department of Electrical and Information Technology
Lund University

Supervisor: Prof. Fredrik Tufvesson, Peyman Hamed Seyed Hosseini

Lund, 2017

Abstract

An indoor positioning system (IPS) is a system to locate objects in indoor environments using radio waves, magnetic fields, acoustic, optical and video signals or other sensory information with help of a number of known reference positions. Nowadays, indoor positioning based services are used in a wide variety of areas and indoor positioning is getting considerable attention from both research and industry. Building indoor positioning systems using off-the-shelf hardware can considerably reduce the cost of the system implementation.

In this master thesis, three kinds of off-the-shelf hardware based on Ultra-Wideband (UWB), WiFi and Bluetooth low energy (BLE) technology respectively are exploited to build up indoor positioning systems. Evaluation and comparison of these three systems are performed through a comprehensive study of the related theory, practical experiments and brief study of off-the-shelf hardware.

Commonly used radio positioning technologies and basic indoor positioning techniques are studied as the foundation of the practical experiments. Accuracy, power consumption, cost and ease of deployment are defined as criteria to evaluate and compare the three systems. A systematic method for deploying these three positioning systems for practical experiments is presented and discussed. A trilateration positioning algorithm is implemented for these three systems to estimate positions and compare accuracy. Results from experiments for both line of sight and none line of sight scenarios are given. Results from a brief study of off-the-shelf hardware for a rough qualitative comparison of power consumption and cost of these three evaluated hardware are presented. Furthermore, obstruction experiments were performed to observe influences of the obstacles on accuracy for these three hardware. Finally, suggestions on future work are provided.

The evaluation shows that the UWB hardware performs the best accuracy for indoor positioning, in centimeter order, but it costs more than the WiFi and BLE hardware. The BLE hardware provides worst indoor positioning accuracy, around 4.5 m in average. However, it is the cheapest and most power consumption efficient among these three evaluated hardware. The WiFi hardware is a kind of a trade-off between the UWB and BLE hardware in terms of indoor positioning, giving medium level accuracy, power consumption and cost. The BLE hardware is easier to deploy compared to the UWB and WiFi hardware as BLE devices are smaller size and able to be powered by coin batteries and thus can avoid external physical connections. However, the RSS-based BLE IPS need proper propagation model to estimate distances, which adds extra workload for the deployment compared to the UWB and WiFi IPSs. Obstruction experiments show that obstacles degrade ranging performance greatly for all of these three hardware and influence on the BLE hardware is the most severe.

Acknowledgments

This project was carried out at Sigma Connectivity in Lund.

First of all, I would like to express my sincere appreciation to my supervisors, Peyman Hamed Seyed Hosseini and Prof. Fredrik Tufvesson, for all the fruitful discussions and guidance throughout the whole work. Special thanks to Peyman Hamed Seyed Hosseini, who guided and helped me for the project step by step and spent a lot of time on proofreading of the report. I am also grateful to my manager Mikael Persson in Sigma Connectivity, for providing me with the great thesis opportunity and helpful guidance.

I want to extend my appreciation to my colleagues in Sigma Connectivity, whom have supported me for this project. This includes but not limited to: Beata Napieraj, Besar Jashanica, Evelina Bui, Henrik Sihm, Hiroshi Watanabe, Igor Egorov, Irina Rezvaya, Joakim Uddenfeldt, Jonas Bergh, Max Kruse, Maziar Haghpanah, Vadim Popov and so on.

Furthermore, I would like to thank my classmate and friend Xuhong Li, Björn Lundquist and Rasmus Ljungberg from Combain, Kenneth John Batstone, PhD student in Lund University, for all their kindly help for my thesis.

Last but not least, I would like to thank my beloved family, my husband and my daughter, for their support, encouragement and accompany all along the project.

I cannot make this project come true without all of your help. I wish you all happiness, health and love.

Table of Contents

Abbreviations

2D	Two-dimension
3D	Three-dimension
AOA	Angle of Arrival
BLE	Bluetooth Low Energy
BS	Base Station
CP	Cement Pillar
CW	Continuous Wave
DOA	Direction of Arrival
GNSS	Global Navigation Satellite System
HF	High Frequencies
IOT	Internet of Things
IPS	Indoor Positioning System
ISM	Industrial Scientific Medical
KNN	K-Nearest Neighbor
LF	Low Frequencies
LOS	Line-of-Sight
MAC	Medium Access Control
ML	Maximum Likelihood
MP	Metal Pillar
MR	Meeting Room
MWB	Metal Writing Board

NLOS	None Line-of-Sight
PDOA	Phase Difference of Arrival
PHY	Physical Layer
RFD	Reduced Functionality Devices
RFID	Radio Frequency Identification
RPs	Reference Points
RSS	Receive Signal Strength
RTT	Round Trip Time
RTOF	Roundtrip Time of Flight
SHF	Super-High Frequencies or microwaves
SLAM	Simultaneous Localization and Mapping
TDOA	Time Difference of Arrival
TG	Task Group
TM	Timing Measurement
TOA	Time of Arrival
TOD	Time of Departure
TOF	Time of Flight
TPs	Test Points
TWR	Two Way Ranging
UWB	Ultra-wideband
WiFi	Wireless Fidelity
WLAN	Wireless Local Area Network
WLAN STAs	WLAN Stations
UHF	Ultra-High Frequencies
WPAN	Wireless Personal Area Network

Chapter 1 Introduction

1.1 Background

Positioning and navigation based services find their applications in a variety of areas, such as industry, commerce, science, sports and personal daily life for both outdoor and indoor environments. The Global Navigation Satellite System (GNSS) is now being widely used in our daily life for outdoor scenarios with global coverage, high accuracy, short latency, high availability and low-user costs. However, GNSS does not work well in indoor environments due to poor link budget when there is no LOS to the open sky.

An indoor positioning system (IPS) is a system to locate objects in indoor environments using radio waves, magnetic fields, acoustic, optical and video signals or other sensory information with help of a number of known reference positions. An indoor positioning system basically consists of a number of reference nodes (often called anchors, beacons, transmitters, senders etc.) deployed at fixed known positions and one or a number of target nodes (usually referred to as readers, tags, mobile devices etc.) to be located. The terminology may be different depending on the indoor positioning technology exploited. For instance, in an Ultra-Wideband (UWB) based IPS, the reference nodes usually are called anchors and the target nodes normally are named tags. In a WiFi based IPS they are often referred to as access points and Wireless Local Area Network (WLAN) stations. The reference nodes, in a Radio Frequency Identification (RFID) based IPS, may be called interrogators while in a cellular network based IPS, they are named Base Stations (BSs).

Following the achievements of GNSS based location services in outdoor applications, the ability to locate objects indoors remains particular challenging for several reasons:

- Severe multipath effects due to walls, ceilings, floors and other obstacles in the indoor environments.
- Low probability for availability of Line-of-Sight (LOS) signal or severe attenuation of LOS signal.
- Specific site parameters such as floor layout, temporally moving objects like opening doors, moving chairs and presence of people.
- There is still not a satisfactory positioning solution applicable to different indoor environments to the same extent as GNSS is for outdoor environments.

1.2 Motivation

Indoor positioning is getting considerable attention from both the research community and industry. Improvements in indoor positioning performance have the potential to create unprecedented opportunities for business. More and more off-the-shelf hardware in the market can enable location based services in indoor environments. Building indoor positioning systems using off-the-shelf hardware can considerably reduce the cost of the system implementation. Among the off-the-shelf hardware, those using wireless radio technologies that make it possible to build cell coin battery powered mobile trackable devices are of special interest.

To realize a reliable and cost efficient indoor positioning system, it is necessary to have an overview of the most commonly used wireless positioning technologies and techniques for indoor positioning. It is also interesting to build up indoor positioning systems using off-the-shelf hardware and evaluate system performances to learn and analyze how wave propagation mechanisms and wireless channel characterization work in real life environment and also how antenna characteristics impact the positioning system performance. Three off-the-shelf hardware based on UWB, WiFi and Bluetooth Low Energy (BLE) technologies are chosen to be evaluated within the scope of this thesis.

The evaluations are planned to be performed in an empty room for LOS scenario and a real life indoor environment with furniture, obstacles and interference from other RF technologies for None Line of Sight (NLOS) scenarios, where stochastic presence of moving people in the room makes study of the impact of human body a necessity.

1.3 Research Questions

Based on the background and motivation of this thesis, the following research questions are established:

- What are the most commonly used RF technologies and positioning techniques for indoor positioning?
- How to set up simple indoor positioning systems using off-the-shelf hardware and evaluate and optimize systems' performance considering different indoor positioning technologies, positioning techniques and indoor environment challenges?
- How is the performance of off-the-shelf hardware to be evaluated when it comes to accuracy, power consumption, cost and ease of deployment for indoor positioning?
- What are pros and cons of the indoor positioning measurement methods Time of Arrival (TOA) and Receive Signal Strength (RSS) that are used with the evaluated off-the-shelf hardware?

1.4 Limitations

- This thesis report involves a literature study on the most commonly used wireless indoor positioning technologies and positioning techniques. However, the evaluation work only

focus on the off-the-shelf hardware in scope. Hence, not all the most commonly used wireless indoor positioning technologies and positioning techniques will be evaluated.
- The evaluation is mainly focused on a 2-dimensional positioning, which means that the Z-axis describing the height of an object is here less focused on and not discussed thoroughly.

1.5 Outline

The remainder of this thesis is structured as follows: In chapter 2, an overview of the commonly used RF technologies for IPSs is presented. Significant advantages of each of the technologies in terms of IPSs are also included. Chapter 3 describes the basic indoor positioning techniques, including various measurement methods for these positioning techniques and the advantages and disadvantages of each of the measurement methods. Experimental setup and evaluation for each of the three IPSs based on the off-the-shelf hardware, results from the evaluation and analyses of results are presented in Chapter 4. In Chapter 5, comparison and discussions are carried out based on the results of the three evaluated IPSs in Chapter 4. Finally, Chapter 6 presents the conclusions and recommendations for future work.

Chapter 2 Commonly Used RF Technologies In IPSs

During the operation of an IPS, signals are exchanged between the reference nodes and the target nodes which enables the localization of the latter. Various signals can be exploited for positioning such as radio waves, magnetic fields, acoustic, optical and video signals. Among them, radio waves based on UWB, WiFi, BLE, RFID and ZigBee technologies are of the most commonly used ones [1-3]. In the following parts of this chapter, an overview of all the mentioned RF technologies commonly used in IPSs is presented.

2.1 UWB

UWB is a radio technology for transmitting signals spreading over a frequency spectrum that occupies minimum 500 MHz bandwidth by employing very short pulses or by OFDM signalling as defined in the IEEE 802.15.4a - 2007 UWB Standard [4]. In the U.S.A., UWB devices can operate in the frequency band between 3.1 GHz and 10.6 GHz.

UWB technology has drawn significant attention and growing interest for indoor localization due to its significant features. The major advantages of an UWB signal as a candidate for indoor positioning against narrow band signals can be seen from the following points of view.

1. Large bandwidth enhances the ability of accurate range estimation with fine time resolution. UWB signals are very narrow pules, usually in nanosecond order, which translates in ranging estimation of centimeter order accuracy.

2. Fine time resolution enhances the immunity to multipath effects. Multipath propagation is one of the main issues of IPS. Radio signal between transmitter and receiver travels over many different paths in indoor environments. There are direct path and also reflections from walls, ceilings, floors and other objects in the buildings. It is important to be able to determine the direct path signal to measure the distance accurately. The fine time resolution of UWB signal enhances the ability for UWB receivers to distinguish between multipath signals and determine the first arriving signal accurately as they arrive at the receivers; therefore, yielding high positioning accuracy.

3. Multiple frequency components enhance the penetration capability to obstacles. Another main challenge of IPS is that LOS signal is severely attenuated or even absent at the receiver because of obstacles in indoor environments, which results in significant error in the positioning results or even stop the functionality of IPS. UWB signals contain multiple

frequency components over the broad range of the bandwidth, making relatively higher probability for them to penetrate a variety of material compared to narrowband signals.

Due to the inherent suitability and fine time resolution of time-based methods for UWB signals, most UWB indoor positioning systems utilize time-based distance measurements to estimate locations.

2.2 WiFi

WiFi technology, using radio waves at the ISM frequencies of 2.4 GHz or 5 GHz to provide WLAN connectivity based on IEEE 802.11 standard, is another commonly used technology for indoor positioning systems. WiFi technology has been widely used all over the world, from public hotspots to private access points and from laptops to mobile devices.

WiFi technology has its own advantages when it comes to IPS. Firstly, the widespread use of WLAN access points and off-the–shelf consumer electronics enables IPSs to use existing infrastructures. Secondly, WiFi modules are quite cheap and small and thus make WiFi-based IPS cost-efficient and flexible. Thirdly, WiFi RSS-based fingerprint positioning systems based on existing WiFi devices can be implemented easily and achieve acceptable accuracy [6-8]. Last but not least, the inclusion of positioning capability of accurate time based distance measurements between WLAN devices using hardware time-stamping techniques in the IEEE 802.11v standard [5] shows that positioning with WiFi technology is expected to continue attracting attention in indoor positioning.

Currently, the most popular WiFi positioning method is to make use of RSS based trilateration [9-10] and fingerprinting [6-8]. However, the accuracy of WiFi RSS-based trilateration systems is severely influenced by the typical indoor propagation phenomena such as shadowing, reflection, refraction and multipath effects. WiFi RSS-based fingerprinting systems, which can achieve acceptable accuracy but need time consuming and labor intensive survey work to construct radio maps and the survey work suffers from changes of environment. TOA-based approaches bypass these problems by relying on the relation between distance and the time it takes a radio signal to travel that distance. TOA method has better accuracy and stability and is less sensitive to the environment than RSS method that make it suitable for achieving high-performance ranging between nodes. Thus, TOA-based trilateration constitutes a promising technique to reach flexible, robust and accurate positioning with WLAN [11-12].

However, TOA-based ranging is not directly available from a standard WiFi device without IEEE 802.11v compliant synchronization support as the time synchronization required by TOA-based ranging is not supported. In order to establish time synchronization for estimating TOA-based ranging in WLAN systems, several methods which can be classified into hardware timestamping based and software timestamping based have been proposed and investigated. Hardware timestamping based methods, taking the timestamp within the WLAN chipset and usually measuring TOA at the PHY of WLAN, have reported good accuracy close to 1 meter in [4] but require specific and complex hardware modification. Software timestamping based methods, which use the system clock to generate a timestamp by WLAN driver and estimate TOA at the upper layer of WLAN, can only provide a time base of 1us resolution corresponding to ranging

accuracy of 300 m and are not able to achieve accurate measurements of time resolution in nanosecond order [11-13].

The IEEE 802.11v standard, which includes mechanisms and guidelines for time synchronization enables TOA based ranging between WLAN devices using hardware time-stamping for WLAN packets. Using hardware timestamps generated inside the 802.11v PHY from hardware counter to synchronize AP and WLAN Stations (WLAN STAs) is done through a procedure called Timing Measurement (TM). The hardware timer can then be synchronized to the system clock with proper hardware support mentioned in IEEE 802.1as [13-14].

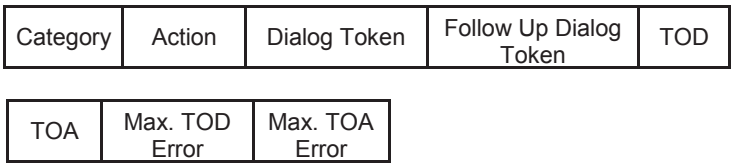

Figure 2.1 Timing measurement frame format defined in IEEE 802.11v

The format of the TM frame is shown in Figure 2.1 [5] and the fields are described below:

- Category: is the value for public action defined in [5].
- Action: is the value indicating TM as specified in [5].
- Dialog Token: This field is set to a non-zero value by the STA initiating the timing measurement to identify the timing transaction.
- Follow Up Dialog Token: Two timing action frames are sent from one WLAN STA to the other to complete synchronization based on timing measurement. For the first message, this field is left blank while in the second message, this field is set to the Dialog Token value used in the first timing message. Additionally, in the first timing message, all the other fields after this field are empty.
- Time of Departure (TOD) and Time of Arrival (TOA): They represent the time of departure and arrival of the WLAN packet at the transmitter and the receiver, respectively. It is the time when the preamble of the packet reaches the transmit (or receive) antenna. Both TOA and TOD are measured in units of 10 ns.
- Max TOD and Max TOA Error: This represents the maximum error in determining the exact TOD or TOA. The content of this field is a numeric value which has to be multiplied with 10 ns to determine the exact error.

Figure 2.2 illustrates the synchronization procedure when an AP is synchronizing a WLAN STA using the TM mechanism. The TM procedure takes advantages of a feature of the IEEE 802.11 protocol by utilizing TWR method for high accuracy synchronization message exchanging and clock offset calculation.

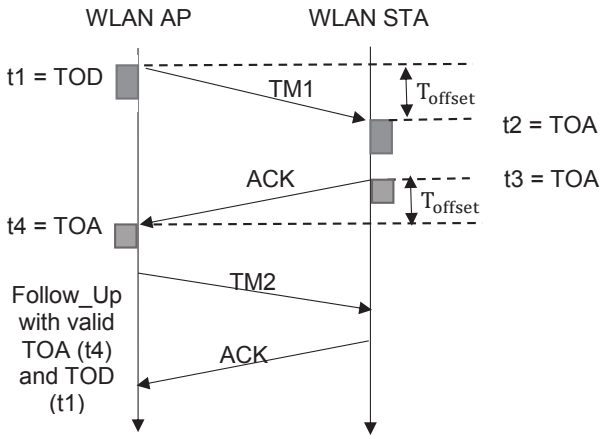

Figure 2.2 Message exchange for synchronization in IEEE 802.11v

The AP sends the first timing measurement action frame TM1 to the WLAN STA. The TOD of TM1 is t1 while this frame arrives at the WLAN STA at t2. Upon successful reception of TM1, the WLAN STA sends an acknowledgement message at t3 which is received at AP at t4. For AP to synchronize to the WLAN STA, the timestamps t1 and t4 should be available at the WLAN STA. Hence, the Follow Up message TM2 is sent by AP which carries t1 and t4 as TOD and TOA, respectively. Upon receiving this message, the node sends another acknowledgement message and uses the timestamps to calculate its clock offset to the AP using:

$$T_{offset} = \frac{(t2-t1)+(t4-t3)}{2}. \qquad (2.1)$$

Although high accurate timestamps can be generated by WLAN receivers, this accuracy cannot be used by most wireless synchronization approaches due to timestamp quantization issues. For example, the timestamps of 802.11v have a quantization of 10ns, which is much larger than a WLAN receiver could achieve [13].

To improve the capability of location reporting accuracy, IEEE 802.11 Task Group (TG) mc who is responsible for developing an IEEE 802.11-2016 standard that is expected to be published in late 2016 has developed a fine timing measurement protocol. This protocol as an extension of the IEEE 802.11v timing measurement protocol is proposed and incorporated in the new IEEE 802.11-2016 standard. When compared with the IEEE 802.11v timing measurement protocol, the fine timing measurement protocol focuses primarily on indoor location determination and has a more accurate requirement for the resolution of the timestamps, which results in a greater location accuracy [15].

2.3 BLE

BLE also known as Bluetooth Smart, was developed to address the power consumption issue of the traditional Bluetooth and released in the Bluetooth core specification version 4.0. BLE devices operate in the unlicensed 2.4 GHz ISM band at 2400 – 2483.5 MHz, providing 40 physical channels separated by 2 MHz and 3 of them are used as advertising channels [16].

Nowadays, BLE has become a commonly used radio standard for the Internet of Things (IOT) and been embedded in the majority of the mobile devices and other consumer electronics. Indoor localization using BLE technology has been widely investigated [17-22]. BLE supports an advertising mode, using this advertising mode a BLE beacon could advertise information repeatedly through three predefined advertising channels. Once the BLE beacon is discovered by a BLE scanner within adverting coverage range, the relative positions of the beacons can be estimated using the received signal strength.

BLE technology has some significant features that makes it an attractive option for indoor positioning [16].

- BLE is a low-power wireless technology suitable for battery-powered mobile devices, which is an ideal option for beacons. Using coin cell battery, a BLE beacon can stay active for months or years without replacing the battery, thus reducing maintenance and support for the location tracking systems.
- As BLE is widely adopted by the majority of the mobile devices and other consumer electronics on the market, a BLE-based IPS can be easily set up using off-the-shelf devices without any specific hardware modification.
- BLE devices can be very low-cost and tiny in size, which makes it even more attractive for indoor localization applications.

Several studies have reported on BLE localization in terms of RSS-based range localization methods [17–20] and fingerprinting methods [21-22].

2.4 RFID

RFID is a generic term used to describe a system that automatically transmits the identity and information of an object wirelessly using radio waves. RFID technology has been widely adopted in many indoor positioning applications [23-27]. A typical RFID positioning system usually includes a number of readers also known as interrogators, tags also called transponders and a host computer which communicates with readers through wire or wireless link. The RFID readers are able to read information from tags.

The most important differentiation criteria of RFID positioning systems are the operating frequency, the type of tags the RFID system uses and the range of the system.

RFID systems operate at specific unlicensed frequencies ranges that can be categorized as Low Frequencies (LF), High Frequencies (HF), Ultra-High Frequencies (UHF) and Super-High Frequencies (SHF) or microwaves. The frequency range that a RFID system operates in

determines key capabilities and limitations of the system. For instance, the lower the frequency, the better penetration for a radio signals to go through obstacles. The higher frequency, the more severe attenuation of a radio signal given a fixed antenna gain.

The communication range of a RFID system is dependent upon several factors such as the type of tag, transmission power, receiver sensitivity, antenna characteristics and propagation environment and so on. The most significant factor is the type of tag. RFID tags can be classified into passive, semi-passive and active tags. Passive tags do not have internal batteries and all the required energy are provided by the magnetic or electromagnetic fields of the readers by means of induction. Passive tags therefore are not able to transmit information when they are not in the zone of magnetic or electromagnetic fields of readers. Semi-passive tags have their own power supply, in form of a battery or solar cell for instance. The magnetic or electromagnetic fields of readers are no longer necessary for powering on the tags, resulting in longer communication range as long as the tags can detect the weaker signals of readers. The typical communication range of RFID systems using passive and semi-passive tags is from few centimeters to few meters. However, semi-passive tags cannot generate their own high frequency signals and still need to modulate the fields of readers for transmitting information, which is similar to passive tags. Active tags not only have their own batteries but also have their own transceivers. Instead of modulating readers' fields, active tags are able to generate their own high frequency electromagnetic fields for transmitting information. RFID system with active tags can have a range up to several hundred meters.

Table 2.1 presents frequency ranges and typical communication range of passive tags and active tags at different frequency ranges of RFID [28].

Frequency Rang (MHz)	LF	HF	UHF	SHF
	< 0.135	3 - 28	433 - 435, 860 - 930	2400 - 2454 5725 - 5875
Range of Passive Tags	≤ 0.5 m	≤ 3 m	≤ 10 m	≤ 6 m
Range of Active Tags	≤ 40 m	300 m	≤ 1 km	≤ 300 m

Table 2.1 RFID frequency range and communication range

RFID technology enables flexible and cheap indoor positioning solutions. The advantage of using passive RFID tags for positioning are their flexibility in size, high level of ruggedness, relatively low-cost of the device, ease of installation and low maintenance needs since they have no batteries. The main drawback of passive tags is the limited detection range. Active tags have relatively larger size and higher cost compared to passive tags. However, the coverage areas of active tags are larger.

The most frequently employed positioning method for RFID positioning systems is that of proximity, also known as Cell of Origin (CoO) [1, 3, 24]. RSS can be used for coarse range estimation in order to apply lateration technique and fingerprinting positioning method for RFID positioning [1-2, 23, 26]. Angle of arrival estimation can also be used as an alternative for RFID positioning systems [3].

2.5 ZigBee

ZigBee is a low-cost, low-power-consumption, two-way wireless communication standard based on the Wireless Personal Area Network (WPAN) IEEE 802.15.4 specification. IEEE 802.15.4-2003 in [29] specifies the PHY and MAC sub-layer while ZigBee protocol in [30] provides network (NWK) layer and the framework for the application layer on the foundation of IEEE 802.15.4-2003.

ZigBee devices operate globally in 2.4 GHz unsilenced ISM band or one of the sub-GHz regional bands (868 MHz European band and 915 MHz used in countries such as USA and Australia) and can transmit data by passing data through a mesh network where each device can communicate directly or through neighbor devices with other devices in the network. There are some indoor location systems using ZigBee technology nowadays [31-34].

A ZigBee mesh network based positioning system contains three types of nodes which are called coordinator, router and end device. There is only one coordinator per system. The coordinator is responsible for establishing and managing the network and normally connected to a host device. Routers, acting as intermediate nodes and relaying data from other devices, are usually deployed strategically at fixed known locations as reference nodes for the rest nodes to be located. End devices, sending and receiving information to/from their parent node (either the coordinator or a router), generally can be attached on the target objects or people to be located. End devices therefore need to be mobile, battery-powered and as small as possible.

ZigBee has some significant features that makes it an attractive option for indoor positioning.

1. ZigBee is specifically designed for low-power and low-cost applications which is suitable for cost-effective IPSs demanding battery operated devices.
2. ZigBee devices in the mesh network can communicate through not only direct connections but also routing paths, resulting in up to 300 meters free-space range, which expands the coverage of positioning systems.
3. ZigBee end devices communicate with their parent node but don’t transmit information to other devices. They are therefore called as Reduced Functionality Devices (RFD) and can be less complex and have small sizes that are easily attached to or integrated into other mobile devices for indoor positioning applications.

The most popular ZigBee positioning method is to make use of RSS based range localization methods and CoO methods [3].

Chapter 3 Basic Indoor Positioning Techniques

Positioning systems determine the location of an object either relative to a known position or within a coordinate system. Various indoor positioning techniques have been proposed in the past few decades. Generally, they fall into three categories: model-based techniques, fingerprint-based techniques and cell-based techniques [9].

Model-based techniques use geometrical models to figure out locations, which is commonly done by measuring geometric relations between reference positions and the tracked target. Based on the measured geometric information and corresponding mathematics, it is possible to calculate the location of the tracked target. Model-based techniques can be further divided into sub-categories called trilateration and triangulation depending on the measured geometric information. Trilateration exploits distance measurements while triangulation primarily employs angle measurements.

The main idea of fingerprint-based techniques is to fingerprint the surrounding signatures at every location in the areas of interests and then build a fingerprint database. The location is then estimated by mapping the measured fingerprints against the database [9].

For cell-based techniques, a user's location is given by the known reference nodes to which it is connected and the localization error depends on the communication range and the distance between the reference nodes [8].

In the remainder of this chapter, different measurement methods are introduced first. Then the fundamental indoor positioning techniques are explained.

3.1 Measurement Methods for Indoor Positioning

There are different measurement methods to estimate the distances or angles required by the basic indoor positioning methods. In this section, we will introduce the most popular distance measurement methods TOA, RSS, Phase Difference of Arrival (PDOA) and Time Difference of Arrival (TDOA) and the commonly used angle measurement method Angle of Arrival (AOA).

3.1.1 TOA

TOA method is sometimes called Time of Flight (TOF). TOA method measures a radio signal propagation time from one node to another node. Once this signal propagation time T_{propag} is obtained, the distance between these two nodes is thus:

$$d = T_{propag} \cdot c, \tag{3.1}$$

where c is the speed of light.

There are usually two ways to determine the signal propagation time T_{propag}, called One Way Ranging (OWR) and Two Way Ranging (TWR).

3.1.1.1 One Way Ranging (OWR)

One way ranging (OWR) simply measures the one way propagation time of a radio signal traveling between two time synchronized nodes. The node receiving the signal can determine the TOA of the received signal that is time-stamped by the transmitting node.

As Figure 3.1 shows, node A sends a message including trimming information to B at T_{send} and the message arrives at B at $T_{receive}$. An additional message may be needed to send from node B to A if the propagation time is calculated at node A.

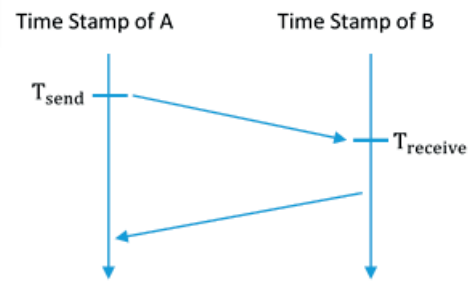

Figure 3.1 One way ranging measurement

As the two nodes are time synchronized, the signal propagating time can be found to be:

$$T_{propag} = T_{receive} - T_{send}. \tag{3.2}$$

3.1.1.2 Two Way Ranging (TWR)

Two Way Ranging (TWR) is also known as Round Trip Time (RTT) or Roundtrip Time of Flight (RTOF). TWR method measures the time taken by a signal to travel from one node to another node and back.

The operation of TWR shows in Figure 3.2. Node A sends a message to node B at a time recorded as T_{AS}. Node B receives the message at time T_{BR} and sends back a reply at T_{BS}. The reply message arrives at node A at time T_{AR}. An additional message may be needed to be sent from node A to B if the propagation time must be known to B.

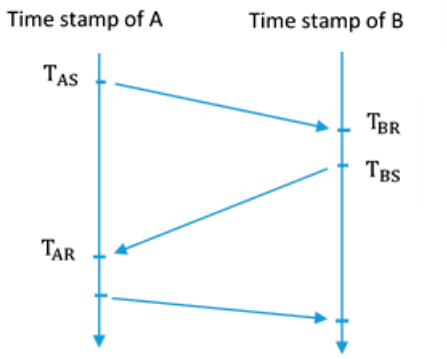

Figure 3.2 Two way ranging measurement

The round trip time of the signal propagation can be calculated through:

$$T_{round-trip} = T_{AR} - T_{AS} - (T_{BS} - T_{BR}). \quad (3.3)$$

And the signal propagation time can be determined as:

$$T_{propag} = \frac{1}{2} T_{round-trip}. \quad (3.4)$$

The propagation time is measured according to both time stamps of node A and node B which means the clock error of both nodes results in TOF estimation error and the error increases as processing delay of node B increases.

In reality, for TWR measurements, the processing delay in the node B also needs to be known and accounted for calculating the signal propagation time. There are various methods that can be adopted to both take this delay into account and to minimize it. For instance, a way of measuring processing delay is to measure TOA by using the clock of receiver node mentioned in [35].

Another new TWR method which exchanges multiple two way messages between node A and B is also proposed in [36] to reduce the effect of processing delay on ranging accuracy.

TOA seems a robust technique due to its advantages:

1. When the signal travels through obstacles such as walls and furniture, the time it takes for the signal to travel will be affected only very slightly compared to the case of RSS measurement.
2. Literature survey shows that TOA is the most accurate technique which can filter out multipath effects in the indoor situations [37-38].

However, TOA based ranging has its own disadvantages:

1. All the transmitters and receivers in an OWR based system are required to be precisely synchronized throughout the TOA measurement. The synchronizations increase complexity and cost of the systems.
2. TOA based ranging relies on the timer accuracy, which means high resolution timers are required for accurate TOA measurement. For instance, a timer with resolution of 1 ns introduces at least 30 cm error on each TOA measurement. Any slight clock drift in the positioning systems might not be negligible.
3. Timestamping in exchanged messages between the reference nodes and target nodes in a TOA based ranging system is needed, to be able to execute TOA measurement. This increases complexity of the exchanged message and may introduce an additional source of error.
4. TWR requires that all the units in the system are transceivers, implying complicated and more expensive devices in the system.
5. Inaccurate estimation of processing delay could degrade the TWR measurement accuracy significantly.

Conventional TOA estimation algorithms use matched filtering or correlation-based TOA to estimate the signal propagation time, the time at which the matched filter output peaks or the time shift of the template signal that produces the maximum correlation with the received signal is used to estimate TOA [39].

3.1.2 RSS

It is very often for indoor positioning systems based on RF technologies that only the RSS is available for determining distance. RSS, reported as an indication of measured power of a received signal. RSS is usually obtained through the voltage measured by a receiver's received signal strength indicator (RSSI) circuit. RSS of radio signals thus can be measured by receivers during normal communication with transmitters, without additional hardware or software requirements.

Distance is correlated with received signal strength represented by RSS, based on the truth that received signal strength is transmit power times channel gain and channel gain decays as distance increases. For instance, in free space, the received signal strength is inversely proportional to square of the separation distance between transmitter and receiver as shown in (3.5) according the Friis' law:

$$P_{Rx} \propto \frac{1}{d^2}, \tag{3.5}$$

where P_{Rx} is the received signal strength and d is the separation distance between transmitter and receiver in free space.

However, the free space Friis' law does not always hold in real indoor environment due to multi-path fading, shadowing and non-uniform propagation of the radio signal. For a specific indoor environment, it is necessary to model the relationship between RSS and distance which is typically done by using theoretical and/or empirical path-loss models. Several empirical and theoretical models have been proposed to translate the difference between the transmitted and the received signal strength into distance estimation.

One of the models for real indoor environments is based on the power law in [40], where the received signal strength inversely proportional to n-th power of the separation distance between transmitter and receiver shown in (3.6):

$$P_{Rx} \propto \frac{P_{Tx}G_{Tx}G_{Rx}}{d^n}, \tag{3.6}$$

Where P_{Rx} is the received signal strength, P_{Tx} is transmit power, G_{Tx} and G_{Rx} are the gains of transmit and receive antenna and d is the distance between transmitter and receiver.

Rewriting the power law on a logarithmic scale, the received power is given by:

$$P_{Rx}(d) = P_{Tx} + G_{Tx} + G_{Rx} - n10log_{10}(d). \tag{3.7}$$

Denoting $A = P_{Tx} + G_{Tx} + G_{Rx}$ and $B = 10log_{10}(d)$, then the received power is:

$$P_{Rx} = A - nB. \tag{3.8}$$

It is trivial to conclude from Equation (3.8) that, given the RSS $P_{Rx}(d)$ at any value of d at a particular location, the separation distance d between a transmitter and receiver can be estimated to be:

$$d = 10^{\frac{A - P_{Rx}}{10*n}}. \tag{3.9}$$

The main advantages of RSS-based positioning methods compared with other methods are:

1. RSS measurement is easily available with ordinary radio transceivers, leading to relatively inexpensive and simple implementation of indoor positioning systems.
2. RSS-based positioning systems do not require time synchronization for any device in the system.

The most relevant drawbacks of RSS-based positioning are:

1. In indoor environments, the propagation phenomena such as reflection, shadowing, refraction and multipath effects can affect the received signal strength constructively or destructively, resulting in the received signal strength to be poorly correlated with distance and thus inaccurate distance estimation.

2. Determining a proper model for correlating RSS with distance is unavoidable for getting good position estimation. The procedure of figuring out the attenuation factor of the received power in a specific environment is usually time consuming.

3.1.3 PDOA

Distance can be estimated based on phase information of a radio signal since the phase of a radio signal changes with wave propagation over distance. Phase based range estimation method is usually termed Phase Difference of Arrival (PDOA) because it is the phase differences of received signals that is used for distance estimation.

Figure 3.3 illustrates an example of PDOA measurement between two nodes A and B. Assuming two pure traveling sinusoidal signals with different operating frequencies f_1 and f_2, they arrive at the receiver after finite time delay ΔT. By measuring the phase difference $\Delta\phi$ of these two received signals, the distance between node A and B can be estimated.

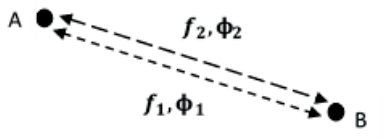

Figure 3.3 PDOA measurement

Let $\Delta\phi$ represents the measured phase difference and it is given by:

$$\Delta\phi = 2\pi\Delta f\Delta T, \tag{3.10}$$

where $\Delta\phi = \phi_1 - \phi_2$ is the measured phase difference and $\Delta f = f_1 - f_2$ is the difference of the operating frequencies.

Denoting $\Delta T = d/c$, the distance d between A and B is then:

$$d = \frac{c\Delta\phi}{2\pi\Delta f}. \tag{3.11}$$

Applying this PDOA measurement between three reference nodes and a tag to provide three distance estimations, a 2D position can be obtained using a trilateration algorithm.

It is possible to measure the phase difference of two signals transmitted or received at the same time if the transmitter or receiver can transmit or receive two signals at the same time as in [41]. In [42], the phase difference is also measured for two different sequentially sent signals.

PDOA can provide range estimation with an error considerably less than the carrier signal wavelength. Due to the small wavelength of RF signals, the distance estimation can be quite accurate.

However, there are several disadvantages with PDOA measurement as below:

1. Phase observations are wrapped within the interval of 2π, resulting in an ambiguity problem in the positioning systems. The receiver can measure the phase of the received signal but it cannot directly measure the integer number of cycles (wavelengths) between the transmitter and receiver.
2. Any frequency deviation in the system can cause phase drift and accuracy of distance measurement, such as the frequency deviation between transmitter and receiver and frequency error due to clock drift.
3. Phase measurement is affected by distortion. Due to interference, for instance multipath effects, the carrier will be distorted, causing error in phase and distance measurements [41-43].

3.1.4 TDOA

The idea of TDOA is to determine the distance difference by measuring the differences in time of arrival between pairs of known reference nodes. TDOA method can be employed when there is no synchronization between a target node and reference nodes, but there is synchronization between reference nodes.

Assuming in a 3-reference-node 2D TDOA system, a signal is transmitted at time t_0 and received at times t_A, t_B and t_C by the three time synchronized reference nodes A, B and C respectively as shown in Figure 3.4.

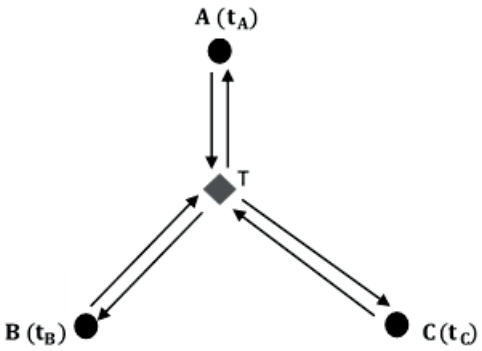

Figure 3.4 TDOA measurement

Two TDOA of received signals Δt thus can be calculated as $t_B - t_A$ and $t_C - t_A$. The difference in distance Δd , corresponding to the time difference, is thus:

$$\Delta d = \Delta t \cdot c, \qquad (3.12)$$

where c is the speed of light.

Two distance differences from three reference nodes can be measured to estimate a 2D position by using hyperbolic trilateration method. Similarly, three distance differences needs to be measured from four reference nodes for 3D positioning.

TDOA is usually estimated by the method known as Generalized Cross-Correlation (GCC) [44]. When all reference nodes share the same clock source, it is possible to obtain the time tag between the received signals at each reference node.

The main advantages of TDOA are:

1. TDOA method doesn't require synchronization of the reference nodes and the target node as required by TOA.
2. Taking time differences of TOA measurements has the advantage to reduce or eliminate common errors experienced at all receivers due to the channel or receiver's clock drift by subtraction.

The drawbacks of TDOA are:

1. Clock synchronization is still required for all receiver nodes used for the position estimation.
2. Solving the non-linear hyperbolic equations can be computationally complex and intensive.

3.1.5 AOA

AOA, also known as Direction of Arrival (DOA), usually determines the incident angles of arriving signals seen by reference nodes through directional antennas or antenna arrays. Adjusting directional antennas mechanically to the point of highest signal strength or employing several spatially separated antennas at reference nodes to measure arriving signals with different incident angles, it is possible to estimate the AOA of the incident signals through basic AOA estimation methods. In practical implementation of AOA systems, antenna arrays are usually exploited due to the complex and maintenance-intensive mechanical adjustment of the directional antenna.

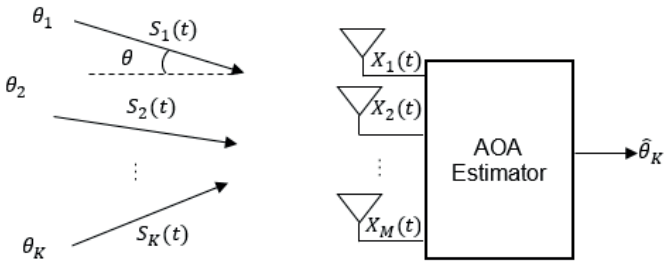

Figure 3.5 The general AOA measurement system

The general AOA measurement system is presented in Figure 3.5 [45-46], which shows K narrowband far-field incident signals on a linear antenna array with M-elements from distinct angles θ_K.

Let $S(t)$ = $[S_1(t)\ S_2(t)\ \dots\ S_K(t)]^T$ indicate the K x 1 vector of incident complex signals and A(θ) = [a(θ_1) a(θ_2) … a(θ_K)] represent the M x K matrix of array factor. Considering a uniformly spaced array with distance between elements d, each array factor vector can be denoted as a(θ_K) = $[1\ e^{jdcos\theta}\ e^{j2dcos\theta}\ \dots\ e^{j(M-1)cos\theta}]^T$. According to [47-48], the received signal can be modeled as:

$$X_M(t) = \sum_{k=1}^{K} a(\theta_k)\, S_k(t), \qquad (3.13)$$

where $S_k(t)$, k = 1, 2, …,K represents the incident signals.

The received signal can be expressed in a more compact form as:

$$X(t) = A(\theta)\, S(t) + n(t), \qquad (3.14)$$

where $X(t) = [X_1(t)\ X_2(t)\ \dots\ X_M(t)]^T$ denotes the received signal vector and n(t) is the additive noise vector.

Given the received signal $X(t)$ and antenna factor A(θ), the AOA estimation $\hat{\theta}_K$ can be obtained by applying basic AOA estimation methods [45, 47]. For example, the conventional beamformer (Barlett) simply uses Fourier-based spectral analysis of all incident signals to estimate the AOA. Capon's beamformer estimates the Maximum Likelikhood of a signal arriving from one direction while the rest of the incident signals are considered as interference with the assumption that the incident signals are uncorrelated. The multiple signal classification (MUSIC), a very popular high resolution method, provides asymptotically unbiased AOA estimations assuming the noise in each signal is uncorrelated.

A key feature of AOA method is the antenna array factor as it contains all the angular information required for the AOA estimation. Therefore, selection of the antenna array is critical to guarantee a good system performance and some considerations about it need to be taken into account such as the number of elements, the distance between the elements, operation frequency and position and direction of the array [46].

The main advantages of AOA methods are:

1. Position estimation can be obtained with less reference nodes compared to distance measurements based positioning method. Two reference nodes in 2D space and three reference nodes in 3D space with known positions can provide a position estimation using AOA method.
2. No time synchronization is required by AOA measurements.

The disadvantage of AOA method includes:

1. Relatively large and complex hardware due to directional antennas or antenna arrays, increasing the cost and size of devices.
2. The accuracy of AOA measurements relies on the antennas exploited. Many factors related to antennas can affect the accuracy of AOA measurements, such as the number of antenna elements, the distance between the elements, operation frequency and position and direction of the antennas.
3. Position estimation performance degrades with target node moving farther from the reference nodes [2].

3.2 Trilateration

As already mentioned, trilateration is the process of determining absolute or relative locations of points by measurement of distances. If measurements of absolute distance are available, it is called spherical trilateration and when only relative distances can be physically measured, it is named hyperbolic trilateration.

3.2.1 Spherical Trilateration

Spherical trilateration, as its name suggests, estimates positions by forming geometry circles in 2D space or spheres in 3D space and looking for intersection points.

Figure 3.6 represents an example of spherical trilateration in 2D space, the points A, B and C are reference points with known coordinates and point T is the target object to be located. As long as the distance d_A between the point T and point A is determined, a circle using this distance d_A as the radius around the point A can be plotted. The location of the point T is somewhere on this plotted circle. If the distance between T and another point B can be obtained as d_B, this distance d_B locates T on another circle around B. Similarly, calculating d_C puts T on a third circle. The location of T is determined as the intersection point or within the intersection area of these circles. In case the absolute locations of the points A, B and C are known, the absolute position of T therefore is determined.

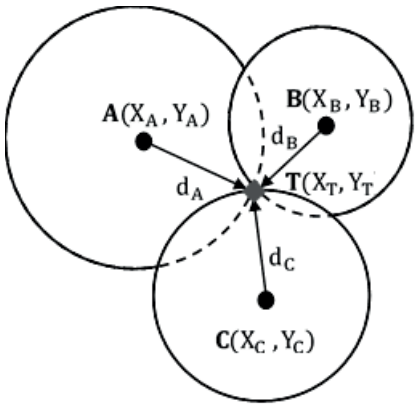

Figure 3.6 Spherical trilateration positioning technique

By using the Euclidean distance equation, we can calculate distance from the known points A, B and C to the unknown point T separately:

$$\begin{aligned} d_A &= \sqrt{(X_A - X_T)^2 + (Y_A - Y_T)^2}, \\ d_B &= \sqrt{(X_B - X_T)^2 + (Y_B - Y_T)^2}, \\ d_C &= \sqrt{(X_C - X_T)^2 + (Y_C - Y_T)^2}. \end{aligned} \qquad (3.15)$$

Solving these three equations in Equation (3.15) determines X_T and Y_T, in other words position of the unknown point T.

However, the equations in Equation (3.15) are nonlinear, overdetermined in the general cases and cannot be solved in an exact closed form. Several methods are proposed to solve the equations in the literature. A straightforward approach to solve the nonlinear equations described in [49]. Another common approach is to use linearization technique to obtain a linear set of equations as in [50]. An iterative algorithm [51] which require an initial estimation to start,

multidimensional scaling [52] and constrained minimization methods [53] are also employed to find the solutions.

Three non-colinear known positions are needed to be able to determine an unknown position in 2D space. In a similar way, in order to determine an unknown position in 3D space, at least 4 non-colinear known positions are needed. Domain-specific knowledge may reduce the number of required distance measurements. For example, when the object is known to be below the anchors plane the position can be estimated through 3 known distance measurements for 3D space.

TOA, RSS, and PDOA are the most popular methods employed to measure the absolute distances for the spherical trilateration positioning technique.

3.2.2 Hyperbolic Trilateration

Hyperbolic trilateration refers to a position estimation technique that determines locations by forming geometric hyperbola or hyperboloid and looking for intersection points. Hyperbolic trilateration technique bases on measurement of difference in distance of two points.

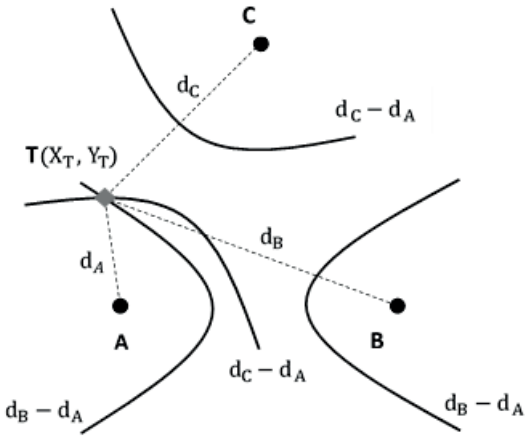

Figure 3.7 Hyperbolic trilateration positioning technique

Figure 3.7 shows an example of hyperbolic trilateration in 2D space. The points A, B and C are reference nodes with known coordinates and point T is the target node to be located. In the case that the absolute distances d_A, d_B and d_C from nodes A, B and C to node T are not available but the differences in distance from nodes A and B and A and C to T are known as d_{BA} and d_{CA}. Given d_{BA}, plotting all potential positions of node T produces two hyperbolic curves with point A and B as the foci because a hyperbola is the set of all points where the difference in the distance to two fixed foci is constant. The equation of the hyperbola is given by:

$$d_{BA} = \sqrt{(X_B - X_T)^2 + (Y_B - Y_T)^2} - \sqrt{(X_A - X_T)^2 + (Y_A - Y_T)^2}. \quad (3.16)$$

Similarly, with knowing the distance difference d_{CA} from nodes A and C to node T, T can be located on another hyperbola with point A and C as the foci. The hyperbola can be expressed as:

$$d_{CA} = \sqrt{(X_C - X_T)^2 + (Y_C - Y_T)^2} - \sqrt{(X_A - X_T)^2 + (Y_A - Y_T)^2}, \quad (3.17)$$

where the two corresponding hyperbolic curves intersect is the position of T. By solving the equation (3.16) and equation (3.17), we can find the coordinates (X_T, Y_T) of point T.

However, the hyperbola equations are non-linear and the procedure to solve a set of non-linear equations can be computationally complex and intensive. There are several methods proposed in the literature to solve the equations such as Taylor-series method [54] and Fang's and Chan's methods [55-56]. The Taylor-series method linearizes the non-linear equations through iterative algorithms while Fang's and Chan's methods determine a unique solution for the non-linear equations from closed-form algorithms.

Similar to spherical trilateration, at least 3 known positions are needed for hyperbolic trilateration to be able to produce two hyperbolas to determine an unknown position in 2D space and 4 known reference positions are needed in order to determine an unknown position in 3D space.

TDOA is the commonly used method to measure the distance differences required by the hyperbolic trilateration positioning technique.

3.3 Triangulation

Triangulation method is used to estimate position when the angles from known reference nodes to the target node can be measured. With the measured angles and the known distances between reference nodes, the position of the target point can be calculated by using the trigonometry laws of sines and cosines.

Figure 3.8 presents an example of 2D triangulation scheme. The circles A and B are reference points with known coordinates and point C is the target node to be located.

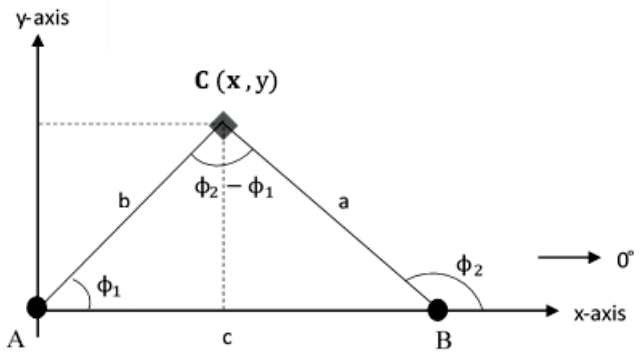

Figure 3.8 Triangulation positioning technique

As long as the two angles ϕ_1 and ϕ_2 from reference nodes to the target node and the distance c between A and B can be measured, according to trigonometry law:

$$\frac{a}{sin\phi_1} = \frac{b}{sin\phi_2} = \frac{c}{sin(\phi_2 - \phi_1)}. \qquad (3.18)$$

Then the coordinates of the target node C can be calculated as:

$$x = \frac{sin\phi_1 \cdot sin\phi_2}{sin(\phi_2 - \phi_1)} \cdot c, \qquad (3.19)$$

and

$$y = \frac{sin\phi_2 \cdot cos\phi_1}{sin(\phi_2 - \phi_1)} \cdot c. \qquad (3.20)$$

At least two reference nodes with known positions are needed for triangulation method to determine an unknown position in 2D space. In 3D space, at least three reference nodes are required to determine position of a target node.

The angle measurements needed for triangulation technique are usually done through the AOA method.

3.4 Fingerprint

Fingerprint-based positioning techniques can be classified into three categories, namely, RF fingerprint, non-RF fingerprint and cross-technology fingerprint [8]. In this thesis, we focus on RF fingerprint-based methods.

RF fingerprint-based methods employed in indoor positioning systems are usually based on measurement of radio signals and the most frequently reported RF fingerprint method is based on received signal strength RSS [8-10]. RSS fingerprint includes two phases: training phase and positioning phase. During the training phase, a radio map composed of the RSS measured at any possible position of the target is constructed. For a typical fingerprint system, the radio map is formed from fingerprints of all possible positions of interest. Each fingerprint is obtained at a specific location by measuring and averaging RSS over time. In the positioning phase, the position is estimated according to the results of comparing the observed RSS and searching matches in the radio map database using appropriate algorithms.

The radio map construction is an inevitable but time consuming, labor intensive and easily affected by environments procedure. Many approaches have been proposed to simplify the procedure, such as crowdsourcing-based approach [57-59] and Simultaneous Localization and Mapping (SLAM) approach [60-62]. Crowdsourcing-based approach encourages volunteer users to participate in data collection. The time and the cost needed by the radio map construction thus shared by the large number of volunteer users instead of skilled surveyors. The SLAM approach focuses on simultaneously localizing the target and constructing the radio maps. For the target location estimation, many algorithms have been reported in the literature, such as the K-Nearest Neighbor (KNN) method [62-63], the weighted nearest neighbors, support vector machine, neural network and Maximum Likelihood (ML) [64]. The idea of KNN is to compute the distance between the observed target and the nearest neighbors around it and then pick the location that minimizes the distance.

The major advantage of the fingerprinting technique is the simple and low-cost hardware implementation required since this technique is usually based on RSS.

Disadvantage of fingerprinting technique as below.

1. Fingerprinting technique requires time consuming and labor intensive survey work to construct radio maps.
2. The final positioning accuracy depends on the number and the distribution of the survey points. Increasing the number of survey points may benefit positioning accuracy, but this needs more efforts on radio map construction.
3. Fingerprinting technique is sensitive to environmental changes. Movement of people or changes of objects can easily degrade the positioning accuracy.

3.5 CoO

CoO, also known as proximity, is a cell-based positioning technique as explained earlier in this chapter. CoO technique estimates the location of a target object with respect to a known position

or an area. The CoO location technique needs to fix a number of reference nodes at known positions. When a target object is detected by a reference node, the position of the target is considered to be in the proximity area covered by the reference node. If the target object is detected by more than one reference node, the reference node that receives the strongest signal is then considered when estimating the target object's position.

One very simple model for CoO is the so-called circular radio coverage model or disk model, where the reading range is modeled by a circle with fixed radius [1]. As Figure 3.9 shows, A and B are the reference nodes and T is the target object. The proximity areas of A and B are marked with dotted circles in the Figure. The position of the target object T is estimated by monitoring in which proximity area it is. Therefore, T is located in the proximity area of A node in the case showing in the Figure.

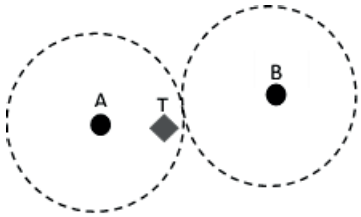

Figure 3.9 CoO positioning technique

The CoO technique only provide approximate position estimation and the achievable positioning accuracy thereby depends on the size of the cell defined by the maximum reading range of the reference nodes and the density of the deployed reference nodes.

The CoO technique is the simplest way to obtain positioning measurement information as it doesn't require any dedicated hardware and time synchronization among the anchor nodes and target object, which make it particularly suited for very low-cost wireless devices such as RFID tags where the deployment of a large number of tags is not an issue.

However, the accuracy of CoO technique can be very poor, especially when "blind points" occur due to the defective coverage of the anchors in indoor environment.

Chapter 4 Evaluation of IPS Using off-the-shelf Hardware

Three indoor positioning systems based on UWB TOF, WiFi TOF and BLE RSS hardware are set up and evaluated in the scope of this thesis. The UWB TOF hardware was chosen due to its attractive ability of accurate range estimation. WiFi and BLE hardware were selected because they are widely adopted by the majority of the mobile devices and other consumer electronics on the market. IPSs based on off-the-shelf WiFi and BLE devices can considerably reduce cost of the system implementation. Moreover, it is interesting to know the positioning performance based on the WiFi TOF technique as it is still an emerging positioning method.

This chapter defines evaluation criteria and describes the evaluation environment where the evaluation experiments were carried out. Considerations for a systematic way of deploying the evaluated IPSs are also presented. In addition, an implemented trilateration positioning algorithm is also introduced and verified in this chapter. Finally, setup of evaluation experiments, experimental results and analysis for each of the three evaluated IPSs are described.

4.1 Evaluation Criteria

To evaluate the performance of these three systems, we defined a set of evaluation criteria which positioning systems will be evaluated and compared against. Different characteristics can be used to judge a positioning system and different applications have different expectations on their systems. We selected the most important characteristics that determine the applicability of indoor positioning systems as evaluation criteria for the indoor positioning systems in this thesis, which are accuracy, power consumption, cost and ease of deployment.

4.1.1 Accuracy

Accuracy of a positioning system is the degree of conformance of the closest estimated position that can be achieved to the true position. Different systems provide different accuracies. In order to compare the accuracy of the systems in this thesis, we defined the term ‘positioning error’ and ‘range error’ as described in the following section.

- Positioning Error

We regard positioning error as the Euclidean distance of the estimated position and true position. If the positions are in two-dimension (2D) Cartesian coordinate we talk about 2D positioning error, while if they are in three-dimension (3D) Cartesian coordinate we refer to 3D positioning error.

Denoting the coordinates of the estimated position as (x_1, y_1) and true position as (x_2, y_2), the 2D positioning error is then:

$$\Delta P_{2D} = \sqrt{(x_1 - x_2)^2 + (y_1 - y_2)^2}. \quad (4.1)$$

Similarly, the 3D positioning error is obtained as:

$$\Delta P_{3D} = \sqrt{(x_1 - x_2)^2 + (y_1 - y_2)^2 + (z_1 - z_2)^2}, \quad (4.2)$$

where (x_1, y_1, z_1) is the estimated position and (x_2, y_2, z_2) is the true position.

The closer the estimated position and the true position, the more accurate the positioning. Thus, we expect the positioning error as small as possible for a high accuracy positioning system.

- Range Error

Range error is the difference between the measured range and true range from a reference device to a target device. Positioning systems in this thesis estimate positions based on measured ranges. Therefore, the positioning error depends on size of the related range error directly. The range error is determined as:

$$\Delta R = R_{Meas} - R_{True}, \quad (4.3)$$

where ΔR is the range error, R_{Meas} and R_{True} are estimated range and true range. The true range R_{True} from a reference device to a target device can be given through Euclidean distance:

$$R_{True} = \sqrt{(x_r - x_t)^2 + (y_r - y_t)^2 + (z_r - z_t)^2}, \quad (4.4)$$

where (x_r, y_r, z_r) and (x_t, y_t, z_t) are the coordinates of the reference device and target device respectively.

4.1.2 Power Consumption

Power consumption is the most important non-location-related parameter of an indoor positioning system because it determines if the terminal devices of the system can be powered by portable batteries and easily attached onto target objects or persons. In some positioning applications, the power consumption of a system may determine if the system can be exploited for the applications. Lots of factors can affect the power consumption of a positioning system such as the positioning technology, hardware and software design of the devices that the system employs, positioning algorithm and different application cases of the system being used.

In this thesis, we emphasize on hardware related power consumption, especially focusing on the power consumption related to the RF technologies and the RF devices exploited by the three evaluated IPSs, providing a generic comparison and a practical benchmark of power consumption for these three technologies and hardware.

4.1.3 Cost

Cost is an important usage requirement that needs to be taken into account for choosing an indoor positioning system. In the case that required performance of a system can be achieved, the lower the cost the better the system. Many factors in a positioning system may affect its cost, like the cost spent on the hardware units and system development, deployment, maintenance costs that the system requires. In this thesis, we mainly discuss the cost related to the hardware units and the technologies the hardware employs.

4.1.4 Ease of Deployment

Positioning systems should be as easy as possible to deploy and set up. If a lot of efforts is required for the system to be operational, the system will not be used as much.

In the remainder of this chapter, evaluation results and discussion are mainly focusing on the accuracy of the three evaluated IPSs. Discussion and comparison of power consumption, cost and ease of deployment for these three evaluated IPSs will be presented in Chapter 5.

4.2 Evaluation Environment

The three mentioned indoor positioning systems were set up in a sports hall in the basement and the office on 3rd floor of Greenland building in Lund separately for evaluating LOS and NLOS scenarios.

(a) Sports Hall (b) Office Area

Figure 4.1 Evaluation areas, (a) The sports hall and (b) the office area

The sports hall, shown in Figure 4.1(a), is a 10.12 m × 15.74 m × 3.28 m rectangular semi-basement room. It is made up of concrete walls and floor covered by wood strips with few glass

windows at one side. The sports hall is empty except for a metal pipe standing at one of the corners.

The office area, shown in Figure 4.1(b), is a typical office with meeting rooms, desks, chairs, cabinets, computers, cables and radio interference like WiFi and Bluetooth. The evaluation area in the office is more open than the sports hall and its size is comparable with the size of the sports hall. The evaluation area in office covers roughly 14.7 m × 16 m × 2.7 m size of rectangular area with meeting rooms in the middle. In addition, there are few cement pillars, metal pillars and metal writing boards in the evaluation area.

To be able to evaluate positioning accuracy of the three systems, the true positions of the target object must be known. Also locations of all reference points (RPs) at where the reference nodes will be deployed are needed for positioning algorithm to estimate positions. We hence defined test points (TPs) at where the target object will be placed and RPs in the sports hall and office evaluation area.

In the sports hall 3 positions close to the roof and at the same height around 2.2 m were defined as RPs marked as triangles while 59 locations were defined as TPs marked with dots and named by numbers in Figure 4.2. The separation distance of two adjacent TPs along the walls is 1 m while TPs in the middle of the area is 2.38m except for the TP50 which is 1.12 m away from its neighbour points TP49, TP51, TP56 and TP57.

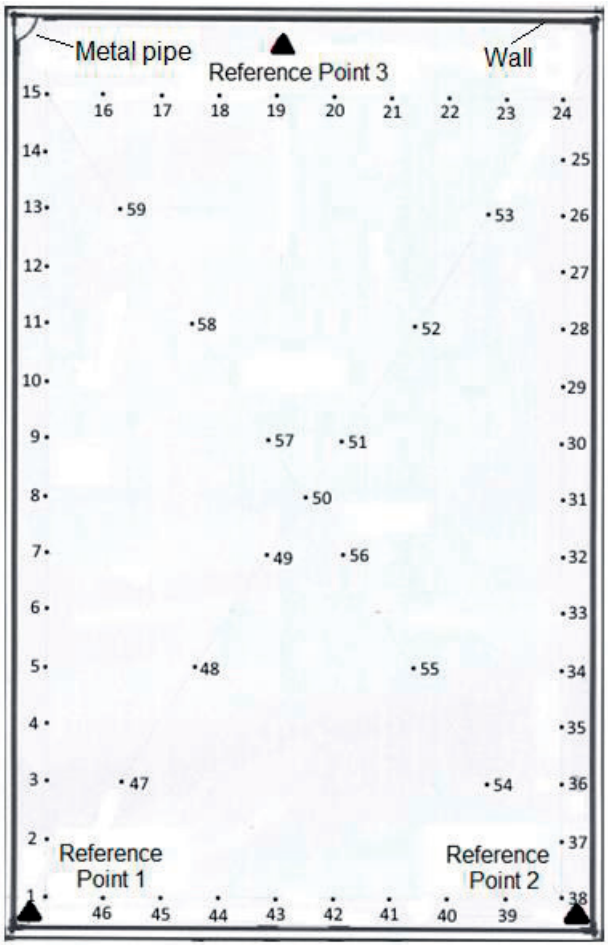

Figure 4.2 Floor plan of the sports hall evaluation area. Triangles are RPs while dots are TPs

In the office evaluation area, 3 locations close to ceiling and at the same height around 2.2 m were chosen as RPs marked as triangles while 90 locations were defined as TPs marked with dots and named by numbers as shown in Figure 4.3. The separation distance of two adjacent TPs in office area is 0.5 m. All the defined points were measured as accurate as possible with help of a laser range finder and an ordinary ruler and their coordinates defined according to a 3D Cartesian coordinate system were labelled on floor and recorded on paper.

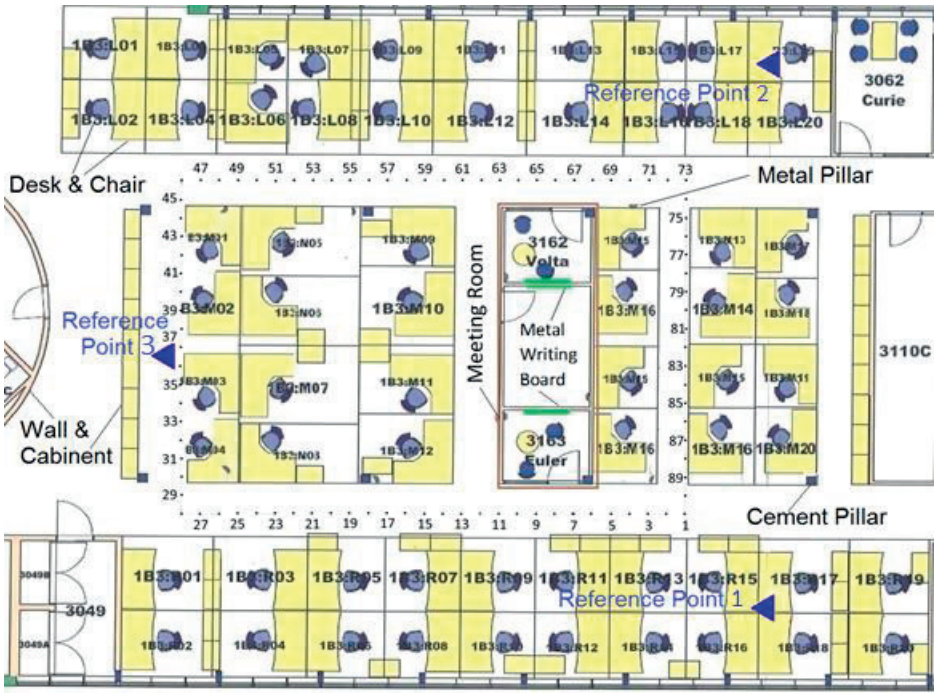

Figure 4.3 Floor plan of the office evaluation area. Triangles are RPs while dots are TPs

In addition, it is necessary to mention that the most important objects in the office area which may affect the evaluation result, those are highlighted in the floor plan as well. The metal pillars and writing boards are originally not included in the floor plan but added with measured positions and approximate scale corresponding to their locations and sizes in the real environment. The dimension and shape of the main obstacles in the office evaluation area are given in Table 4.1.

Obstacles	Dimension (cm^3) (Height x Width x Depth)	Shape	Comments
Meeting Room (MR)	285 x 750 x 268.8		Stands on the floor
Metal Pillar (MP)	(12+9) x 3 x 246		Stands on the floor
Cement Pillar (CP)	25 x 25 x 268.8		Stands on the floor
Metal Writing Board (MWB)	151.5 x 121.5 x 1.5		Hangs on wall

Table 4.1 Main obstacles in the office evaluation area

Moreover, the significant obstacles existing between each RP and TP in the office evaluation area are listed in Table 4.2. With denoting meeting room as MR, metal pillar as MP, cement pillar as CP and metal writing boards as MWB.

Points	Obstacles between TP and RP1	Obstacles between TP and RP2	Obstacles between TP and RP3
1	LOS	LOS	MR & edge of CP
2	LOS	LOS	MR
3	LOS	LOS	MR
4	LOS	LOS	MR
5	LOS	LOS	MR
6	LOS	LOS	MR
7	LOS	Corner of MR & CP	edge of MR
8	LOS	MR	LOS
9	LOS	MR	LOS
10	LOS	MR	LOS
11	LOS	MR & MWB	LOS
12	LOS	MR & MWB	LOS
13	LOS	MR & MWB	LOS
14	LOS	MR	LOS
15	LOS	MR	CP
16	LOS	MR	LOS
17	LOS	MR	LOS
18	LOS	MR & MWB	LOS
19	LOS	MP & MR & MWB	LOS
20	LOS	MP & CP & MR & MWB	LOS
21	LOS	MR & MWB	LOS
22	LOS	MR & MWB	LOS
23	LOS	MR & MWB	LOS
24	LOS	MP & MR	LOS
25	LOS	MP & CP & MR	LOS
26	LOS	MR & MP	LOS
27	LOS	MR	LOS
28	LOS	MR	LOS
29	LOS	MP & MR	LOS
30	LOS	MP & CP & MR	LOS
31	MP	MR	LOS
32	LOS	MR	LOS
33	CP	MR	LOS
34	LOS	MR	LOS

Points	Obstacles between TP and RP1	Obstacles between TP and RP2	Obstacles between TP and RP3
35	LOS	MR	LOS
36	LOS	LOS	LOS
37	LOS	LOS	LOS
38	MR	LOS	LOS
39	MR	LOS	LOS
40	MR	LOS	LOS
41	Corner of MR	CP & MP	LOS
42	Corner of MR	LOS	LOS
43	Corner of MR	MP	LOS
44	Corner of MR	LOS	LOS
45	MR & CP	LOS	LOS
46	MR & CP & MP	LOS	LOS
47	MR & edge of CP	LOS	LOS
48	MR	LOS	LOS
49	MR & MWB	LOS	CP
50	MR & MWB	LOS	LOS
51	MR & MWB	LOS	LOS
52	MR & MWB	LOS	LOS
53	MR & MWB	LOS	LOS
54	MR & CP & MWB	LOS	LOS
55	MR	LOS	LOS
56	MR	LOS	LOS
57	MR & MP	LOS	edge of MP
58	MR & MP	LOS	CP
59	MR & MP	LOS	CP
60	MR	LOS	LOS
61	MR & MWB	LOS	LOS
62	MR & MWB	LOS	LOS
63	MR & MWB	LOS	LOS
64	MR	LOS	LOS
65	MR	LOS	LOS
66	MR	LOS	LOS
67	MR & CP	LOS	MR
68	LOS	LOS	MR
69	LOS	LOS	MR
70	LOS	LOS	MR
71	LOS	LOS	MR

Points	Obstacles between TP and RP1	Obstacles between TP and RP2	Obstacles between TP and RP3
72	LOS	LOS	MR
73	LOS	LOS	MR & CP
74	LOS	LOS	MR
75	LOS	LOS	MR
76	LOS	LOS	MR & MP
77	LOS	LOS	MR & MWB
78	LOS	LOS	MR
79	LOS	LOS	MR
80	LOS	LOS	MR
81	LOS	LOS	MR
82	LOS	LOS	MR
83	LOS	LOS	MR
84	LOS	LOS	MR
85	LOS	LOS	MR & edge of MP
86	LOS	LOS	MR
87	LOS	LOS	MR
88	LOS	LOS	MR
89	LOS	LOS	MR
90	LOS	LOS	MR

Table 4.2 Main obstacles between RPs and TPs in the office evaluation area

It is necessary to mention that the obstacles in Table 4.1 and Table 4.2 are just the main obstacles we can see in the environment and they are listed between different RPs to TPs just based on optical LOS observation. Radio signal propagation in indoor environment is far more complicated. We believe there are more obstacles which may affect the communication of radio signals that not listed in the Table 4.1 and Table 4.2.

4.3 Positioning Algorithm

All the three indoor positioning systems to be evaluated in this thesis are able to measure distance. The UWB IPS and WiFi IPS measure distance through TOA measurement while the BLE IPS measures distance via RSS measurement. Based on the theory study of basic indoor positioning techniques in chapter 3, the trilateration positioning algorithm is suitable for all these three systems and hence is implemented to estimate the positions and provide a fair comparison with regard to accuracy for all these three systems.

4.4 Deployment Methodology

When it comes to deployment of an IPS, the first question that pops up is how to place the hardware units to optimize the system performance. Many factors can affect performance of an IPS and thus need to be taken into account for deploying an IPS. We try to find a systematic way of deployment to achieve optimal coverage and accuracy for the systems to be evaluated based on the allowed conditions of the hardware units that these systems exploited. The main considerations are described in the following sub-sections.

4.4.1 Numbers of Reference Points (RPs)

To be able to make use of trilateration positioning algorithm for the UWB TOA, WiFi TOA and BLE RSS based positioning systems, 4 RPs with known position are needed for 3D positioning and 3 RPs are required for 2D positioning. However, since all of our predefined RPs are at the same height and above the target object, the number of RPs can be minimized to 3 for 3D positioning. We therefore decided to deploy 3 reference nodes for all these three system.

4.4.2 Positions of Reference Points

When it comes to considering positions for the 3 defined RPs, the first consideration is the coverage. Considering rectangular shape evaluation area of the sports hall, the primary plan is to place two RPs at two of the corners and the third one in the middle of the other side of the two corners. However, this consideration doesn't take the communication range that the hardware support into account, which actually is the most important factor to secure coverage. Moreover, the supported communication range may vary depending on environments. We therefore carried out specific range measurements with all three kinds of hardware units in both the sports hall and office area to figure out if the primarily defined area can be covered. In addition, for the office evaluation area, except for considering coverage we also tried to make sure all 3 RPs have optical LOS to each other to get as good as possible performance for the systems.

The range measurements performed for several separation distances d with two hardware units from each system acting as reference device and target object respectively. For each separation distance, both hardware units were placed stationary with same height h and same orientations. The setup is shown in Figure 4.4.

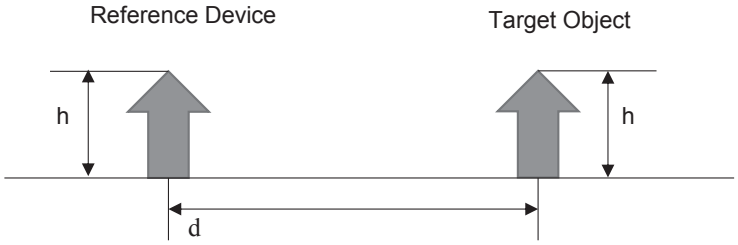

Figure 4.4 Range measurement setup

At each distance, k samples ($x_1, x_2 \dots x_k$) are collected and then averaged according to Equation (4.5) to give the measured range:

$$R = \frac{1}{k}\sum_{i=1}^{k} x_i. \qquad (4.5)$$

According to the size of the evaluation area and pre-defined locations of RPs, the ranges required for covering the sports hall and office evaluation area are approximately 17 m and 20 m respectively. The measured results showing in Table 4.3 indicate that all three hardware could fulfil the required coverage ranges.

Hardware	Measured Range in Sports Hall (m)	Measured Range in Office Area (m)
UWB (k = 1000)	18.05	30.17
WiFi (k=200)	18.2	23.17
BLE (k=200)	18	29

Table 4.3 Range measurement result

We have to emphasise that the measured range in Table 4.3 doesn't mean the maximum range the corresponding hardware supports. Due to the special purpose of this range experiment, we stopped the test as long as we confirmed that the ranges of interests can be supported by the hardware under evaluation.

4.4.3 Placement Orientation

In the previous section, during the range experiments the reference device and target object were placed in fixed orientations. However, placement orientation of a RF hardware unit may affect the accuracy of an IPS because antenna radiation pattern of an off-the-shelf hardware unit is usually not expected to be uniform, which means placing hardware units in different orientation may play an important role in the performance of IPS. An investigation was carried out to observe the influence of the orientation.

First of all, we tried to obtain the antenna radiation pattern of all the three hardware. Moreover, we performed an orientation experiment to observe the influence of placing a hardware unit in different orientations. The experiment was carried out in the sports hall with two hardware units from each system acting as reference device and target object respectively. During the experiment, the two hardware units were placed with 1 m separation distance from each other and the target object was kept stationary while the reference device was placed in different orientations ($0^\circ, 90^\circ, 180^\circ, 270^\circ$) but maintaining 1 m separation distance. In each orientation, samples were collected and then averaged according to Equation (4.5). In case different range errors were compared, they were calculated according to Equation (4.3). Based on the limitations of the three hardware units, different measurements were conducted.

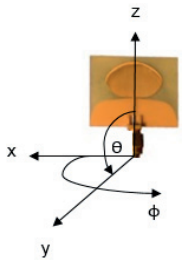

(a) Antenna placement during measurement of the radiation pattern

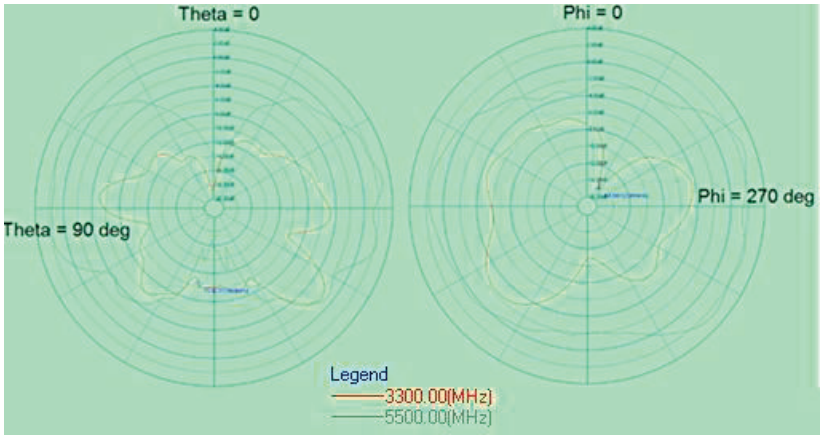

(b) Antenna gain, E-Plane, Phi = 90˚ (c) Antenna gain, H-Plane, Theta = 90˚

Figure 4.5 Antenna radiation pattern of the UWB Hardware

For the UWB hardware, antenna radiation pattern was measured and also an orientation experiment was conducted. The antenna placement during radiation pattern measurement and the measured results are shown in Figure 4.5.

Range error results of the orientation experiment from the UWB hardware is shown in Table 4.4. According to the results, the orientation which has maximum antenna gain at 5500 MHz in H-plane as shown by the gray curve in the Figure 4.5 provides smallest range error as shown in Table 4.4.

Angles of ϕ (Deg.)	Range Error (cm)
0	5.6
90	0.1
180	3.2

270	4.5

Table 4.4 Orientation test result for the UWB hardware

For the BLE beacon, the simulated antenna radiation pattern is shown in Figure 4.6. According to the figure, the BLE Beacon has best antenna gain along z axis, i.e., Theta = 0˚ and 180˚ directions.

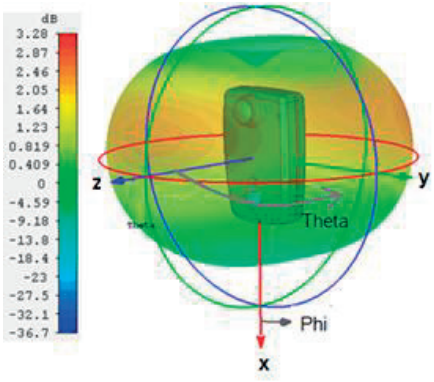

Figure 4.6 Antenna radiation pattern of the BLE Beacon

RSS results of the orientation experiment from a BLE Beacon are shown in Table 4.5. According to the results, the orientation which has best antenna gain according to the antenna radiation pattern of the BLE Beacon provides highest RSS. In other words, the BLE Beacon has better radiation at its front and back sides.

Angles of θ (Deg.)	RSS (dBm)
0	-47
90	-48.5
180	-47.3
270	-47.5

Table 4.5 Orientation test result with the BLE hardware

For the WiFi hardware, neither measurement nor simulation for the antenna of the hardware unit was possible. We thus only conducted orientation measurement with two WiFi hardware units as shown in Figure 4.7.

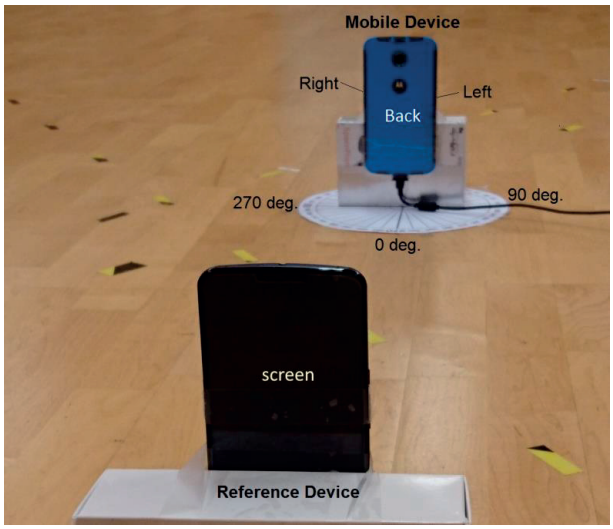

Figure 4.7 Antenna orientation experiment setup for the WiFi hardware

Range error results of the orientation experiment from the WiFi hardware unit are shown in Table 4.6. According to the results, the WiFi hardware unit has best radiation from its back and left sides.

Angles (Deg.)	Range Error (cm)
0	7.8
90	8.9
180	26.7
270	21.4
Screen to screen	22.5

Table 4.6 Orientation test result with the WiFi hardware

During the deployment, the reference devices were placed in orientations with highest gain facing the positioning area to be evaluated for all the three evaluated IPSs.

4.4.4 Placement Distance against Disturbance

Reference devices of an IPS are usually deployed on the walls or ceiling. However, indoor positioning systems based on RF technologies are generally sensitive to walls or other obstacles. We conducted an experiment with the BLE beacon to investigate the impact that walls have on RSS. The BLE beacon was chosen as test system because it is based on RSS measurement and theoretically RSS is usually more sensitive to obstacles compared to TOA measurement.

This experiment was conducted for two scenarios: deploying a BLE beacon on the wall and deploying the BLE beacon 20 cm away from the wall. For both scenarios, the BLE beacon was kept stationary while a target device was placed at three difference separation distances d (0.5 m, 1 m, 2 m) from the Beacon to read the RSS from it. At each distance of a scenario, five RSS samples were collected and then averaged as a RSS result. The delta RSS of the two scenarios is defined as:

$$\Delta RSS = RSS_{Beacon\ 20cm\ from\ wall} - RSS_{Beacon\ on\ wall}. \quad (4.6)$$

The results are shown in Table 4.7.

d (m)	RSS (dBm) with Beacon on wall	RSS (dBm) with Beacon 20 cm away from wall	Δ RSS (dB)
0.5	-41	-37	4
1	-49.9	-43.7	6.1
2	-53.6	-49	4.6

Table 4.7 Result of placement experiment for the BLE hardware

According to Table 4.7, the RSS reduction can reach 6.1 dB due to placement of the Beacon on the wall based on the three distances tested. According to the propagation model of this BLE hardware in Figure 4.31, such RSS reduction can cause distance error up to 6 m when separation distance of the BLE Beacon and target device is around 12 m and even within a very short separation distance 1 m the distance error can be 0.5 m. We therefore recommend to keep the reference devices away from walls and ceilings during deployment. In our experiments in the sports hall, we keep all deployed reference hardware units at least 20 cm away from the walls and ceilings.

With similar principle, we try to avoid other disturbance during system deployment. For example, we use cardboard stands to fix the reference hardware units as much as possible and we try to keep antenna of the deployed hardware units above any high attenuation level of obstructions, for instance, metal stands.

4.5 Evaluation of UWB-based IPS

4.5.1 UWB Anchors and Tag

The UWB Anchors and Tags we employed are TREK1000 evaluation kit from DecaWave. This evaluation kit contains four evaluation boards called EVB1000 which integrate DecaWave's DW1000 low power, single chip CMOS radio transceiver IC compliant with the IEEE 802.15.4-2011 Ultra-Wideband (UWB) standard. These four evaluation boards are identical and each board as shown in Figure 4.8 can be configured either as an Anchor or as a Tag. Two of the evaluation

boards can be used to run a pre-programmed two-way ranging (TWR) application which controls the DW1000 IC to exchange messages, calculate the time-of-flight and estimate the resultant distance between the two boards. The evaluation kit alternatively enables evaluation for Real Time Location Systems (RTLS) using two-way ranging (TWR) RTLS application. The application connecting to anchors or tags receives the Time of Flight (TOF) reports and estimates tag's location based on the anchors position. None of these EVB1000 boards have internal batteries and need to be powered up by external power.

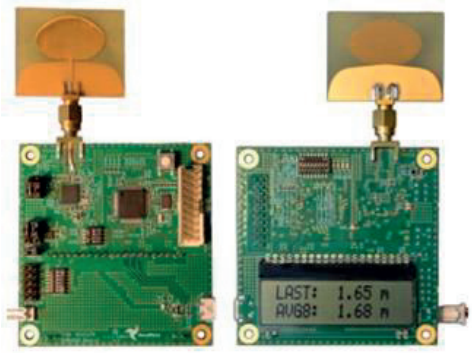

Figure 4.8 DecaWave EVB1000 evaluation board, component side (left) and display side (right)

4.5.2 UWB IPS System Setup and Configuration

The UWB-based IPS was deployed separately in the sports hall and office area to evaluate both LOS and NLOS scenarios. For both scenarios the system has the similar setup with placing three EVB1000 boards at the RPs named 1, 2 and 3 as Anchors and one EVB1000 board configured as Tag acted as target object. The configurations of the evaluation boards is shown in Table 4.8.

Role	Center Frequency	Bandwidth	Data Rate
Anchor	6.489 GHz	500 MHz	110 kbps
Tag	6.489 GHz	500 MHz	110 kbps

Table 4.8 Configurations of the UWB IPS

During the evaluation, the Anchor at the RP1 acted as a master Anchor and was connected to a computer through USB cable to run a pre-programmed application software for positioning estimation and reporting estimated results. The Tag acted as target object supposed to place at TPs is responsible for ranging measurement from all Anchors to itself and exchanging estimated ranges with the Master Anchor through its on-chip ARM based software. The master Anchor does the positioning estimation based on the gathered ranging results and reports it to the connected computer. Both the Tag and Anchors are powered on by external portable Batteries. The Tag was placed at all predefined TPs in Figure 4.2 for LOS case and Figure 4.3 for NLOS scenario one by one. The Tag was kept stationary at each TP until 1000 set of measurement samples were

collected as per plan. The Tag was then moved to the next TP and the procedure was repeated until all planned TPs were tested. For this UWB system, we tested all 59 predefined TPs in the sports hall and the 90 TPs in the office. For each TP, ranges from all three Anchors to Tag was calculated respectively by averaging 1000 collected samples from corresponding Anchors to Tag. This UWB IPS measures and calculates distance based on TOA and then reports both the measured TOA and the range.

4.5.3 Evaluation Result and Analysis

This section presents evaluation results including positioning error and range error for both LOS and NLOS scenarios from the evaluated UWB IPS. Thorough analysis of the given results are also provided in this section.

4.5.3.1 Positioning Error

The positioning result was derived by computing the coordinates through the trilateration algorithm introduced in section 4.3 based on the collected range measurement results from the UWB IPS. The positioning error is given as the Euclidean distance of the estimated position and its true position. 2D positioning error is calculated according to Equation (4.1) and 3D positioning error is derived through Equation (4.2). The 2D and 3D positioning error distribution from UWB IPS for both LOS and NLOS scenarios are presented in Figure 4.9 and Figure 4.10.

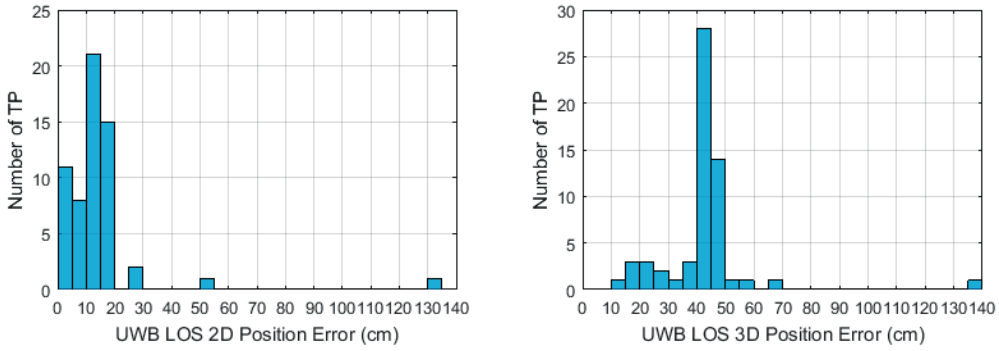

Figure 4.9 LOS positioning error distribution of the UWB IPS

Figure 4.9 shows that in LOS scenarios the 2D positioning error of all evaluated TPs are centrally distributed within 20 cm and only 4 TPs have position error bigger than 20 cm. The 3D positioning result is worse than that of 2D case. The 3D positioning error spreads between 10 and 70 cm with two exceptions at about 70 cm and 140 cm and the majority of calculated errors distributes around 40 cm.

As we expected the positioning result from NLOS scenario is worse than that of LOS scenario. According to the positioning error distribution in Figure 4.10, only about 70% of 2D positioning error is smaller than 20 cm while the rest are widely distributed up to around 1 m. When it comes

to 3D positioning error, the distribution spreads widely up to around 130 cm with a considerable part locating within 60 cm and another big group concentrating around 70 cm.

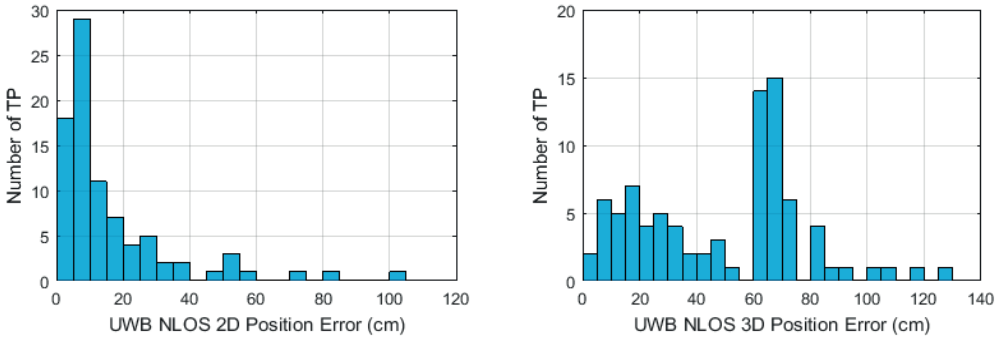

Figure 4.10 NLOS positioning error distribution of the UWB IPS

For both LOS and NLOS scenarios, it is easy to conclude that the 3D positioning result is worse than 2D positioning result. However, the worse 3D positioning result is expected because we only have 3 known RPs. It is mainly the positioning algorithm which estimates coordinate in a mathematical way. The 3D positioning accuracy could be improved by either adding a 4^{th} RP in the system where gives an absolute solution to the spherical equations introduced in section 3.2.1 in this report or improving positioning algorithm. Since this UWB IPS system only uses 3 Anchors, regardless of the impact of positioning algorithm, we assume 3D positioning result can be reflected from the 2D positioning result. Therefore, in the rest of this section, we will mainly discuss 2D positioning error.

To be able to have a clear picture on the estimated positions relative to their true positions, the anchors and the evaluation areas, we plotted the estimated positions as blue plus signs together with their true positions as black dots and three anchors as blue triangles in a 2D Cartesian coordinate system scaled according to the real size of the evaluation areas in Figure 4.11 and Figure 4.12 for LOS and NLOS scenarios respectively.

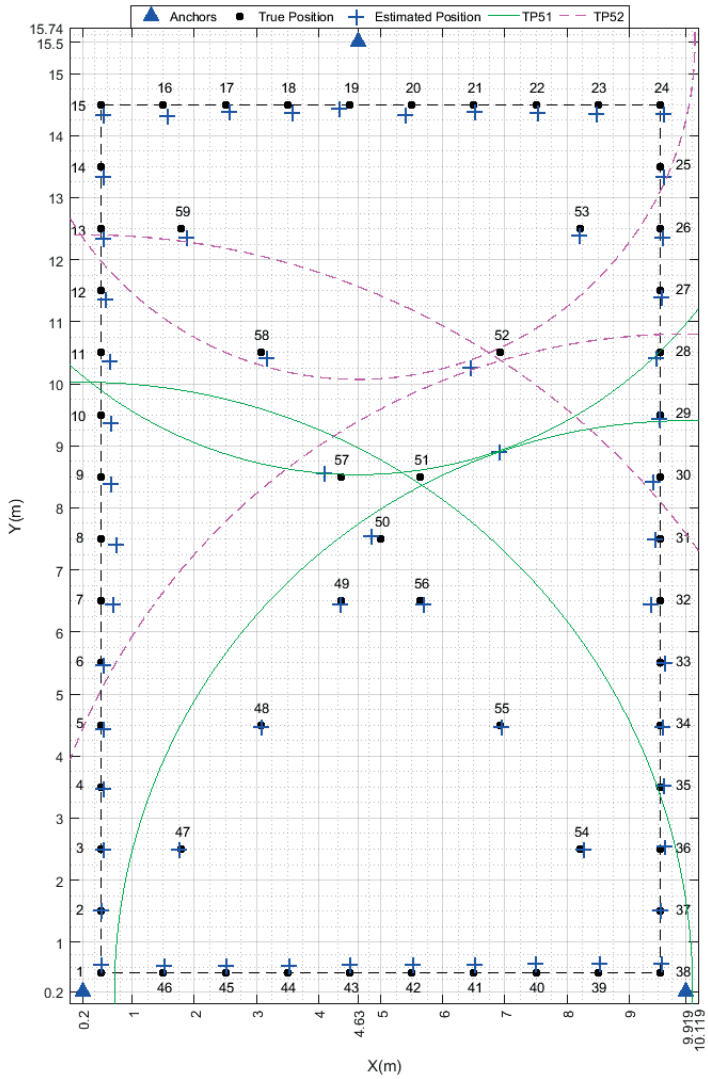

Figure 4.11 LOS estimated positions of the UWB IPS

In Figure 4.11 of LOS case, now one could easily find that two of the mentioned 4 TPs which have position error bigger than 20 cm are TP51 and TP52. For each point of TP51 and TP52, we plotted their three circles formed by its three measured ranges in Figure 4.11. The green-solid-line circles are for TP51 while pink-dot-line circles are for TP52. From the intersection status of these circles, we conclude that the biggest positioning error given by TP51 and TP52 are mainly caused by the

trilateration positioning algorithm. This error should be possibly minimized by optimizing the positioning algorithm if time allows.

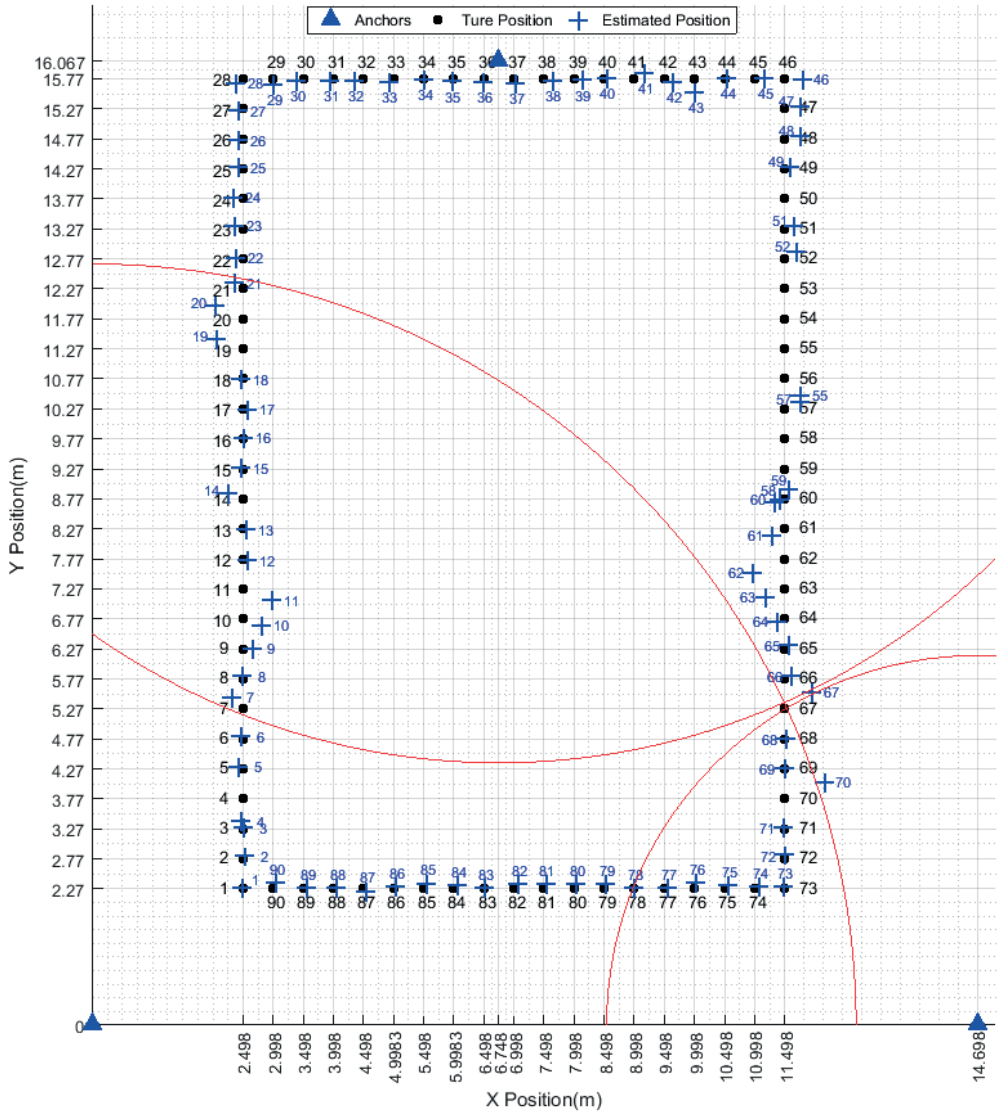

Figure 4.12 NLOS estimated positions of the UWB IPS

For NLOS scenario, we added indexes for all the estimated positions as blue numbers In Figure 4.11 as well. One may notice that there are four points TP50, TP53, TP54 and TP56 without estimated positions in the figure, which we will discuss later in this section.

In addition, in Figure 4.13 and Figure 4.14 we can numerically inspect the 2D positioning error at each test point through the positioning error plot versus all TPs for both LOS and NLOS scenarios. In Figure 4.13 positioning error for LOS case, we replaced the biggest positioning errors of TP51 and TP52 with 0 in order to have better resolution at the rest points. The big error of TP51 and TP52 is mainly caused by the trilateration algorithm as we already discussed. In Figure 4.13 and Figure 4.14, there are sharp peaks at TP8 and TP57 with positioning error in LOS case and at TP55, TP58, TP62, TP67 and TP70 with positioning error in NLOS scenario.

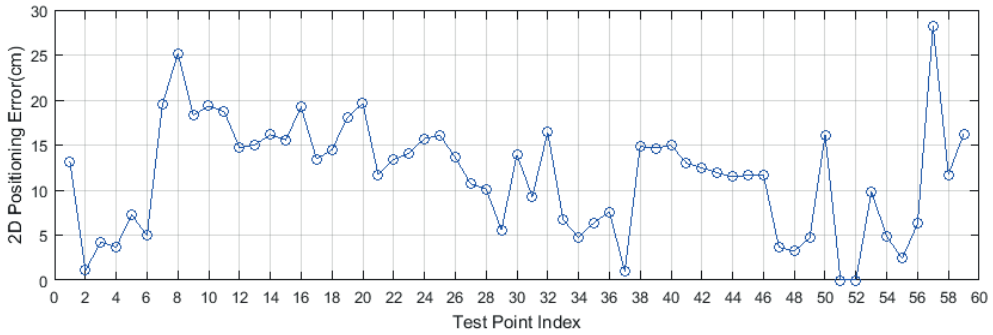

Figure 4.13 LOS positioning error vs. TPs of the UWB IPS

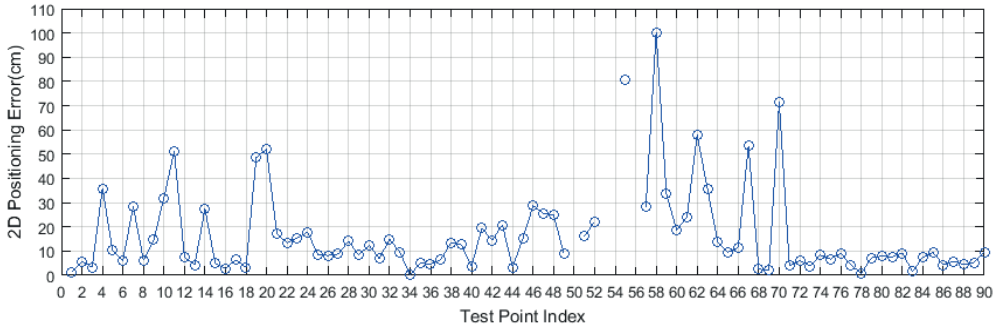

Figure 4.14 NLOS positioning error vs. TPs of the UWB IPS

From what has been presented so far, we know how the positioning error distributed and how the values relate to TPs in both a graphic and numerical way. However, we still have no clear clue about the detailed behaviour of different TPs and especially the NLOS scenario require further investigation. For instance, we can see from positioning error versus TP plots in Figure 4.13 and Figure 4.14, there are sharp peaks at TP8 and TP57 for LOS case and TP55, TP58, TP62, TP67

and TP70 for NLOS scenario. But the root cause of these peaks is not clear from all presented positioning error results so far.

As already mentioned, the positioning estimation works by using trilateration algorithm based on measured range results for this UWB IPS. The trilateration algorithm itself could affect the estimation result somehow but the basis is the accuracy of the measured range. In other words, the result of measured range affect the positioning result directly. Hence, it is interesting to see the measured range results from the UWB IPS.

4.5.3.2 Range Error

As coordinates of all RPs and TPs are recorded and known, the true ranges from all three Anchors to Tag at any TP can be given via Equation (4.2). Based on the measured range, then the range error can be calculated according to Equation (4.3). We calculated range error for all measured TPs in the sports hall and office evaluation area for the UWB IPS.

Figure 4.15 and Figure 4.16 illustrate the distribution of range error from the sports hall and office.

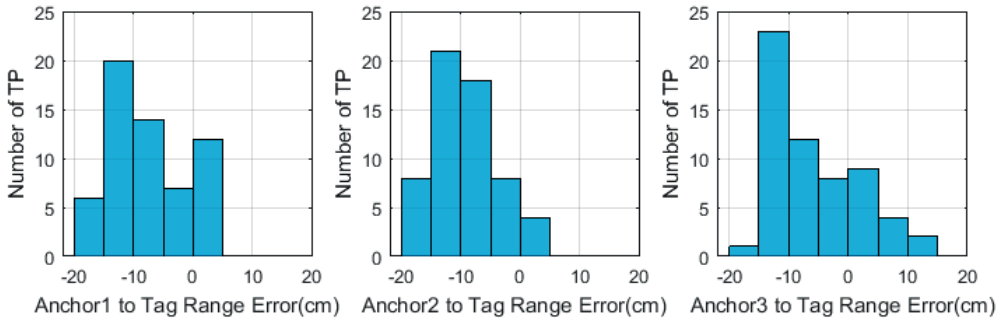

Figure 4.15 LOS range error distribution of the UWB IPS

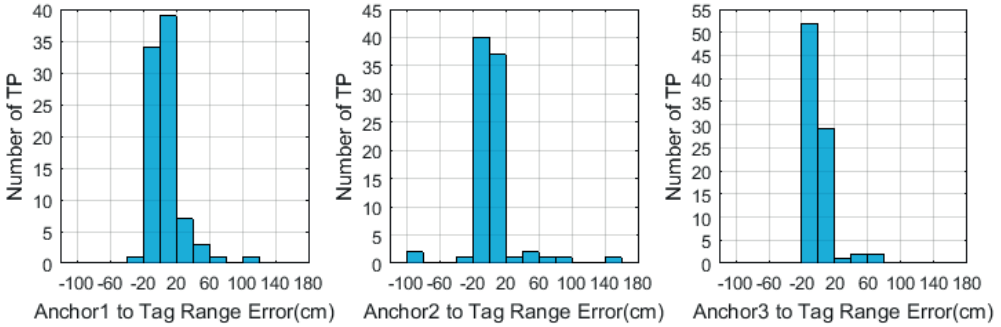

Figure 4.16 NLOS range error distribution of the UWB IPS

It is easy to see from the distributions that all range errors of the three Anchors to Tag are within 20 cm for LOS scenario while for NLOS scenario majority of the range errors are within 20 cm but few range errors are bigger than 20 cm. It is worth to mention in LOS case most points have negative range errors which means their measured ranges are smaller than corresponding true ranges according to the range error definition. However, this is not always true for NLOS case. For NLOS case, the bigger range errors are mainly positive values which means their measured ranges are bigger than their corresponding true ranges.

Moreover, the range error plus the true range of all TPs from all three Anchors to tag are plotted in Figure 4.17 and Figure 4.18 for LOS and NLOS scenario respectively.

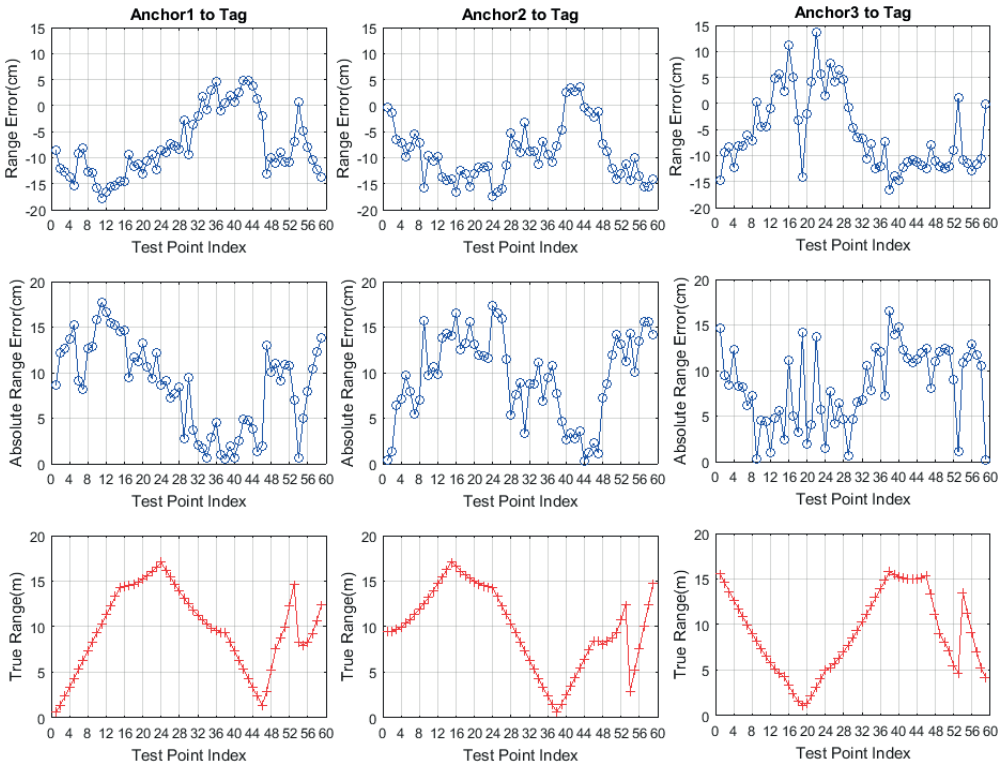

Figure 4.17 LOS range error and true distance vs. TPs of the UWB IPS

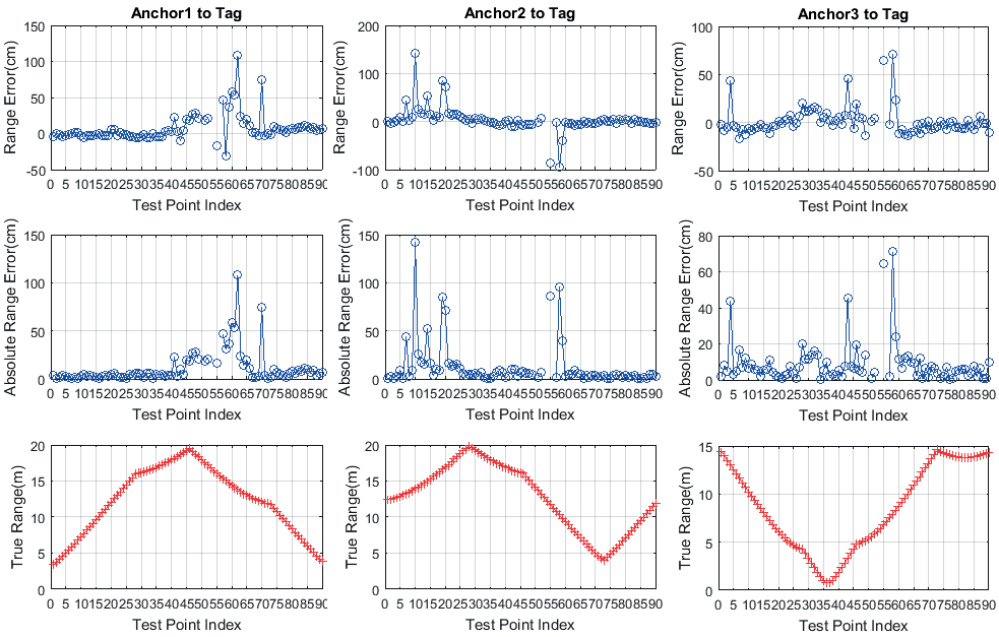

Figure 4.18 NLOS range error and true distance vs. TPs of the UWB IPS

Now it can be observed clearly from Figure 4.17 and Figure 4.18 that the sharp peaks shown in positioning error plots are due to the presence of big range error from at least one anchor to the tag. For example, those mentioned TPs, TP8 and TP57, presenting peaks in LOS positioning error plot, have at least a high range error from anchor 1 to the tag and anchor 2 to the tag respectively. Similarly, TP55, TP58, TP62, TP67 and TP70, showing peaks in NLOS positioning error plot, have at least one big range error except for TP67. TP 55 has at least the big range error from anchor 3 to the tag, TP58 and TP55 have big range error from anchor 2 to the tag and TP62 and TP70 have big range errors from anchor 1 to the tag. TP67, as an exception, has quite small range error from all three anchors to the tag. Its big positioning error is mainly due to inaccurate estimation by the positioning algorithm as we can see from the intersection result of its three circles shown in Figure 4.12.

For LOS scenario, few more conclusions can be drawn from Figure 4.17. Firstly, according to the absolute range error plots, all the three absolute range error curves basically fluctuate with the trend of true distances excluding exceptions at few points, which means in LOS situation, distance is the main cause of range error for this UWB IPS. With distance increasing range error grows and with distance decreasing the range error becomes smaller. Secondly, it shows in Figure 4.17 that the range error at all TPs is below 20 cm which means the range error mainly caused by distance is less than 20 cm within 20 m true distance for this UWB IPS. Last but not least, in the range error plots, we see that most range errors are negative values, which means the measured range is smaller than corresponding true range when distance is the main cause of this UWB IPS.

However, the conclusion drawn in LOS case is not completely reflected in Figure 4.18 for NLOS scenario. For NLOS scenario, we can see that the big range errors usually occur where relatively long true distances are measured. For instance, the big range error areas between TP41 and TP63 in the Anchor1 to Tag absolute range error plot and between TP7 and TP25 in the Anchor2 to Tag absolute range error plot are mapped to a region where relatively long true distances are measured as seen in the true distance plots. And it is not obviously visible that the range error changes with the trend of true distance like we saw in LOS scenario. In addition, based on LOS result we know that the range error caused by true distance is below 20 cm, so there must be some other factors affecting range estimation except true distance. This is understandable as the NLOS environment is much more complicated and thus results in more impacts on the IPS' performance.

It is necessary to do some further analysis in order to understand the causes of range error in office evaluation area for this UWB IPS. As we know the center frequency of the UWB signal for the evaluated UWB IPS is 6489.6 MHz and the wavelength of the signal is about 4.6 cm which means an obstacle with dimension comparable to 4.6 cm could have influence on the UWB signal propagation. Based on this basic rule, all the listed main obstacles in Table 4.1 may affect the UWB signal.

Keeping this basic principle in mind, now let us first have a look at those already mentioned 4 TPs, TP50, TP53, TP54 and TP56, at which we couldn't get estimated positions. We did the investigation for these four positions by repeating the test at these points. The symptom is repeatable and thus we are able to discover there was no range measurement result from Anchor 1 to these points at all but there were ranging results from Anchor2 and Anchor3 to these points showing on the on-board display of the Tag EVB1000 board, which means the communication link between Anchor 1 and these points was not established at all. Anchor 1 is the master Anchor responsible for exchanging information with Tag, estimating position and reporting results. That's why we couldn't get any data from logs at these points. From Figure 4.18, we can see the true distance from these TPs to Anchor 1 is around 18 m. On the other hand, according to Table 4.2, there are meeting rooms, metal writing boards and cement pillar between these points to Anchor 1 which could affect the UWB signal. Such a far true distance plus poor communication condition may make the UWB signal not go through and thus the communication link cannot be established.

Except those 4 TPs, TP50, TP53, TP54 and TP56, at which we couldn't get estimated positions, the peak area in the range error plots are also interesting. The peak area of range error between Anchor 1 and Tag occurs from TP41 to TP63 according to Figure 4.18. Consulting Table 4.2, these points locate in the areas which have lot of obstacles between them and Anchor 1. Same for the range error from Anchor 2 to Tag, the range error plot from Anchor 2 to Tag has a peak area between TP7 and TP25 and the Table 4.2 shows these TPs have at least one obstacle from them to Anchor 2. The range error from Anchor 3 to Tag has no obvious peak area instead there are only few peak points in the plot. They are TP4, TP43, TP58 and TP59. Except for TP43, we can see there are obstacles between TP4, TP58, TP59 and Anchor 3.

In addition, we can see most range errors are positive values, especially in the area that obstacles exist. This is probably due to NLOS propagation. When the direct LOS between the Anchors and Tag is blocked, only reflections of the UWB signals from obstacles reach the receiver. Therefore,

the time of the first arriving signal does not represent the true distance, resulting in longer estimated distance and positive range error.

Last but not least, the range error can be as large as 1.5 m when there is NLOS, which is much bigger than the error due to distance.

Based on all the analysis, we can draw the conclusion that for this UWB IPS, in LOS scenarios, distance is the main factor affecting the positioning accuracy of the system while, in NLOS scenario, both distance and obstacles in the communication environment play a significant role on the performance of the UWB IPS. Obstacles usually cause bigger range errors than errors caused by distance and give longer measured ranges than their corresponding true ranges.

4.6 Evaluation of WiFi-based IPS

4.6.1 WiFi Anchors and Tag

The WiFi anchors and tag we evaluated are Nexus 6 mobile phones from Motorola as shown in Figure 4.19. This mobile phone integrates Broadcom's 5G WiFi (802.11ac) BCM43462 system-on-chip (SoC), featuring AccuLocate indoor positioning technology which enables TOA ranging based on WiFi technology.

Figure 4.19 Motorola Nexus 6 used for the WiFi IPS

4.6.2 WiFi IPS System Setup and Configuration

The WiFi-based IPS was deployed separately in the sports hall and office area to evaluate both LOS and NLOS scenarios. For both scenarios, the system has the similar setup with placing three Motorola Nexus 6 phones at the RP 1, 2 and 3 as anchors and one Motorola Nexus 6 phone at predefined TP as tag. The configurations of the WiFi Anchors and Tag are shown in Table 4.9.

Role	Center Frequency	Bandwidth
Anchor	5220 MHz	80 MHz
Tag	5220 MHz	80 MHz

Table 4.9 Configurations of the WiFi IPS

During our evaluation, all anchors were kept at the known reference positions while the tag, which acted as target object, was placed at predefined TPs while connected to a computer through USB cable to run a pre-programmed application software for measuring range and reporting measured results.

Both the tag and anchors are powered on by internal batteries. At each TP, the Tag initiated the range measurement and waited for the pre-programmed application software estimating ranges from all three anchors to it. The Tag was kept stationary at each TP and waited for until about 70 set of measurement samples were collected for LOS case and 100 set of measurement samples collected for NLOS scenario and then was moved to the next TP. This procedure was repeated over 59 predefined TPs in the sports hall and 46 TPs in office for this WiFi IPS. For each TP, ranges from all three anchors to tag were calculated respectively by averaging collected samples from corresponding anchors to tag. This WiFi IPS measures and calculates distance based on TOA and then reports both the measured TOA and range.

4.6.3 Evaluation Result and Analysis

This section presents evaluation results including positioning error and range error for both LOS and NLOS scenarios from the evaluated WiFi IPS. Thorough analysis of the given results is also provided in this section.

4.6.3.1 Positioning Error

The positioning results are derived by computing the coordinates through the trilateration algorithm introduced in section 4.3 based on the collected range measurement results from the WiFi IPS. The positioning error is given as the Euclidean distance of the estimated position and its true position. 2D positioning error is calculated according to Equation (4.1) and 3D positioning error is derived through Equation (4.2).

The 2D and 3D positioning error distribution from WiFi IPS for both LOS and NLOS scenarios are presented in Figure 4.20 and Figure 4.21.

It is obvious to see from Figure 4.20 that for LOS scenario in 2D the positioning error of most TPs are distributed within 1 m and the positioning error of the rest 12 out of 59 points spreads between 1 m and 2.4 m with one exception that has about 4.8 m positioning error. 3D positioning results are mainly divided into two groups. One group distributes between 20 cm and 1.4 m while the range of the other positioning error group is from 1.6 m to 2.4 m. There are 5 points which even have positioning errors greater than 2.4 m.

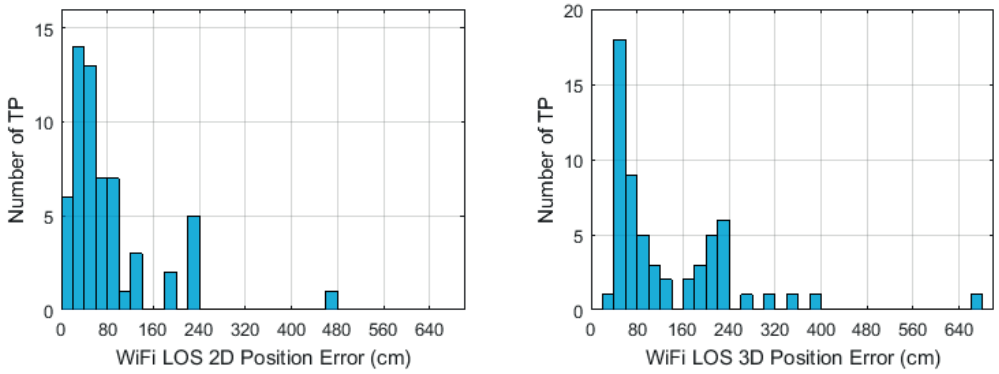

Figure 4.20 LOS positioning error distribution of the WiFi IPS

The positioning result from NLOS scenario is worse than that from LOS. According to the positioning error distribution in Figure 4.21, the majority of NLOS positioning error is within 2.8 m and the few remaining positioning errors are widely distributed up to 6.4 m. When it comes to 3D positioning error, the distribution spreads widely up to around 7.2 m with a considerable part being within 4.4 m.

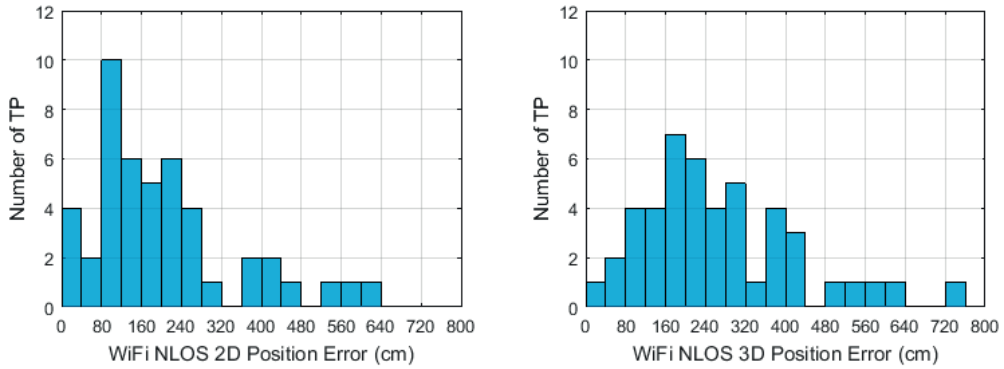

Figure 4.21 NLOS positioning error distribution of the WiFi IPS

Same as for the UWB IPS, in the rest of this section, we will mainly discuss 2D positioning error for the WiFi IPS.

To be able to have a clear picture on the estimated positions relative to their true positions, the anchors and the evaluation areas; we plotted the estimated positions as blue plus signs together with their true positions as black dots and three anchors as blue triangles in a 2D Cartesian coordinate system scaled according to the real size of the evaluation areas in Figure 4.22 and Figure 4.23 for LOS and NLOS scenario separately.

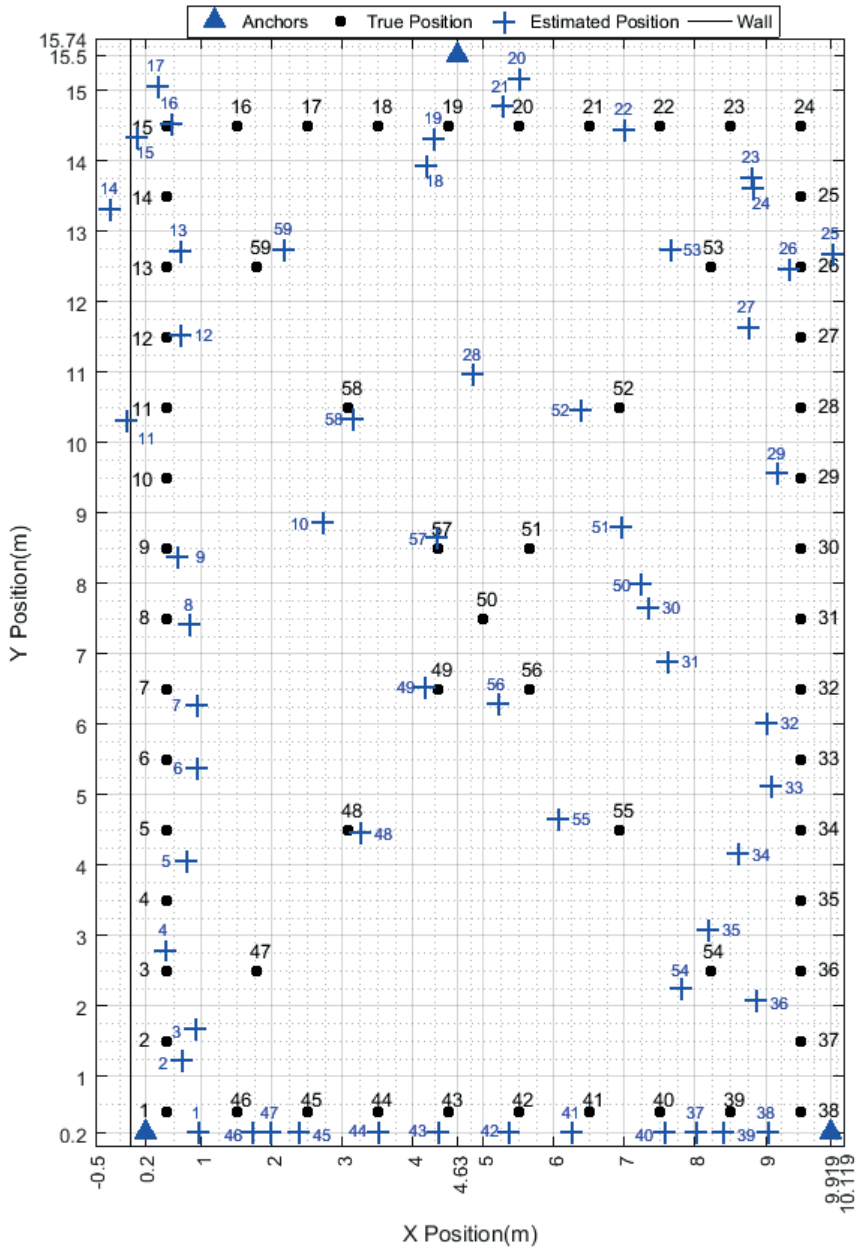

Figure 4.22 LOS estimated positions of the WiFi IPS

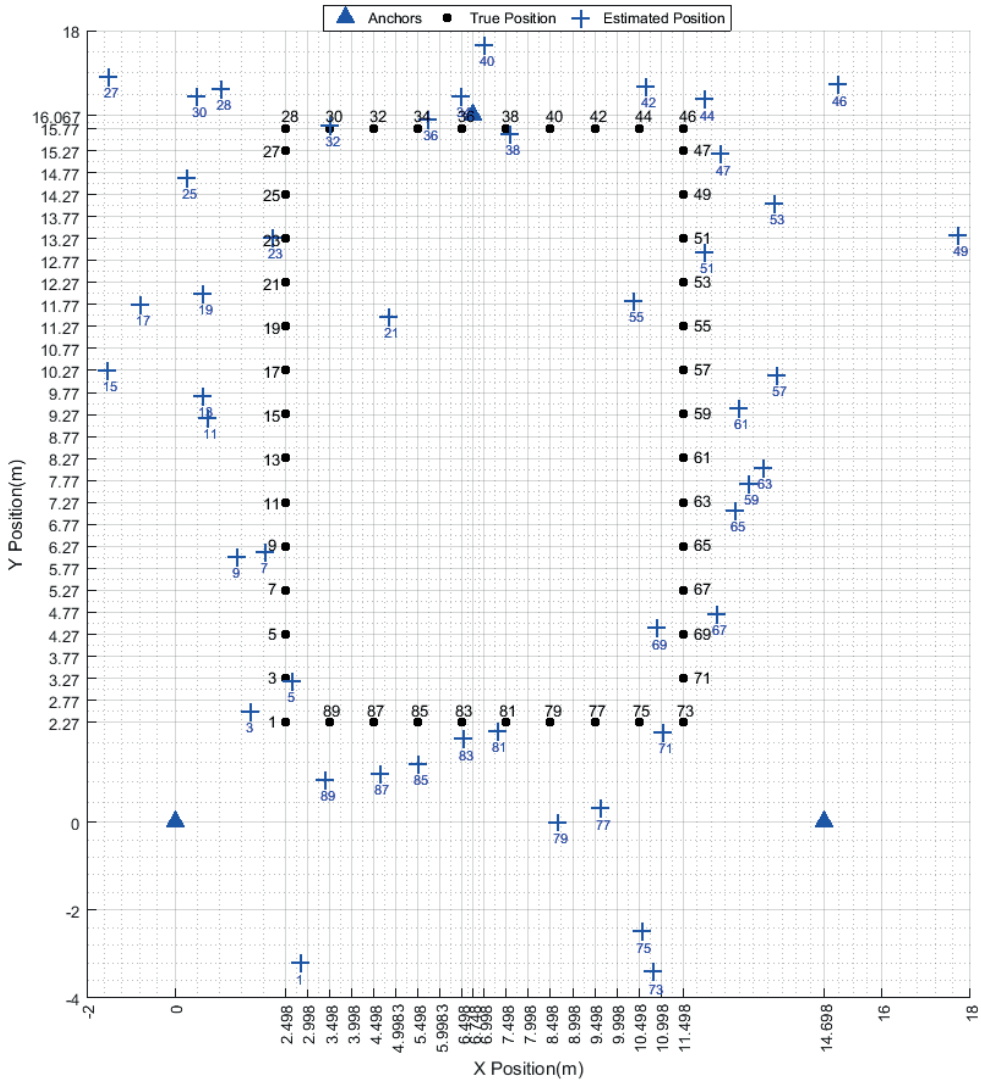

Figure 4.23 NLOS estimated positions of the UWB IPS

In addition, in Figure 4.24 and Figure 4.25 we can numerically inspect the 2D positioning error at each test point through the positioning error plot versus all TPs for both LOS and NLOS scenarios. For LOS case, we can see from positioning error versus TP plots in Figure 4.24, the highest peak is at TP28 with the positioning error of around 4.8 m and the biggest errors occur at TP1, TP49 and TP73 with values greater than 5.5 m for NLOS.

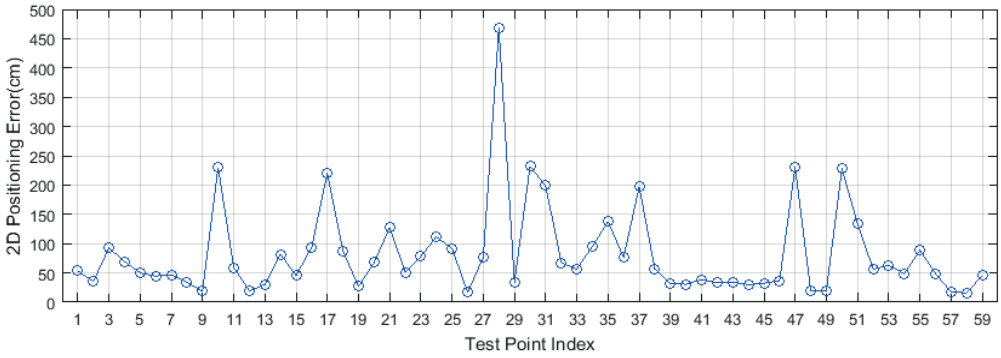

Figure 4.24 LOS positioning error vs. TPs of the WiFi IPS

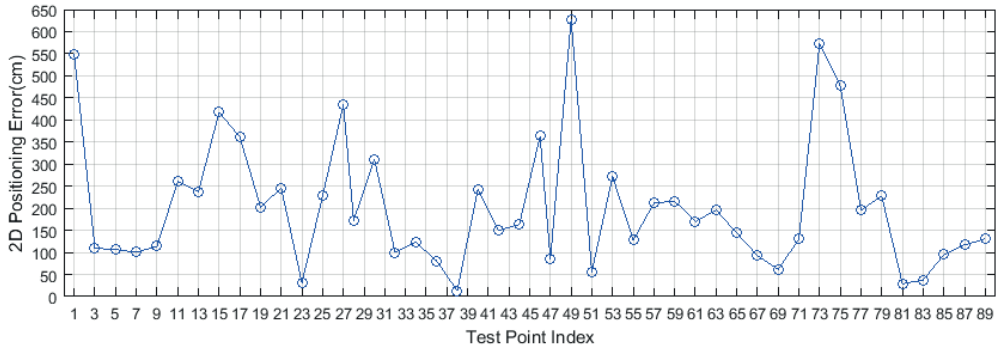

Figure 4.25 NLOS positioning error vs. TPs of the WiFi IPS

The measured range results from this WiFi IPS will be given in the following section for further analysis for the accuracy performance of this IPS.

4.6.3.2 Range Error

As coordinates of all RPs and TPs are recorded and known, the true ranges from all three anchors to tag can be given via Equation (4.2). Based on the measured range, then the range error can be calculated according to Equation (4.3). We calculated range error for all measured TPs in the sports hall and office evaluation area for the WiFi IPS.

Figure 4.26 and Figure 4.27 illustrate the distribution of range error for the sports hall and office. It is easy to see the distributions of all range errors from all three anchors to tag are within 50 cm for LOS scenario while for NLOS scenario majority of the range errors are within 1 m and the rest range errors widely spread up to 8 m. It is worth to mention in LOS case there are more points that have negative range errors, which means the measured ranges are smaller than corresponding true ranges according to the range error definition. However, this is not true for

NLOS case. For NLOS case there are more positive range errors and the bigger range errors are all positive values as well which means in NLOS scenario this IPS measured ranges greater than the true range more frequently.

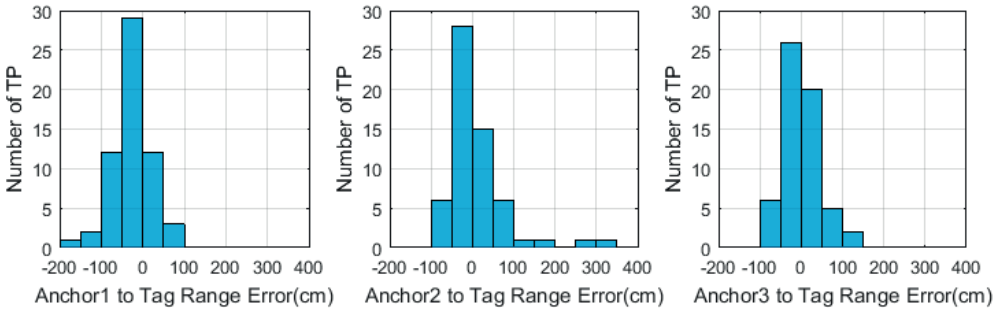

Figure 4.26 LOS range error distribution of the WiFi IPS

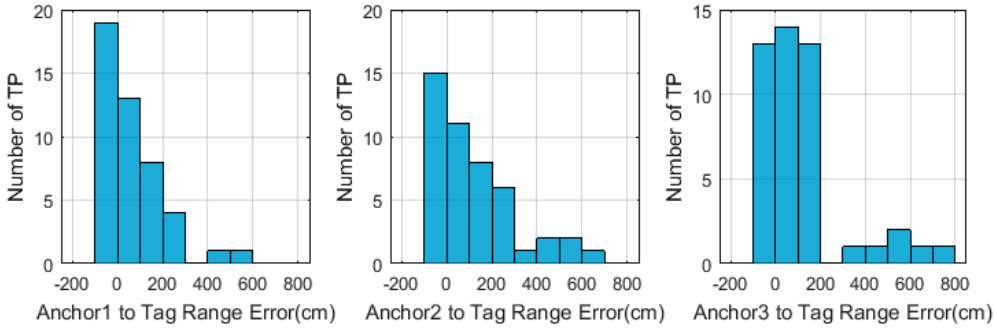

Figure 4.27 NLOS range error distribution of the WiFi IPS

Moreover, the absolute range errors plus the true ranges of all TPs from all three Anchors to tag are plotted in Figure 4.28 and Figure 4.30 for LOS and NLOS scenarios respectively.

In Figure 4.28 for LOS scenario, the range error curves do not show obvious tendency to change with true distances like the range error curves of UWB IPS do in LOS scenario. However, we noticed that the range errors are relatively bigger at those TPs located at the right side of the anchor phones or under the anchor phones. Based on the conclusion drawn from the orientation test result with the WiFi hardware units in section 4.4.3, that the WiFi hardware units have best radiation from their back and left sides, the potential influence on range error could be the antenna directivity. The approximate deployment orientations of the WiFi anchors are depicted as green markers in Figure 4.29. The bigger range errors shown in Figure 4.28 are mainly at TPs between TP28 and TP47 from anchor 1 to the tag, between TP17 and TP35 from anchor 2 to the tag and between TP3 and TP25 from anchor 3 to the tag. These points basically are located either at the

right sides of the anchor phones or under the anchor phones, where the antennas have the least directivity.

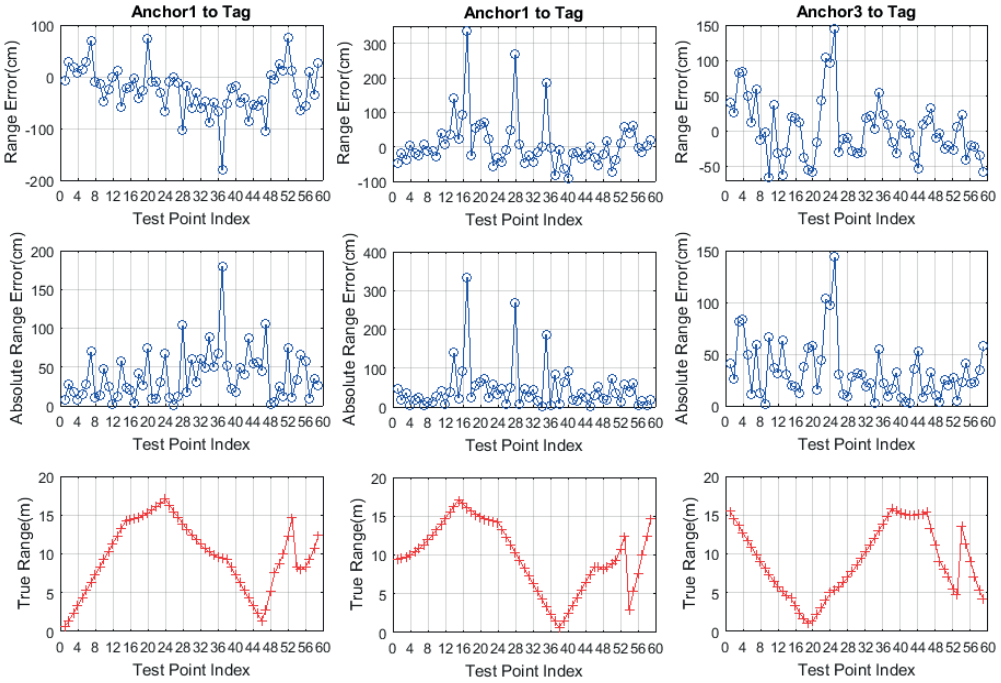

Figure 4.28 LOS range error and true distance vs. TPs of the WiFi IPS

In NLOS scenario, Figure 4.30 shows that most of the sharp peaks shown as green circles on the absolute range error curves locate in relatively big true distance areas. In addition, the peak areas on range error curves from all three Anchors to Tag look quite similar to those shown on UWB range error curves. Base on the experience from UWB IPS, we compared the wavelength of the WiFi signal with the dimension of the obstacles in Table 4.1. As we knew the center frequency of the WiFi signals is 5220 MHz and the wavelength of the signal is about 5.7 cm which means an obstacle with dimensions comparable to 5.7 cm could have influence on propagation of the WiFi signals. Based on this basic rule, all the listed main obstacles in Table 4.1 may affect the WiFi signal.

The peak values of range error between Anchor 1 and Tag occurs from TP42 to TP63 according to Figure 4.30. Looking these points up in Table 4.2, these points are located in the area, which has lot of obstacles blocking LOS to Anchor 1. For the range error from Anchor 2 to Tag, the peak values of range error occurs betweenTP15 and TP30 and the Table 4.2 shows that these TPs have at least one obstacle between them and Anchor 2. The range error from Anchor 3 to Tag has no obvious peak area, instead there are only few peak points in the plot. They are TP1, TP49 TP 75 and TP79. Except for TP43, there are obstacles between TP4, TP49, TP 75, TP79 and

Anchor 3. However, the range errors caused by obstacles in WiFi IPS are much bigger than the range errors resulted by obstacles in UWB IPS. In UWB IPS, the peak errors were smaller than 1.5 m while in WiFi IPS this error can be as high as 7 m.

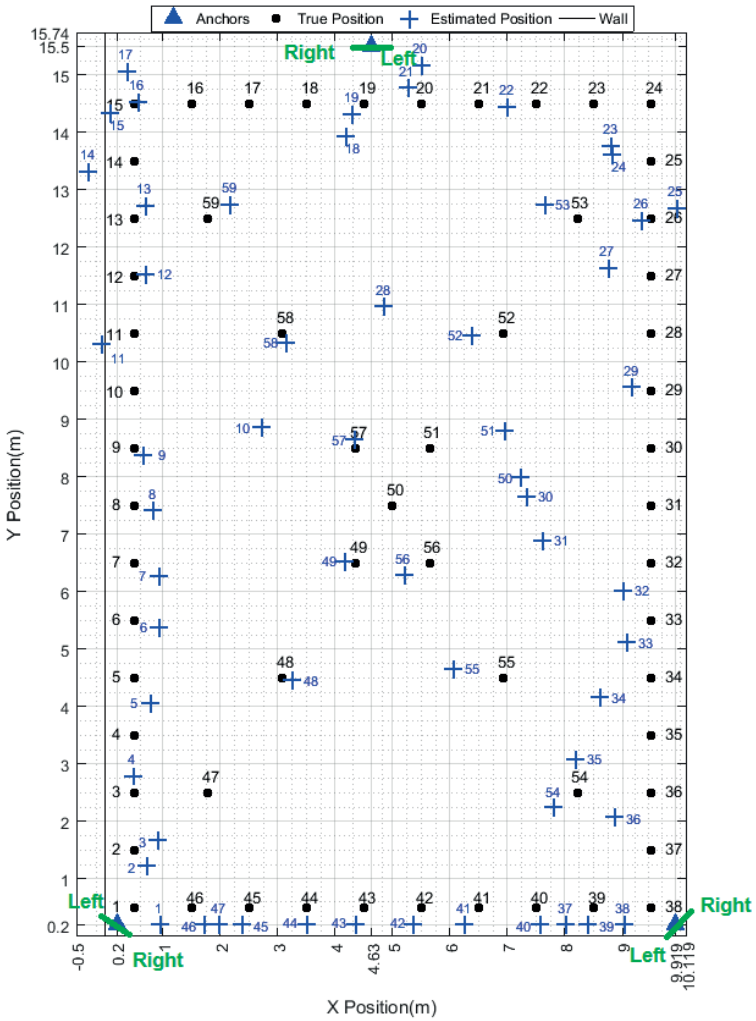

Figure 4.29 LOS anchors deployment orientation of the WiFi IPS

In addition, we can see most range errors are positive values especially in the area that obstacles exists. This is probably due to NLOS propagation. When the direct LOS between the Anchors and Tag is blocked, only reflections of the WiFi signals from obstacles reach the receiver. Therefore,

the time of the first arriving signal does not represent the true distance and the longer travelled distance results in positive range error.

Last but not least, the range error can be as large as around 7 m when NLOS propagation exists, which is much bigger than the range error due to distance as we can see in figure 4.28.

Based on all the analysis, we can draw the conclusion that, in LOS scenario, distance is the main factor affecting the positioning accuracy, while in NLOS scenario, both distance and obstacles in the communication environment play a significant role on the performance of the of the WiFi IPS. When the true distance is big and obstacles exist, the range error could be very big.

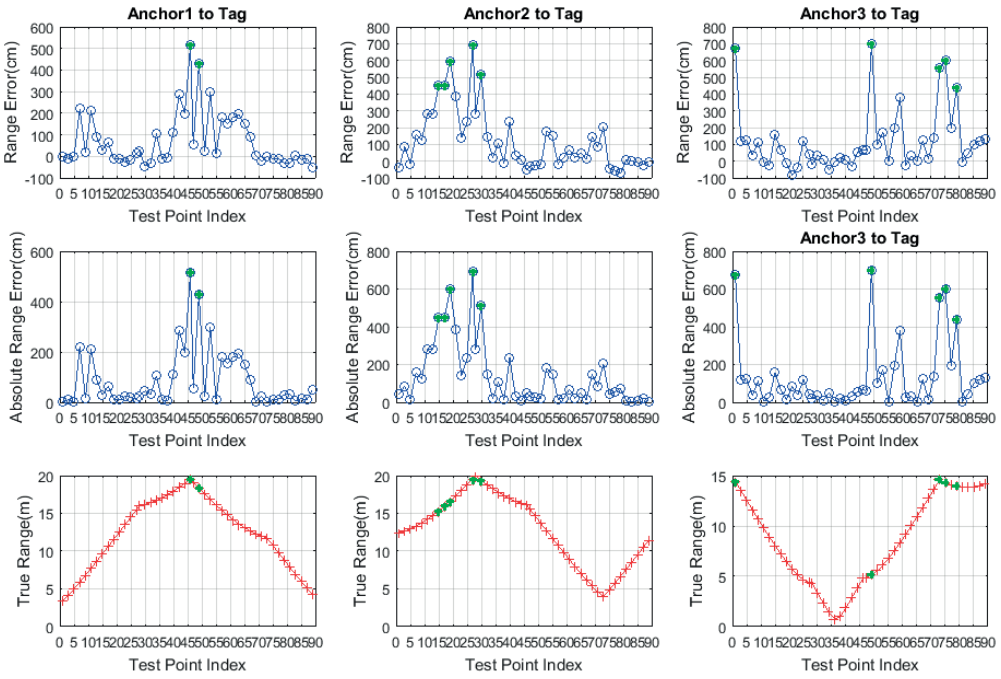

Figure 4.30 NLOS range error and true distance vs. TPs of the WiFi IPS

4.7 Evaluation of BLE-based IPS

4.7.1 BLE Beacons and Mobile Device

The evaluated BLE beacons use Nordic Semiconductor nRF51822 chip which is an ultra-low power 2.4 GHz wireless System on Chip (SoC) supporting Bluetooth low energy. The Figure 4.31 represents the BLE beacon.

Figure 4.31 BLE beacon

4.7.2 BLE IPS System Setup and Configuration

The BLE-based IPS was deployed in the sports hall and office area to evaluate both LOS and NLOS scenarios. For both scenarios the system has the similar setup with placing three BLE Beacons at the RPs and one BLE MD at predefined TPs. The configurations of the BLE Beacons and MD are shown in Table 4.10.

Role	Frequency	RSSI Resolution
Beacons	2.4 GHz	1 dB
Mobile Device (MD)	2.4 GHz	1dB

Table 4.10 Configurations of the BLE IPS

During evaluation, all BLE Beacons were kept at the known reference positions while the MD acted as target object was placed at predefined TPs while connected to a computer through USB cable to run a pre-programmed application software for measuring range and reporting measured results. The Beacons were powered on by internal Batteries and the MD was powered on by the connected computer via USB cable. The MD was placed at each TP and kept for the pre-programmed application software to measure RSS from all three Beacons to it. The MD was

moved to the next TP until 200 set of measurement samples were collected as per plan. This procedure was repeated over 32 predefined TPs in the sports hall and 44 TPs in the office.

4.7.3 RSS Propagation Model

As the collected RSS samples do not reflect distance directly, a propagation model to setup a relationship between RSS and distance is needed for this BLE IPS. We therefore carried out experiments to set up a propagation model according to the power law introduced in section 3.1.2. We compared three propagation models from three experiments with different setup and chose the best propagation model which gives most accurate position estimation. The experiments and results of all these three models are explained as below.

Experiment I: The experiment was carried out in an office area that has similar structure, same construction materials and locates at the same floor with the office evaluation area introduced in Section 4.2. But this office area is quite empty. There are several cerement pillars, metal pillars and meeting rooms in the room but there is no other obstacles in the area. During the experiment, a BLE Beacon was placed at a fixed position with its antenna height from the floor set to 2.355 m and the BLE MD antenna height set to 1.735 m was placed a fixed distance away from the BLE Beacon.

Experiment II: The experiment was carried out in the empty sports hall as described in Section 4.2. During the experiment, a BLE Beacon and a BLE MD were placed at same height approximately 0.23 m from antenna to floor and they are kept a fixed distance away from each other.

Experiment III: The experiment was carried out in the same sports hall as Experiment II. But this time the BLE Beacon and MD were placed at different heights. The BLE Beacon was placed at one of the corners in the room with its antenna height from the floor set to 2.13 m while the BLE MD antenna height set to 1.735 m was placed a fixed distance away from the BLE Beacon.

There is no obstacle between the LOS of the BLE Beacon and BLE MD during all these three experiments. In the experiments the BLE MD was connected to a computer and kept at the specific known position until 200 RSS samples were collected and then moved to a new position. This procedure was repeated for collecting more data at different positions. After the experiments were done, by averaging 200 collected values, the RSS values at all measured positions were calculated and then based on the calculated RSS values, a propagation model was set up according to the power law introduced in section 3.1.2. The parameters of A and n in Equation (3.9) were given by using polynomial curve fitting and they are shown in Table 4.11 for all three experiments.

Parameters	Experiment I	Experiment II	Experiment III
A (dBm)	- 41.9604	- 42.9768	- 44.1105
n	1.5731	2.1636	1.5607

Table 4.11 Parameter values of RSS propagation model from different experiments

Based on the propagation model, given a measured RSS from a BLE Beacon to the MD, the corresponding distance between BLE Beacon to the MD can be estimated according to Equation (3.9).

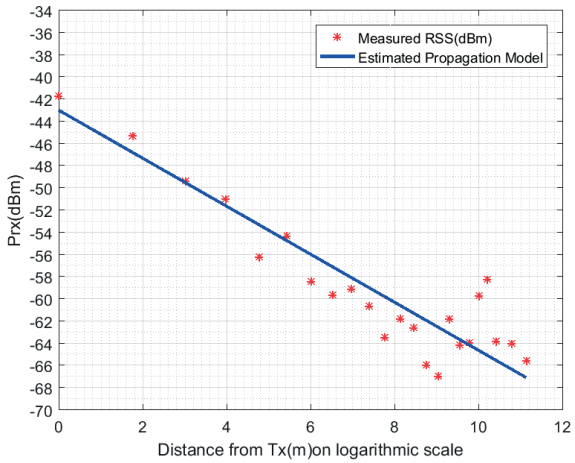

(a) On log logarithmic scale

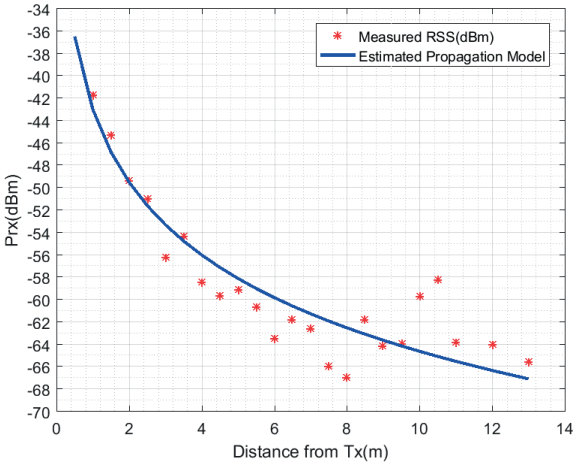

(b) On linear scale

Figure 4.32 RSS propagation over distance from experiment II for the BLE IPS

We have compared positioning results from these three different propagation models for both the sports hall for LOS scenario and office for NLOS scenario respectively and results show that the parameters from experiment II illustrated in Figure 4.32 are best for both LOS and NLOS cases. Therefore, the evaluation results from the BLE IPS presented in this thesis are obtained according to experiment II.

4.7.4 Evaluation Result and Analysis

This section presents evaluation results including positioning error and range error for both LOS and NLOS scenarios from the evaluated BLE IPS. Thorough analysis of the given results are also provided in this section.

4.7.4.1 Positioning Error

The positioning results were derived by computing the coordinates through the trilateration algorithm introduced in section 4.3 based on the collected range measurement results from the BLE IPS. The positioning error is given as the Euclidean distance of the estimated position and true position. 2D positioning error is calculated according to Equation (4.1) and 3D positioning error is derived from Equation (4.2). The positioning error distribution from BLE IPS for both LOS and NLOS scenarios are presented in Figure 4.33 and Figure 4.34.

It is obvious to see from Figure 4.33 that for LOS scenario the 2D and 3D positioning error show almost same distribution. This is because most of the 2D positioning errors are very big compared to the range errors of the 3rd dimension, which are always smaller than the height of the BLE beacons, around 2.2 m. Therefore, the contribution of the 3rd dimension to the 3D positioning errors is not obviously visible compared to the big 2D positioning errors.

In both 2D and 3D result, there are only 3 TPs have positioning error smaller than 1 m. The major error values distribute widely between 1 m and 8 m. 2 TPs have even bigger error around 9.5 m.

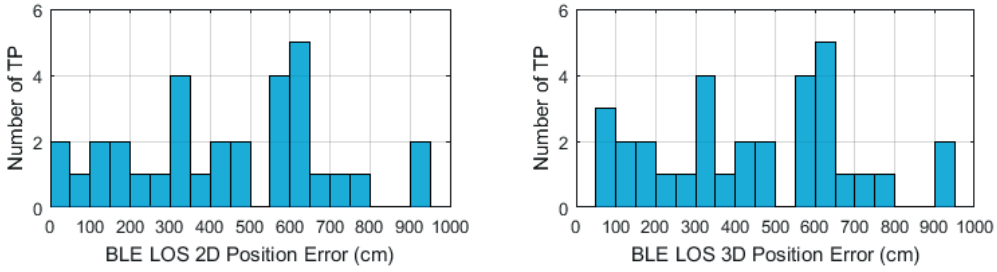

Figure 4.33 LOS positioning error distribution of the BLE IPS

The positioning error for NLOS scenario shows similar result as LOS case. The 2D and 3D positioning error distribution are quite alike and widely spread from 0.5 m to 8 m with majority between 3 m and 6.5 m. In addition, it is not obvious to see the NLOS results are worse than the LOS results for this IPS as observed in both UWB and WiFi systems.

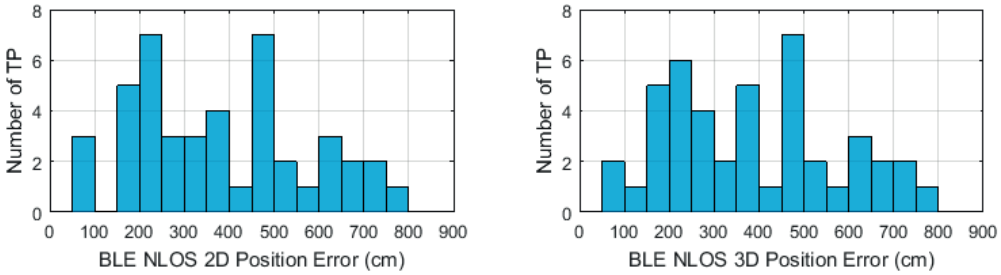

Figure 4.34 NLOS positioning error distribution of the BLE IPS

In the remaining of this section, we will mainly discuss 2D positioning error for this BLE IPS.

To be able to have a clear picture of the estimated positions relative to their true positions, the Beacons and the evaluation areas, we plotted the estimated positions as blue plus signs together with their true positions as black dots and three Beacons as blue triangles in a 2D Cartesian coordinate system scaled according to the real size of the evaluation areas in Figure 4.35 and Figure 4.36 for LOS and NLOS scenario separately.

In Figure 4.35 for LOS scenario, it is hard to match the estimated points with their true positions without markers due to the big errors. It is interesting to see the estimated points are mainly divided into two groups. One group locate in the middle of the room on the left while the other group are on one side of the room close to the wall. We plotted three circles formed by three measured ranges for one point of each group as shown in Figure 4.35. The green-solid-line circles are for TP49 on one side of the room close to the wall while pink-dot-line circles are for TP15 one the left side of the room. From the intersection status of these circles, the big positioning errors of TP15 is mainly caused by inaccurate measured ranges. For TP49 the estimation accuracy probably could be improved by positioning algorithm but still the root caused is the inaccurate measured ranges.

For NLOS scenario, it is almost not possible to match the estimated points with their true positions due to the big errors. And the estimated points are also divided into groups like in LOS case. In Figure 4.36, two groups located in the middle of the evaluation area while another group are on one side of the evaluation area close to Beacon1 and Beacon2. We plotted three circles formed by three measured ranges for one point of each group in Figure 4.36. The green-solid-line circles are for TP23 on the left side of the evaluation area. The pink-dotted-line circles are for TP38 on the right side of the evaluation area and the red-star-line circles are for TP68 one side of the evaluation area close to Beacon1 and Beacon2. According to the intersection status of these circles, the big positioning errors of TP23 and TP38 are mainly caused by inaccurate measured ranges. For TP68 the estimation accuracy probably could be improved by positioning algorithm but still the root caused is the inaccurate measured ranges.

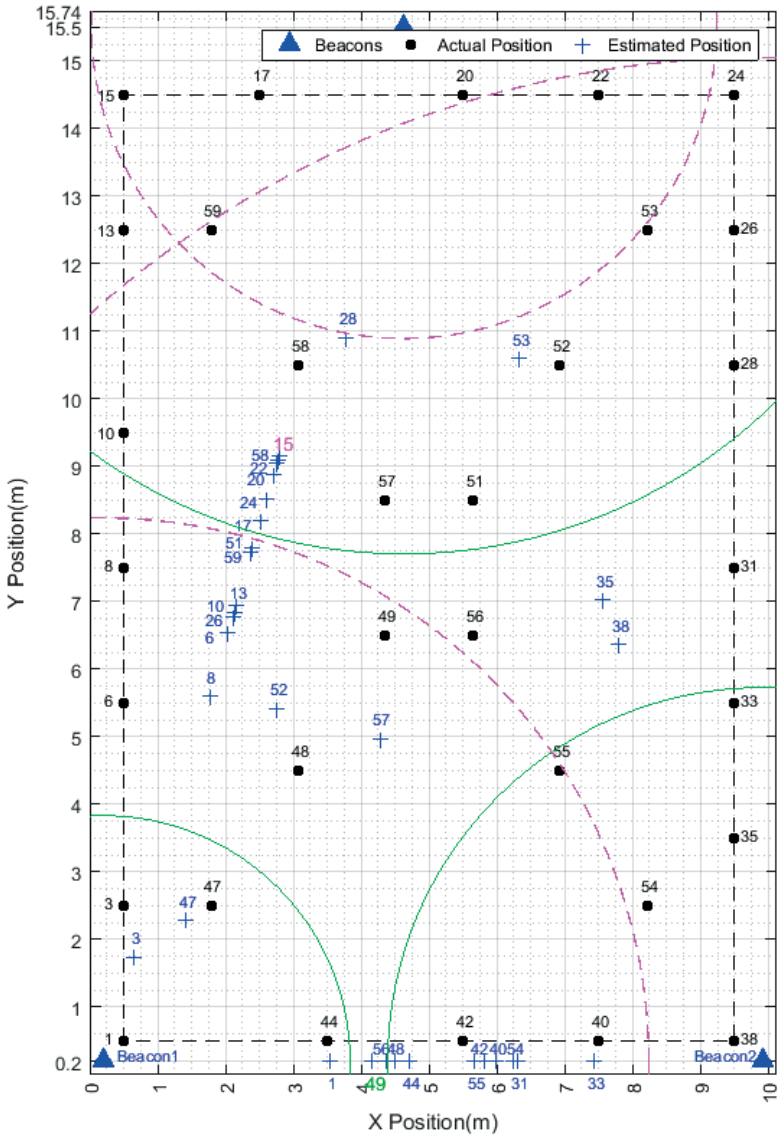

Figure 4.35 LOS estimated positions of the BLE IPS

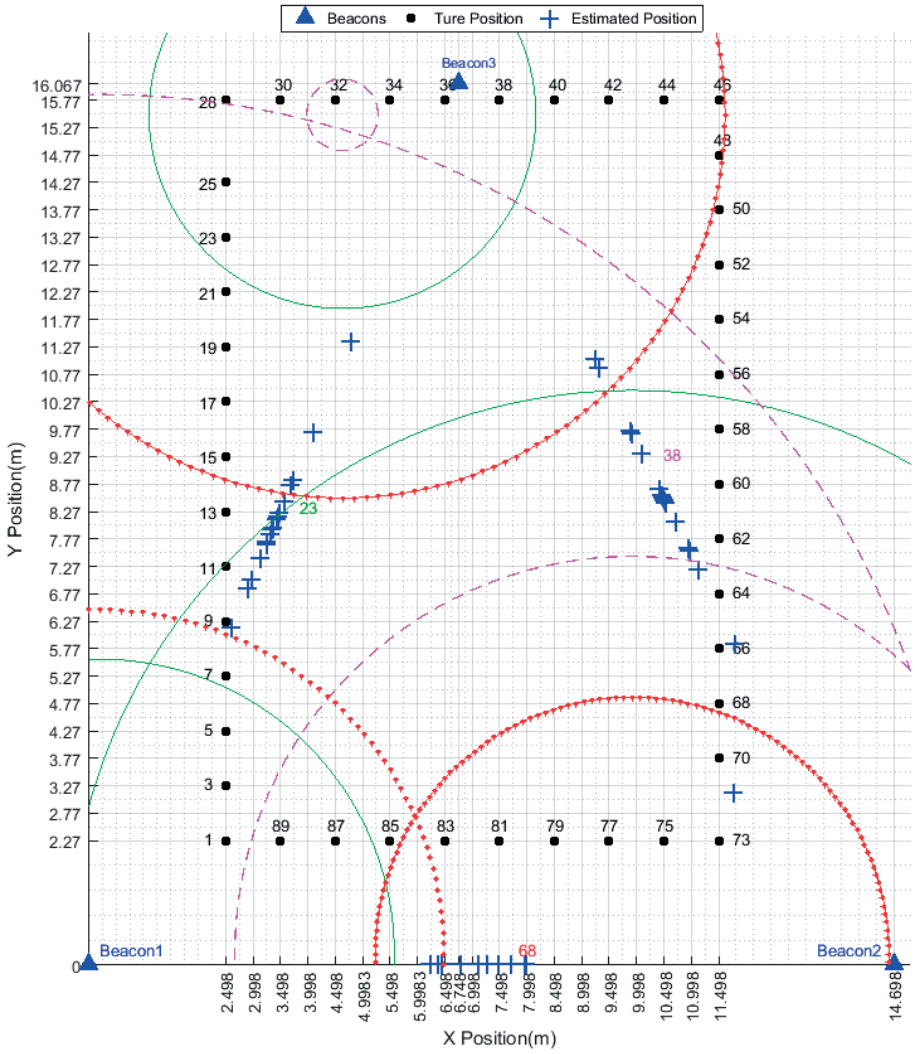

Figure 4.36 NLOS estimated positions of the BLE IPS

In addition, in Figure 4.37 and Figure 4.38 we can numerically inspect the 2D positioning error at each test point through the positioning error plots versus all TPs for both LOS and NLOS scenarios. Figure 4.37 shows the positioning error curve fluctuates between TP24 and TP38 and have a sharp peak around TP26 with positioning error around 9.5 m for LOS case. In NLOS scenario, the big positioning error occurs between TP30 and TP44 and highest value at TP30 with a value around 8 m.

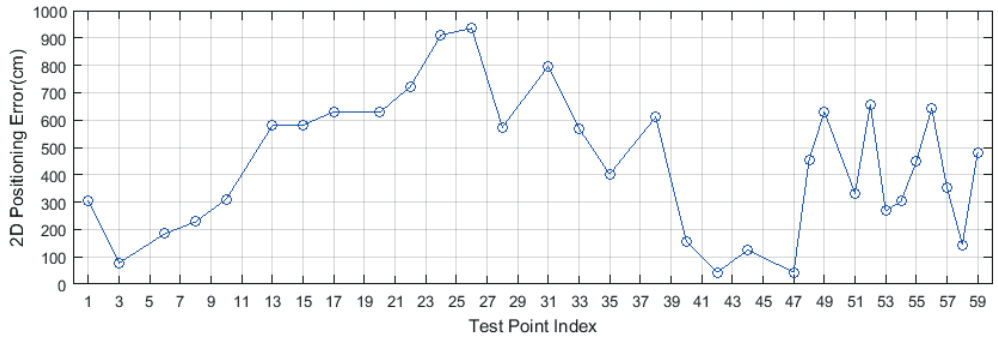

Figure 4.37 LOS positioning error vs. TPs of the BLE IPS

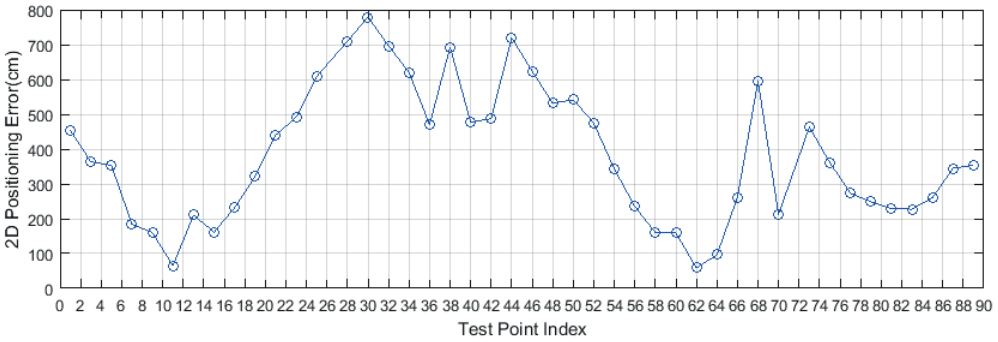

Figure 4.38 NLOS positioning error vs. TPs of the BLE IPS

In the following section, the measured range results from this BLE IPS will be illustrated and discussed in order to better understand the positioning accuracy of this system.

4.7.4.2 Range Error

As coordinates of all Beacons and TPs are recorded and known, the true ranges from all three Beacons to MD can be given via Equation (4.2). Based on the measured range, then the range error can be calculated according to Equation (4.3). We calculated range error for all measured TPs in the sports hall and office for the BLE IPS.

Figure 4.39 and Figure 4.40 illustrate the distribution of range errors from the sports hall and the office. It is easy to see the distributions of almost all the range errors from the three Beacons to MD are within 10 m and more than half of range errors are between 0 and 4 m in LOS scenario. NLOS range results are a little bit worse than LOS results and most errors are within 6 m. In addition, the range errors of this BLE IPS from both LOS and NLOS cases are more negative values, which means more than half of the measured ranges are smaller than corresponding true

ranges according to the definition of the range error and more measured RSS values are bigger than the values they should be according to the RSS propagation curve in Figure 4.32.

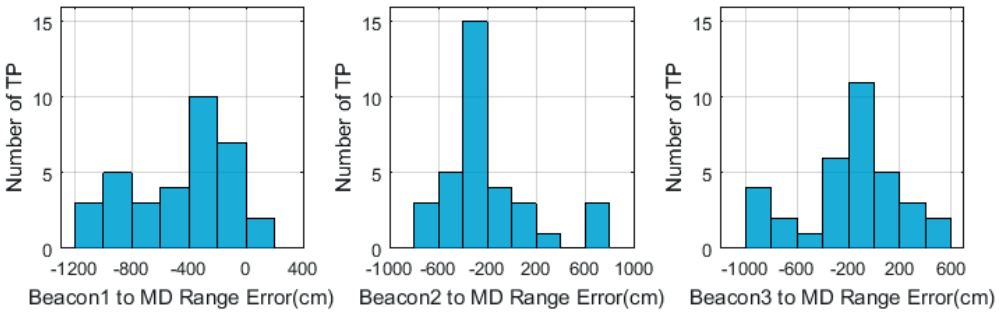

Figure 4.39 LOS range error distribution of the BLE IPS

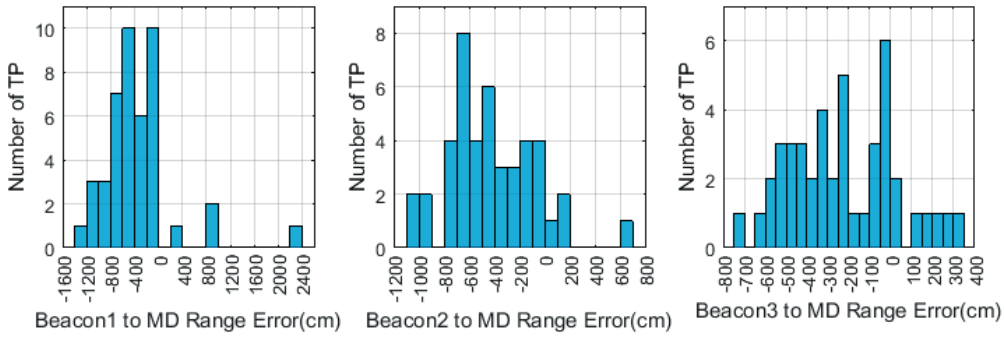

Figure 4.40 NLOS range error distribution of the BLE IPS

Moreover the range errors and the true ranges of all TPs from all three Beacons to MD are plotted in the Figure 4.41 and Figure 4.42 for LOS and NLOS scenarios respectively.

For LOS scenario, few conclusions can be drawn from Figure 4.41. First, from the absolute range error plots, all the three absolute range error curves basically fluctuate with the trend of true distances excluding exceptions at few points, which means in LOS situation distance is the main cause of range error for this BLE IPS. With distance increasing range error grows and with distance decreasing the range error becomes smaller as the propagation model in Figure 4.32 indicates. Secondly, the fluctuation of the absolute range error is very large, from about zero at a minimal true distance up to about 8 m or 10 m when true distance is about 16 m. Therefore, the impact of true distance on the range accuracy for this BLE IPS is significant. Last but not least, according to the range error plots, most of the range errors are negative values, which means most of the measured ranges are smaller than their corresponding true ranges. This potentially can be due to the improper propagation model used for the range estimation of the BLE system.

The propagation model used for the range estimation of the BLE system may not consider all propagation phenomena in the evaluated NLOS environment.

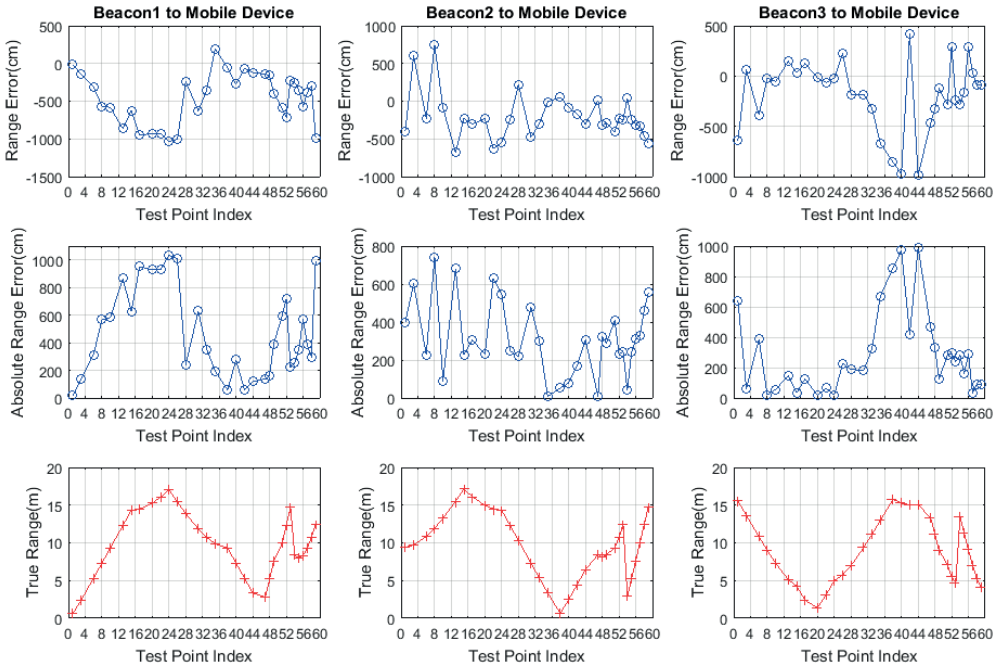

Figure 4.41 LOS range error and true distance vs. TPs of the BLE IPS

In Figure 4.42 for NLOS scenario, the absolute range errors almost follow the changes of the true distances like in LOS scenario. Same as LOS scenario, most of the range errors are negative values according to the range error plots which is also probably due to the improper propagation model used for the range estimation of the BLE system. The propagation model used for the range estimation of the BLE system may not consider all propagation phenomena in the evaluated NLOS environment. Moreover, the variance of the range error in NLOS case is a little bit worse than the variance of the range error from LOS scenario.

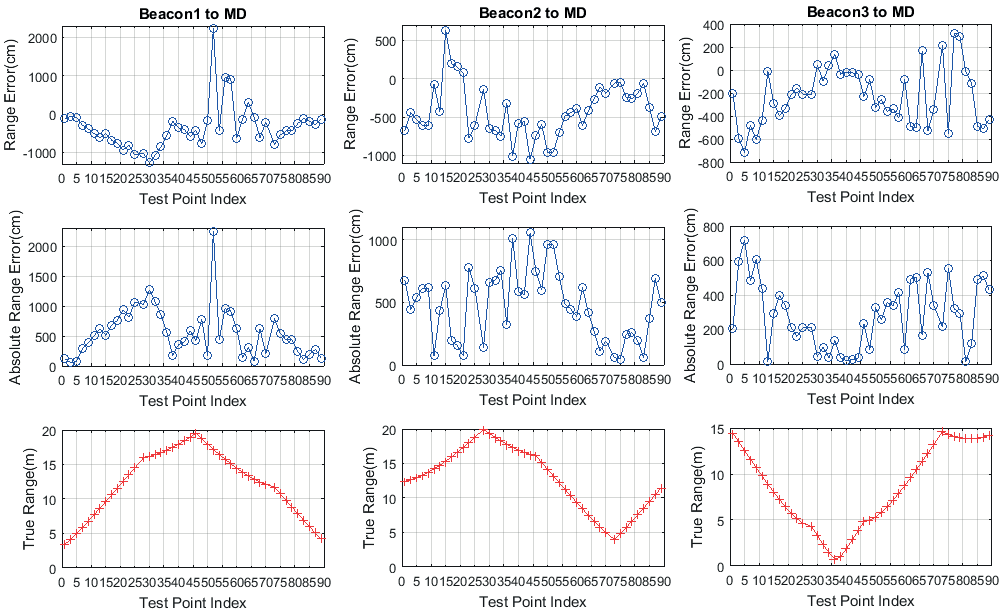

Figure 4.42 NLOS range error and true distance vs. TPs of the BLE IPS

Chapter 5 Comparison and Discussion

This chapter compares and discusses the performance of the three off-the-shelf UWB, WiFi and BLE hardware for indoor positioning purpose from the accuracy, power consumption, cost and ease of deployment point of view.

5.1 Accuracy

In order to compare accuracy of the three evaluated IPSs in this thesis, we introduce a term circular error probability (CEP) which is defined as percent of the estimated positions showing an absolute position or distance error less than a specific value. For instance, CEP50 means 50% of estimated positions, which show an absolute position or distance error, less than the corresponding given value in this section.

5.1.1 Positioning Error

In chapter 4, both 2D and 3D positioning error results of all evaluated positions for each evaluated IPS were presented and discussed, respectively. There, calculation of both 2D and 3D positioning error for each evaluated position for different IPSs was explained in detail. In this section, a comparison of both 2D and 3D positioning error for these three IPSs is given in Table 5.1 and Table 5.2 for LOS and NLOS separately. The 2D and 3D positioning errors in both tables are obtained by averaging positioning errors based on different CEP, in other words, different percent of evaluated positions, for each of evaluated IPSs.

As can be concluded from the Table 5.1 and Table 5.2, the positioning error differs significantly among these three IPSs. UWB IPS provides the most accurate position estimation while BLE IPS gives the worst positioning accuracy among these three systems and WiFi shows medium positioning accuracy. More specifically, the UWB IPS provides centimeter order 2D and 3D positioning accuracy for both LOS and NLOS scenarios. The WiFi IPS have around 70 cm 2D and 1.2 m 3D positioning error in LOS scenario and 1.8 m 2D and 2.5 m 3D positioning accuracy in NLOS scenario for CEP95 case. BLE IPS shows the worst positioning accuracy around 4.5 m but it can provide approximately 3 m accuracy if considering CEP68 for both LOS and NLOS scenarios.

LOS positioning error(cm) for different CEP												
Positioning	CEP50			CEP68			CEP95			CEP100		
Error	UWB	WiFi	BLE	UWB	WiFi	BLE	UWB	WiFi	BLE	UWB	WiFi	BLE
2D	7.6	34.8	232.8	9.2	42.9	316.5	11.7	70.2	409.3	14.7	82.4	441.4
3D	35.3	57.9	237.9	37.5	73.7	321.6	40.0	116.0	413.4	42.5	134.0	445.4

Table 5.1 LOS Positioning Error Comparison

NLOS positioning error(cm) for different CEP												
Positioning	CEP50			CEP68			CEP95			CEP100		
Error	UWB	WiFi	BLE	UWB	WiFi	BLE	UWB	WiFi	BLE	UWB	WiFi	BLE
2D	5.4	95.6	218.1	7.2	122.3	272.6	13.5	186.1	363.2	16.5	204.2	380.7
3D	25.0	152.8	228.5	35.3	182.8	281.4	46.2	251.3	370.4	49.4	269.8	387.8

Table 5.2 NLOS Positioning Error Comparison

It is necessary to mention that, in some cases, the positioning error of NLOS scenario in Table 5.2 is smaller than the corresponding positioning error for LOS scenario in Table 5.1, which may be due to the bigger number of evaluated test positions in NLOS than LOS and the potential existence of indoor propagation effects in the evaluation area.

5.1.2 Range Error

For a more equitable comparison mainly focusing on the hardware performance of these three evaluated IPSs and excluding the impact of positioning algorithm, a comparison of range error is shown in Table 5.3 and Table 5.4 for LOS and NLOS respectively. Calculation of range error for each evaluated position for different hardware units is depicted in detail in chapter 4.The range errors presented in this section are for both average and maximum range errors. The average range errors are obtained by averaging range errors based on different CEP, in other words, different percent of evaluated positions, for each of evaluated IPSs. The maximum range error is the biggest error occurred among the considered percentage of evaluated positions. In both Tables, the first 3 rows provide range error comparison for measured range from each different reference point to tag and also the average of measured ranges from all reference points to the tag is shown in the last row.

Range error result also show that the UWB IPS has the best accurate range estimation while range estimation from BLE IPS is the worst. More specifically, the UWB IPS gives approximately 10 cm range error in the worst case for both LOS and NLOS scenarios. The range error value from BLE IPS in CEP95 case is about 3 m for LOS case and 4 m for NLOS situation respectively. The WiFi IPS provides medium level range accuracy among these three systems. For example, in CEP95 case, its average range error around 30 cm for LOS scenario and 1 m for NLOS scenario.

It also can be observed form the tables that difference of the average range error between LOS scenario and NLOS scenario from the UWB IPS is the smallest while from BLE IPS is the biggest.

For instance, in CEP95 case, the difference of average range error in LOS and NLOS case for UWB IPS is very small and about 1 cm. However, the figure under the same condition from BLE IPS is about 1 m. This means the UWB IPS is the most robust system to combat indoor propagation effects and the BLE is the most sensitive one to indoor environments among these three evaluated systems.

LOS range error(cm) for different CEP													
Different	Average/	CEP50			CEP68			CEP95			CEP100		
RP to Tag	Maximum	UWB	WiFi	BLE	UWB	WiFi	BLE	UWB	WiFi	BLE	UWB	WiFi	BLE
RP1 - Tag	AVG.	4.6	14.4	199.7	6.0	20.9	285.6	8.2	33.5	430.7	8.3	34.8	467.5
	MAX.	9.1	28.3	352.8	11.2	49.6	592.2	15.5	88.7	991.0	17.8	179.8	1032.3
RP 2 - Tag	AVG.	5.7	14.0	162.7	7.1	19.9	203.5	9.1	33.9	285.1	9.3	36.6	311.8
	MAX.	9.8	26.9	288.4	12.0	45.6	330.2	15.9	139.4	629.4	17.3	334.1	741.6
RP3 - Tag	AVG.	4.7	14.2	88.4	6.1	18.5	137.7	7.9	29.0	237.3	8.0	30.2	283.7
	MAX.	8.3	27.4	188.0	11.2	35.9	293.7	14.1	83.8	854.2	16.5	144.0	988.3
RP1,2,3 to Tag	**AVG.**	**5.0**	**14.2**	**150.3**	**6.4**	**19.8**	**208.9**	**8.4**	**32.1**	**313.7**	**8.5**	**33.9**	**354.3**
	MAX.	**9.8**	**28.3**	**352.8**	**12.0**	**49.6**	**592.2**	**15.9**	**139.4**	**991.0**	**17.8**	**334.1**	**1032.3**

Table 5.3 Comparison of LOS range error of the UWB, WiFi and BLE IPSs

NLOS range error(cm) for different CEP													
Different	Average/	CEP50			CEP68			CEP95			CEP100		
RP to Tag	Maximum	UWB	WiFi	BLE	UWB	WiFi	BLE	UWB	WiFi	BLE	UWB	WiFi	BLE
RP1 - Tag	AVG.	2.5	12.8	247.9	3.4	22.3	333.9	7.8	69.8	491.6	10.9	87.2	549.1
	MAX.	4.8	29.0	438.4	7.2	88.4	624.2	46.8	297.8	1069.0	107.8	514.5	2244.9
RP 2 - Tag	AVG.	2.3	25.3	244.0	3.1	48.0	332.8	7.7	120.2	448.3	12.1	143.0	474.8
	MAX.	4.4	69.2	487.9	6.5	147.3	613.8	71.7	513.1	961.7	141.9	692.2	1052.2
RP3 - Tag	AVG.	2.8	25.2	118.9	3.8	43.4	173.9	6.4	106.3	263.0	8.7	131.6	281.2
	MAX.	5.9	63.4	255.7	7.6	121.1	357.5	23.8	599.8	595.8	71.0	701.1	717.9
RP1,2,3 to Tag	**AVG.**	**2.5**	**21.1**	**203.6**	**3.4**	**37.9**	**280.2**	**7.3**	**98.7**	**401.0**	**10.6**	**120.6**	**435.0**
	MAX.	**5.9**	**69.2**	**487.9**	**7.6**	**147.3**	**624.2**	**71.7**	**599.8**	**1069.0**	**141.9**	**701.1**	**2244.9**

Table 5.4 Comparison of NLOS range error of the UWB, WiFi and BLE IPSs

Figure 5.1 and Figure 5.2 illustrate range error verses true distance as per each reference point to Tag in LOS scenario and NLOS scenario for all three evaluated IPSs.

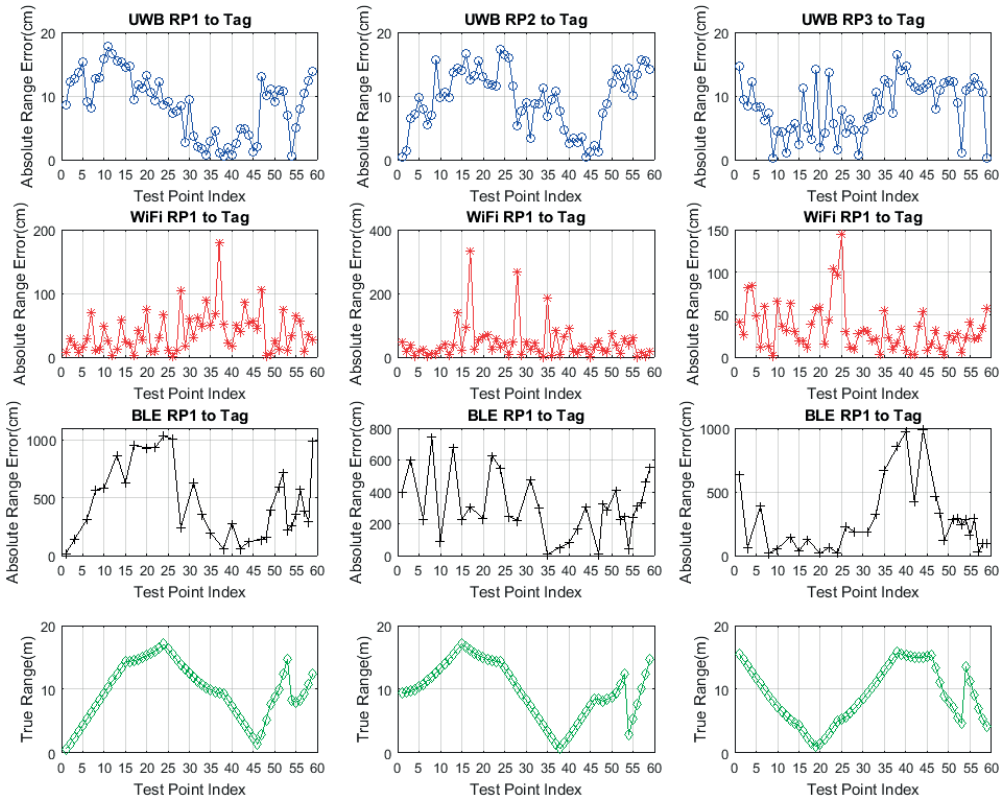

Figure 5.1 Comparison of LOS absolute range error and true range vs. TPs of the UWB, WiFi and BLE IPSs

In LOS scenario, the range errors of both UWB IPS and BLE IPS are mainly affected by true distance. With increasing distance, range error grows and with distance decreasing the range error becomes smaller. However, the influence of true distance on range error of BLE IPS is much more significant than the impact on range error of UWB IPS as shown in Figure 5.1.

In NLOS scenario, all three IPSs have big range errors at almost same evaluated positions, which means the accuracy of all these three systems was degraded by the NLOS environment. The influence of NLOS environment on BLE IPS is most severe compared to UWB IPS and WiFi IPS and on UWB IPS is slightest. Except for the impact from the evaluation environment, the impact from true distance also can be observed from the range plots of all these three evaluated systems in Figure 5.2. However, the influence of the environment is more significant compared to the impact of true distance.

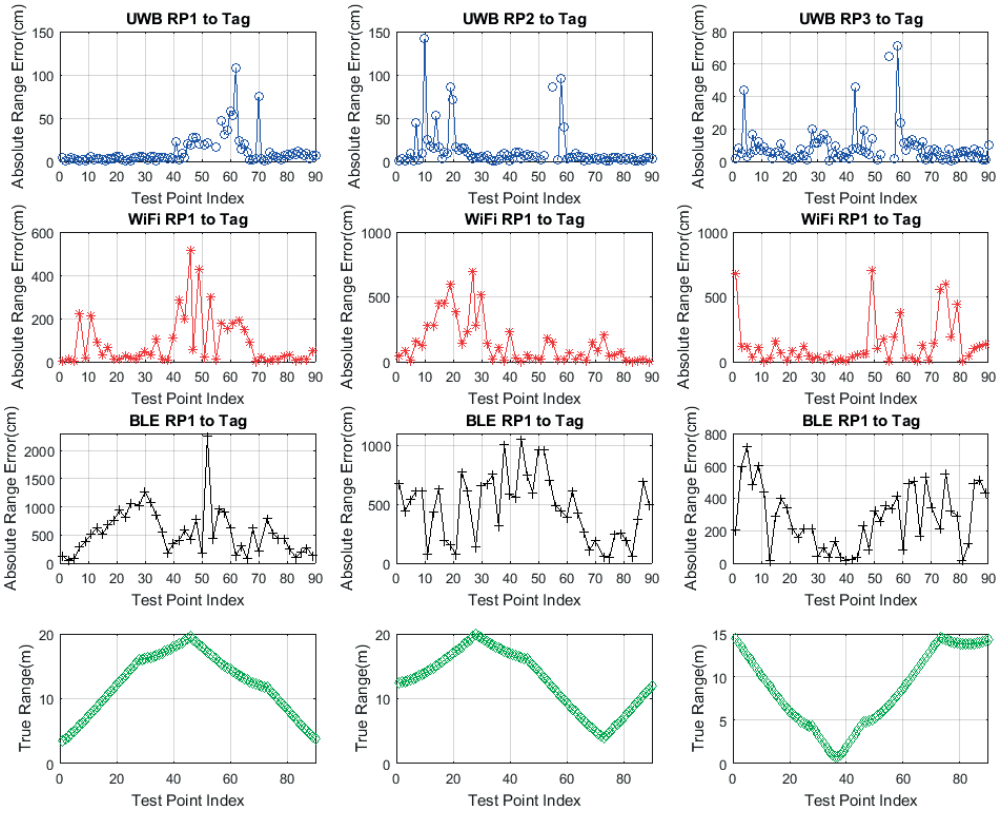

Figure 5.2 Comparison of NLOS absolute range error and true range vs. TPs of the UWB, WiFi and BLE IPSs

5.1.3 Obstruction Evaluation

Indoor environments, especially the presence of obstacles, may degrade the accuracy of indoor positioning systems. In order to get more knowledge about the impact of obstacles on the ranging performance for these three evaluated hardware, a dedicated evaluation was carried out in the LOS evaluation area, the sports hall. During the experiment, a mobile tag and an anchor or beacon from each kind of hardware were placed stationary at a fixed separation distance from each other with same height of about 1 m. Totally 5 separation distances (1 m, 4 m, 8 m, 12 m, 15 m) were tested for each hardware. For each separation distance, a metal writing board and human body act as obstacles at different positions to obstruct the LOS between the tag and anchor or beacon in different ways. Totally 8 cases were tested including LOS and 200 data samples collected for each case.

The detailed setup of these 8 cases are explained as below and few test setup examples are given in figure 5.3.

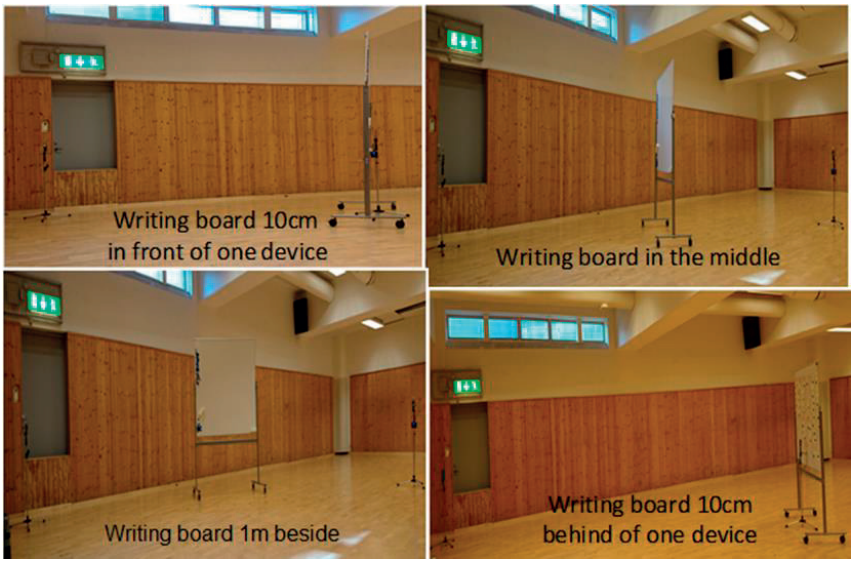

Figure 5.3 Examples of the obstacle experiment setup

1. **LOS:** After placing the two devices at a fixed separation distance, measurements and data collecting were done without any obstacle in between.

2. **Writing board in the middle (WB Mid) or body in the middle (Body Mid):** The metal writing board was placed in the middle between the two test devices. For instance, if the two devices were 1 m away from each other, the writing board was placed in the middle with 0.5 m away from them.

3. **Writing board beside of the two test devices (WB Beside):** The metal writing board was placed in parallel with the straight line connecting the two tested devices and in the middle with 1 m distance away from the straight line.

4. **Writing board in front (WB Front) or body in front (Body Front) of one of the device:** The metal writing board was placed or a person stood with 10 cm distance in front one of the devices.

5. **Writing board behind (WB Behind) or body behind (Body Behind) of one of the device:** The metal writing board was placed or a person stood with 10 cm distance behind one of the devices.

Figure 5.4 and Figure 5.5 show the results from the obstacle test. The range errors shown in both figures are calculated as differences between the measured ranges and their corresponding true ranges, same as the range error calculation defined in chapter 4.

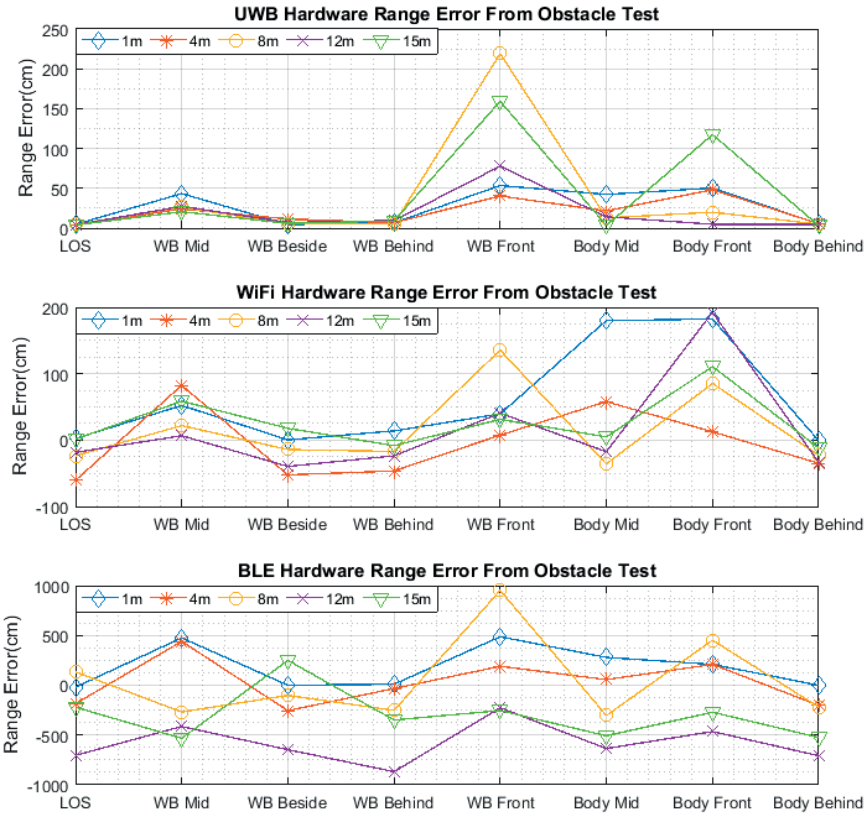

Figure 5.4 Range error of different obstacle test cases for the UWB, WiFi and BLE hardware

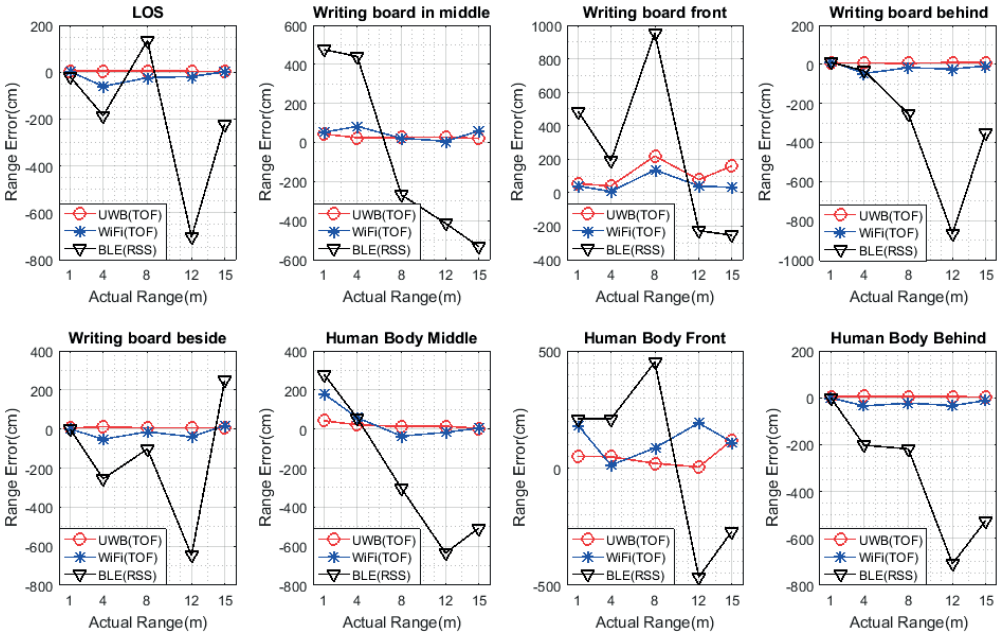

Figure 5.5 Comparison of range error of the UWB, WiFi and BLE hardware in different obstacle test cases

Few conclusions can be drawn from the Figures.

1. BLE hardware has worst ranging accuracy compared to UWB and WiFi hardware. This is because the BLE hardware measures range based on RSS whilst UWB and WiFi hardware measure range based on TOA and RSS based range measurement is more affected by the environment than TOA based range measurement, particularly when obstacles are present.

2. UWB hardware has better ranging accuracy than WiFi hardware in most cases even though both of them measure ranges through TOA. This is because UWB hardware has larger bandwidth and better time resolution, which enhances the ability for the UWB receiver to distinguish between multipath signals and determine the first signal accurately when reflections exist. In addition, UWB hardware is more robust to frequency selective obstruction due to its larger bandwidth.

3. For all three hardware, the range measurement shows bigger error in the cases that there is a writing board or human body in front of one of the devices. This is probably due to the absence of LOS path in these cases that only reflected signals were measured.

5.2 Power Consumption

This section provides discussion on power consumption of UWB, WiFi and BLE hardware from the used protocol point of view. Furthermore, an example with typical current consumption of these three hardware is presented. At the end, discussion about feasibility of using non-rechargeable portable battery for these three hardware is carried out based on theoretical discussion and practical data.

By transmitting very short pulses as defined in the IEEE 802.15.4a - 2007 UWB Standard [4], UWB devices reduce their current consumption significantly. BLE, also known as Bluetooth Smart, is a low-power aimed technology according to the Bluetooth core specification version 4.0. Consequently, it offers very low power consumption. A typical WiFi device, advantaging for longer range connections, high data rate and supporting devices with a substantial power supply, is relatively less power efficient and consumes more power than UWB and BLE.

However, these IEEE standards defines only the PHY and MAC layers of the technologies. The network, security and application profile layers usually developed and defined by separate alliances of companies, which means power consumption of different hardware varies depending on implementation of specific chipsets. Therefore, it is necessary to have some investigation on the power consumption of general UWB, WiFi and BLE hardware.

A brief survey for the some popular UWB, WiFi and BLE chipsets on the market shows that the current consumption of UWB chipsets is on the order of 50 mA on active transmit or receive mode, the current consumption of WiFi and BLE chipsets is approximately in the order of few hundreds of milliampere at its maximum output power and 10 to 20 mA on active transmit or receive mode, respectively.

In addition, Table 5.5 shows an example which compares the typical current consumption of the UWB, WiFi and BLE chipsets used by these three evaluated hardware. The detailed chipset characteristics of the BCM43462 WiFi chipset are confidential and not publicly available. Therefore, the power consumption data of BCM43570 chipset is used as a reference for the discussion and comparison instead. It is necessary to mention that even though the data in Table 5.5 are based on the specific hardware units, they are broadly representative for examples of the same technology.

Technology	UWB	WiFi	BLE
Chipset	DecaWave dw1000 [65]	BCM43570 [66]	nRF51822 [67]
VDD (V)	3.3	3.3	3
Tx (mA)	42	~500	12
Rx (mA)	65	~200	9.7

Table 5.5 Current consumption of the UWB, WiFi and BLE chipset

Figure 5.6 indicates the power consumption in mW unit for each technology based on data from Table 5.5. Obviously, the BLE consumes least power compared to UWB and WiFi while WiFi consumes highest power among them.

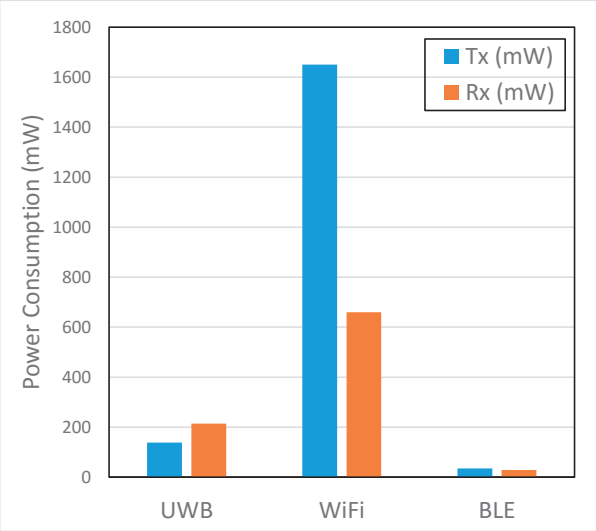

Figure 5.6 Comparison of power consumption of the UWB, WiFi and BLE chipset

In order to practically investigate the feasibility of using non-rechargeable battery for these three kinds of RF hardware, specifications and dimensions of the 3V non-rechargeable lithium coin cell battery CR2477N from Renata that supports the maximum rated capacity of 950 mAh are given in Table 5.6 and Figure 5.7.

CR2477N 3V Lithium Battery [68]	
Nominal Voltage	3 V
Rated Capacity	950 mAh
Standard Discharge Current	1.0 mA
Max. Cont. Discharge Current	2.5 mA

Table 5.6 Specifications of Renata 3V non-rechargeable lithium battery CR2477N

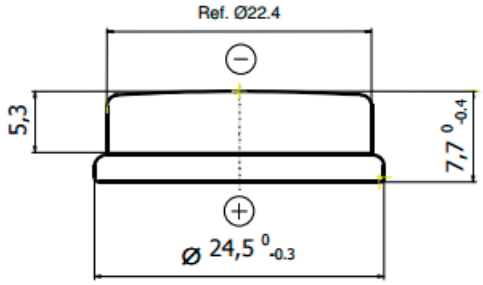

Figure 5.7 Dimensions of Renata 3V non-rechargeable lithium battery CR2477N

Due to the low power consumption, BLE modules are capable of working with the non-rechargeable coin batteries like CR2477N for few months or years, for instance, by adding a capacitor in parallel with the battery to increase the maximum discharge current of the battery in order to fulfil the required current consumption of BLE modules.

However, this solution is impractical for UWB and WiFi modules due to their higher current consumption. UWB and WiFi products are better to be powered through power outlets or by rechargeable Lithium-ion/polymer batteries which can provide much higher discharge current compared to non-rechargeable batteries however such batteries provide lower volumetric energy density compared to non-rechargeable batteries.

Table 5.7 and 5.8 show specifications and dimensions of the rechargeable lithium Ion polymer battery ICP621333PA from Renata as an example.

ICP621333PA 3.7V Rechargeable Lithium Ion Polymer Battery [69]	
Nominal Voltage	3.7 V
Nominal Capacity	240 mAh
Max Discharge Current	2.0 C – 480 mA (for non continues discharge) 1.0 C – 240 mA (for continues discharge)

Table 5.7 Specifications of Renata rechargeable lithium Ion polymer battery ICP621333PA

ICP621333PA 3.7V Rechargeable Lithium Ion Polymer Battery [69]	
Thickness (t)	Max. 6.7 mm
Length (l)	Max. 13.0 mm
Width (w)	Max. 35.0 mm

Table 5.8 Dimensions of Renata rechargeable lithium Ion polymer battery ICP621333PA

This rechargeable lithium Ion polymer battery ICP621333PA has comparable dimensions to the non-rechargeable coin battery CR2477N and could support maximum non-continues discharge current of 480 mA and fulfil the required current consumption of WiFi and UWB modules. However, its volumetric energy density is only about 25 percent of that of the non-rechargeable coin battery CR2477N, which means the dimension of the rechargeable lithium Ion polymer battery will be at least 4 times bigger than the dimension of the non-rechargeable coin battery in order to provide the same capacity as the non-rechargeable coin battery does, making battery driven small size of WiFi and UWB devices impractical, as opposed to BLE beacons.

In summary, BLE consumes lower power than UWB and WiFi and is able to use non-rechargeable coin batteries while UWB and WiFi consume higher power and are better to be powered through power outlets or by rechargeable batteries directly or indirectly when they are embedded in a system such as a phone or a computer.

5.3 Cost

This section provides discussion on cost of UWB, WiFi and BLE hardware, especially from the perspective when they are employed for indoor positioning. Furthermore, an example with approximate cost of these three hardware is presented.

As we discussed in the theory part, the large bandwidth of UWB signals enable fine time resolution. However, it also imposes challenges to UWB hardware design and implementation when it comes to accurate TOA measurement. First of all, clock jitter becomes extremely sensitive for UWB positioning systems as the fact that 1ns clock drift can result in 30 cm ranging error. UWB systems thus require precisely synchronized and high resolution clocks, which is often very expensive. Secondly, due to the large bandwidth of UWB signals, in order to sample received signals at or above the Nyquist rate, UWB receivers are necessary to have higher speed signal processing capability, which means higher costs. Thirdly, UWB positioning systems usually employ two way ranging method, which require all anchors and tags in the system to be transceivers, increasing the cost of the system. A UWB positioning system can be relatively more expensive due to the high requirements on the hardware. Last but not least, UWB has not been widely used in the consumer electronics devices, unlike WiFi and BLE, therefore it has not gained the high volume cost reduction benefits.

WiFi hardware needs to be designed with tight tolerances to ensure that radio specific performance and certification criteria are achieved. This imposes cost on design process and certification. For instance, more efforts are needed to integrate WiFi technology into a system due to various needed drivers, a complex protocol stack, high requirements on power amplifiers and so on. All these mentioned factors increase the cost of WiFi devices. However, WiFi has been widely adopted all over the world, from public hotspots to private homes and from laptops to mobile devices nowadays due to its recognised performance. It thus gains high volume cost reduction benefits. Positioning systems using conventional WiFi RSS-based measurement can take advantages of existing WiFi infrastructure and readily available mobile devices and hence the specific cost needed for positioning purpose can be very low.

However, WiFi TOA-based ranging is not directly available from a standard WiFi device as the time synchronization required by TOA-based ranging is not provided by a standard WiFi device

without IEEE 802.11v compliant synchronization support. In order to establish time synchronization for estimating TOA-based ranging in WLAN systems, specific and complex hardware or software development and modification are required. The IEEE 802.11v standard provides possibility for TOA based ranging between WLAN devices, which was officially included in IEEE 802.11 standard in 2011. But it needs more efforts for enabling TOA measurement and it is not widely implemented yet, resulting in extra cost for WiFi devices to provide TOA measurement. In addition, OWR measurement requires precisely synchronized timer for accurate ranging and TWR measurement requires all the units in the system are transceivers. Therefore, WiFi devices providing TOA-based positioning capability are more costly compared to standard WiFi devices.

A BLE hardware can be very simple and cheap. BLE is intended for portable products, short ranges, and limited battery power. Moreover, BLE has been widely used in the consumer electronics, therefore it gains high volume cost reduction benefits.

Table 5.9 shows an example price for the UWB, WiFi and BLE chipset respectively. There is of course cost on system level, but this is an indication. The cost of the UWB hardware is higher compared to the WiFi and BLE hardware.

Technology	UWB	WiFi	BLE
Price	Sub 10 USD	Sub 5 USD	Sub 2 USD

Table 5.9 Typical costs of UWB, WiFi and BLE chipset [70]

5.4 Ease of Deployment

Both the UWB and WiFi hardware require connections to external power supplies or chargers to be able to get the systems up and running. This could be a key limitation for applications that external physical connections have to be avoided.

The BLE hardware can avoid external physical connections as they are able to be powered by coin batteries. In addition, the BLE devices have very small size. Therefore, it is easier to deploy the BLE hardware compared to the UWB and WiFi hardware.

However, the RSS-based BLE IPS needs proper propagation model to estimate ranges, which adds extra workload for the system deployment compared to the UWB and WiFi IPSs.

There is no absolute conclusion regarding which system is the easiest to deploy among the UWB, WiFi and BLE IPSs. The ease of deployment of the IPSs hould be considered together with other factors like accuracy, power consumption, cost and so on, according to requirements of practical applications.

Chapter 6 Conclusion and Future Work

This chapter presents the conclusion reached through theoretical study and evaluation in the thesis. Advices for future work that would be of interest in the indoor positioning area are also provided in this chapter.

6.1 Conclusion

Indoor positioning based on three off-the-shelf hardware: Ultra-Wideband, WiFi and Bluetooth low energy has been evaluated for both LOS and NLOS scenarios. The goal was to evaluate the parameters that determine the applicability of indoor positioning systems, which are accuracy, power consumption, cost and ease of deployment.

Comprehensive theory study of the commonly used radio positioning technologies and basic indoor positioning techniques was done to gain related theoretical knowledge as foundation of the evaluation. Accuracy, power consumption, cost and ease of deployment were defined as criteria to evaluate and compare these three systems. A systematic method for deploying these three positioning systems for practical experiments is presented and discussed. Sufficient practical experiments were executed to collect data for the evaluation. A trilateration positioning algorithm was implemented to estimate position based on collected experimental data for comparing positioning accuracy for these three systems. Discussion, analysis and comparison of the performance of these three employed hardware in terms of indoor positioning are performed and stated in detail. Results from brief study of off-the-shelf hardware for a rough qualitative comparison of power consumption and cost of these three evaluated hardware are presented. Furthermore, obstruction experiments were performed to observe influences of the obstacles on accuracy for these three hardware. Finally, suggestions on future work is provided.

The evaluation shows that the the Ultra-Wideband hardware performs the best accuracy for indoor positioning, in centimeter order, due to its large bandwidth and fine time resolution but the cost of the Ultra-Wideband hardware is more expensive than the WiFi and BLE Bluetooth low energy hardware, which make it best suited for applications that require high accuracy but cost is less of an issue. The Bluetooth low energy hardware provides worst accuracy, about 4.5 m in average, because its receive signal strength based ranging provides poor correlation with distance in indoor environments. However, it is the cheapest and most power consumption efficient among these three evaluated hardware. It is therefore the best option for the applications that only require coarse position estimation but have to set up positioning systems as easily as possible and with limited budget. For instance, when power outlets or rechargeable batteries are not available for reference nodes or positioning systems prefer to track objects by utilizing existing

mobile devices, BLE beacons with coin batteries and BLE mobile phones are the best choose in these cases. The WiFi hardware is a kind of a trade-off between UWB and BLE hardware in terms of indoor positioning, providing medium level of accuracy, power consumption, cost and deployment complexity. Thanks to the relatively newly available TOA ranging technique in WiFi, the TOA based WiFi IPS is able to give about 1 m positioning accuracy in LOS scenario and 2 m 2D positioning accuracy in NLOS situation. When it comes to ease of deployment of these three IPSs, the BLE IPS is easier to deploy compared to the UWB and WiFi IPSs as BLE devices are small size and able to be powered by coin batteries and thus can avoid external physical connections. However, the RSS-based BLE IPS needs proper propagation model to get the system up and running, which adds extra workload for the system deployment compared to the UWB and WiFi IPSs. The ease of deployment should be considered together with other factors like accuracy, power consumption, cost and so on, according to requirements of practical applications.

The evaluation also shows that obstacles affect ranging accuracy greatly for all these three evaluated hardware, particularly in the cases that obstacles are close and in front of one of the tested hardware, and influence of obstacles on the BLE hardware is the most severe.

6.2 Future Work

Even though the evaluation was done according to plan, several improvements could be added if the time and the budget would have permitted.

The positioning algorithm was implemented and exploited for the position estimation in this thesis is not the optimal and positioning errors due to the algorithm itself were discovered during the evaluation. Optimizing the existing algorithm or implementing a more robust algorithm would improve the positioning accuracy of these evaluated systems.

The evaluation for all these three systems are carried out in limited size areas with minimal required 3 anchors and beacons for both LOS and NLOS scenarios. In other words, the scalability of these systems are unknown. However, the scalability is also an important parameter to IPSs in practical applications. Evaluation of these systems with more than 3 anchors and beacons to cover bigger positioning areas would provide more valuable usage information for these systems.

The author tried to evaluate the systems with a mobile tag and started for UWB IPS with carrying the tag and walking along a predefined path but the results showed unpredictable error introduced by the author's movement due to factors such as controlling constant walking speed, walking steps and so on. Therefore, the later evaluation experiments were all carried out with placing tag stationary at defined test points and all the results presented and discussed in this thesis are also from these static tag experiments. The latency and updating rate of the positioning could benefit from evaluation with moving tag in a known average speed with the help of a robot for example.

Finally, the evaluation were performed only for the three most popular RF technologies UWB, WiFi and BLE, including two different positioning methods TOA and RSS, based positioning systems. Further evaluation for other commonly used RF technologies and positioning methods based indoor positioning systems will expand the understanding and experience in this area.

Chapter 7 Bibliography

[1] D. Dardari, P. Closas, and P. Djuric, “Indoor tracking: Theory, methods, and technologies,” IEEE Trans. Veh. Technol., 2015, in publication.

[2] H. Liu, H. Darabi, P. Banerjee, and J. Liu, “Survey of wireless indoor positioning techniques and systems,” IEEE Transactions on Systems, Man, and Cybernetics Part C, vol. 37, no. 6, pp. 1067–1080, Nov 2007.

[3] Dr. Rainer Mautz, “Indoor Positioning Technologies”, Institute of Geodesy and Photogrammetry, Department of Civil, Environmental and Geomatic Engineering, ETH Zurich, Feb. 2012.

[4] Part 15.4: Wireless Medium Access Control (MAC) and Physical Layer (PHY) Specifications for Low-Rate Wireless Personal Area Networks (WPANs). Amendment 1: Add Alternate PHYs, IEEE, 2007.

[5] Part 11: Wireless Medium Access Control (MAC) and Physical Layer (PHY) Specifications: Amendment 8: Wireless Network management. IEEE Std 802.11v - 2011. IEEE, New York, Feb. 2011.

[6] X. Liu, S. Aeron, V. Aggarwai, X. Wang and M. Wu, “Adaptive Sampling of RF Fingerprints for Fine-Grained Indoor Localization,” IEEE J. Trans. Mobile Computing, vol. 15, pp. 2411-2423, 2016.

[7] S. He and S. H. G. Chan, “Wi-fi fingerprint-based indoor positioning: Recent advances and comparisons,” IEEE Communications Surveys Tutorials, vol. 18, no. 1, pp. 466–490, Firstquarter 2016.

[8] Q. Jiang, Y. Ma, K. Liu and Z. Dou, “A Probabilistic Radio Map Construction Scheme for Crowdsourcing-Based Fingerprinting Localization”, IEEE J. Sensors Journal, vol. 16, pp. 3764-3774, May. 2016.

[9] M. Shchekotov, ‘‘Indoor localization methods based on Wi-Fi lateration and signal strength data collection,’’ in Proc. 17th Conf. Open Innov. Assoc., Yaroslavl, Russia, 2015, pp. 186–191.

[10] C. Yang and H.-R. Shao, "WiFi-Based Indoor Positioning," IEEE Communications Magazine, pp. 150-157, March 2015.

[11] M. Ciurana, D. Lopez, and F. Barceló-Arroyo, “SofTOA: Software Ranging for TOA-Based Positioning of WLAN Terminals,” Location and Context Awareness, pp. 207–221, May. 2009.

[12] A. Gunther and C. Hoene, “Measuring Round Trip Times to Determine the Distance between WLAN Nodes”, NETWORKING 2005. Networking Technologies, Services, and Protocols; Performance of Computer and Communication Networks; Mobile and Wireless Communications Systems, pp. 303–319, May. 2005.

[13] A. Mahmood, R. Exel, and T. Sauter, “Impact of hard-and software timestamping on clock synchronization performance over ieee 802.11,” in Factory Communication Systems (WFCS), 2014 10th IEEE Workshop on. IEEE, 2014, pp. 1–8.

[14] IEEE, “802.1AS-2011 - IEEE Standard for Local and Metropolitan Area Networks - Timing and Synchronization for Time-Sensitive Applications in Bridged Local Area Networks”, 2011.

[15] E. Au, “The Latest Progress on IEEE 802.11mc and IEEE 802.11ai [Standards]”, IEEE J. Vehicular Technology Magazine, Vol. 11, pp. 19-21, Sep. 2016.

[16] Bluetooth SIG, “Specification of Bluetooth System, Version 4.0”, Kirkland, WA, USA, 30 June 2010

[17] J. Neburka, Z. Tlamsa, V. Benes et al., “Study of the Performance of RSSI based Bluetooth Smart Indoor Positioning”, IEEE Int. Conf. Radioelektronika (RADIOELEKTRONIKA).

[18] J. Zhu, Z. Chen, H. Luo et al., “RSSI Based Bluetooth Low Energy Indoor Positioning,” in Proc. Int. Conf. Indoor Positioning and Indoor Navigation (IPIN), Oct. 2014, pp. 526–533.

[19] A. I. Kyritsis, P. Kostopoulos, M. Deriaz and D. Konstantas, “A BLE-Based Probabilistic Room-Level Localization Method”, IEEE Int. Conf. on Location and GNSS (ICL-GNSS), 2016, pp. 1-6.

[20] S. Bertuletti; A. Cereatti; U. Della; M. Caldara; M. Galizzi, “Indoor distance estimated from Bluetooth Low Energy signal strength: comparison of regression models”, IEEE Conf. Sense Applications Symposium (SAS), 2016, pp. 1-5.

[21] Y. Wang, Q. Yang, G. Zhang and P. Zhang, “Indoor Positioning System Using Euclidean Distance Correction Algorithm with Bluetooth Low Energy Beacon,” IEEE Int. Conf. Internet of Things and Applications (IOTA), Jan. 2016, pp. 243-247

[22] R. Faragher and R. Harle, “Location fingerpriting with Bluetooth low energy beacons,” IEEE J. Sel. Areas Commun., vol. 33, no. 11, pp. 2418–2428, Nov. 2015.

[23] S. S. Saab and Z. Nakad, “A standalone RFID indoor positioning system using passive tags,” IEEE Trans. Ind. Electron., pp. 24–40, Jun. 2011.

[24] Miodrag Bolic, Majed Rostamian, and Petar M. Djuric. Proximity Detection with RFID: A Step Toward the Internet of Things. Pervasive Computing, IEEE, 14(2):70–76, Apr 2015.

[25] M. Scherhaufl, M. Pichler, E. Schimback, D.J. Muller, A. Ziroff, and A. Stelzer. Indoor Localization of Passive UHF RFID Tags Based on Phase-of-Arrival Evaluation. IEEE Transactions on Microwave Theory and Techniques, 61(12):4724–4729, Dec 2013.

[26] A. Bekkali, H. Sanson, and M. Matsumoto, “RFID indoor positioning based on probabilistic RFID map and Kalman filtering,” in Proc. 3rd IEEE Int. Conf. Wireless Mobile Comput. WiMOB, 2007, pp. 1–7.

[27] J. A. Fisher and T. Monahan, "Tracking the social dimensions of RFID systems in hospitals,” 2008, International Journal of Medical Informatics, pp. 176-183.

[28] Y. Bai, S. Wu, H. Wu, K. Zhang, “Overview of RFID-Based Indoor Positioning Technology”, RMIT University, Australia. Dec. 2012.

[29] “IEEE standard for information technology - telecommunications and information exchange between systems - local and metropolitan area networks specific requirements part 15.4: Wireless Medium Access Control (MAC) and Physical layer (Phy) specifications for low-rate wireless personal area networks (lr-wpans)”, IEEE Std 802.15.4-2003, pages 1 –670, 2003.

[30] ZigBee Alliance, “Zigbee specification,” ZigBee Alliance, Jan. 2008.

[31] Chan, H. K.: ‘Agent-Based Factory Level Wireless Local Positioning System with ZigBee Technology’, IEEE Systems Journal, 2010, 4(2), pp. 179-85.

[32] S. H. Fang, C. H. Wang and T. Y. Huang, “An Enhanced ZigBee Indoor Positioning System With an Ensemble Approach,” IEEE Communications Letters, Vol: 16, pp. 564-567, 2012.

[33] T. Alhmiedat, G. Samara, A. O. Abu Salem, “An Indoor Fingerprinting Localization Approach for ZigBee Wireless Sensor Networks”, European Journal of Scientific Research, ISSN 1450-216X / 1450-202X Vol. 105 No 2, pp.190-202, July, 2013.

[34] Y. Alvarez, F. L. Heras, “ZigBee-based Sensor Network for Indoor Location and Tracking Applications”, IEEE Latin America Transactions, Vol. 14, pp. 3208 – 3214, 2016.

[35] A. I. Baba, “Calibrating time of flight in two way ranging,” in Proc. 7th IEEE Int. Conf. Mobile Ad-hoc Sensor Netw., 2011, pp. 393–397.

[36] C. Hoene and J. Willmann, "Four-way TOA and software-based trilateration of IEEE 802.11 devices," in 19th International Symposium on Personal, Indoor and Mobile Radio Communications (PIMRC), 2008, pp. 1-6.

[37] S. Lanzisera, D. T. Lin, and K. S. J. Pister, “RF time of flight ranging for wireless sensor network localization,” in in Workshop on Intelligent Solutions in Embedded Systems (WISES, pp. 1–12, 2006.

[38] W. N. B. A. Thorbjornsen, B. and J. Reeve, “Radio frequency (rf) time-of-flight ranging for wireless sensor networks,” Measurement Science and Technology, pp. 1–12, 2010.

[39] S. Gezici, Z. Tian, G. B. Giannakis, H. Kobayashi, A. F. Molisch, H. V. Poor, and Z. Sahinoglu, “Localization via ultra-wideband radios: A look at positioning aspects for future sensor networks,” IEEE Signal Process. Mag., vol. 22, no. 4, pp. 70–84, Jul. 2005.

[40] Andreas F. Molisch, “Wireless Communications”, Wiley-IEEE Press, 2005.

[41] T. Nowak, M. Hierold, A. Koelpin, M. Hartmann, H.-M. Troger, and J. Thielecke, “System and signal design for an energy-efficient multi-frequency localization system,” in Wireless Sensors and Sensor Networks (WiSNet), 2014 IEEE Topical Conference on, Jan. 2014, pp.55–57.

[42] M. Pelka, C. Bollmeyer, and H. Hellbr¨uck, “Accurate radio distance estimation by phase measurements with multiple frequencies,” in 2014 International Conference on Indoor Positioning and Indoor Navigation, Oct. 2014.

[43] Y. Schröder, G. von Zengen, S. Rottmann, F. Busching and L. Wolf, “InPhase: An Indoor Localization System based on Phase Difference Measurements”, Institute of Operating Systems and Computer Networks, Technische Universit¨at Braunschweig.

[44] R. I. Reza, “Data fusion for improved toa/tdoa position determination in wireless systems,” Ph.D. dissertation, Virginia Polytechnic Institute and State University, 2000.

[45] A. D. Redondo, T. Sanchez, C. Gomez, L. Betancur, and R. C. Hincapie, “Mimo sdr-based implementation of aoa algorithms for radio direction finding in spectrum sensing activities,” in Communications and Computing (COLCOM), 2015 IEEE Colombian Conference on, May 2015, pp. 1–4.

[46] T. Sanchez, C. Gomez, L. Betancur; A.Garcia, R. Hincapie, “From theory to practice: Implementations issues for techniques based on AoA and TDoA”, IEEE 2016 8th Euro American Conf. on Telematics and Information Systems (EATIS), pp. 1–4, Apr 2016.

[47] H. Krim, M. Viberg, Two decades of array signal processing research: The parametric approach, IEEE Signal Processing Magazine 13 (4) (1996) 67–94.

[48] R. Schmidt, “Multiple emitter location and signal parameter estimation,” Antennas and Propagation, IEEE Transactions on, vol. 34, no. 3, pp. 276–280, Mar 1986.

[49] F. Seco, A. R. Jimenez, C. Prieto, 1. Roa, and K. Koutsou, "A survey of mathematical methods for indoor localization," in Intelligent Signal Processing, 2009. WISP 2009. IEEE International Symposium on. IEEE, 2009, pp. 9-14.

[50] J. Caffery, “A new approach to the geometry of TOA location,” in Vehicular Technology Conference, 2000. IEEE VTS-Fall VTC 2000. 52nd, vol. 4, 2000, pp. 1943–1949.

[51] W. Navidi, W. S. Murphy, and W. Hereman, “Statistical methods in surveying by trilateration,” Computational Statistics & Data Analysis, vol. 27, no. 2, pp. 209–227, 1998.

[52] H.-W. Wei, Q. Wan, Z.-X. Chen, and S.-F. Ye, “A novel weighted multidimensional scaling analysis for time-of-arrival-based mobile location,” Signal Processing, IEEE Transactions on, vol. 56, no. 7, pp. 3018–3022, July 2008.

[53] K. W. Cheung, H. C. So, W. K. Ma, and Y. T. Chan, “Least squares algorithms for time-of-arrival-based mobile location,” IEEE Trans. on Signal Processing, vol. 52, no. 4, April 2004.

[54] W.H.Foy, "Position location solutions by Taylor-series estimation", IEEE Trans. on AES, vol. 12, no.2, pp. 187-194, March 1976.

[55] B. T. Fang. “Simple solutions for hyperbolic and related position fixes”, IEEE Trans. Aerosp. Electron. Syst., vol., 26, pp.748-753, Sept. 1990.

[56] Y. T. Chan and K. C. Ho, “A simple and efficient estimator for hyperbolic location,” IEEE Transactions on Signal Processing, vol. 42, no. 8, pp. 1905–1915, 1994.

[57] A. Rai, K. K. Chintalapudi, V. N. Padmanabhan and R. Sen, “Zee: Zero-effort crowdsourcing for indoor localization,” in Proc. ACM MobiCom, 2012, pp. 293–304.

[58] Z. Yang, C. Wu, and Y. Liu, “Locating in fingerprint space: Wireless indoor localization with little human intervention,” in Proc. ACM MobiCom, 2012, pp. 269–280.

[59] S. Yang, P. Dessai, M. Verma, and M. Gerla, “FreeLoc: Calibration-free crowdsourced indoor localization,” in Proc. IEEE INFOCOM, Apr. 2013, pp. 2481–2489.

[60] M. Montemerlo, S. Thrun, D. Koller, and B. Wegbreit, “FastSLAM: A factored solution to the simultaneous localization and mapping problem,” in Proc. AAAI/IAAI, 2002, pp. 593–598.

[61] B. Ferris, D. Fox, and N. Lawrence, “WiFi-SLAM using Gaussian process latent variable models,” in Proc. IJCAI, vol. 7, 2007, pp. 2480–2485.

[62] Y. Gu, A. Lo, and I. Niemegeers, “A survey of indoor positioning systems for wireless personal networks,” IEEE Communications Surveys & Tutorials, vol. 11, 2009.

[63] P. Bahl and V. Padmanabhan, "RADAR: An InBuilding RF-Based User Location and Tracking System," Proc. IEEE Infocom 2000, IEEE CS Press, Los Alamitos, Calif. 2000, pp. 775-784.

[64] N. Pritt, “Indoor positioning with maximum likelihood classification of Wi-Fi signals,” IEEE Sensors, Baltimore, Maryland, 4-6 Nov 2013.

[65] DecaWave Ltd, “DW1000 Datasheet, Version 2.11”, Dublin, Ireland, 2016.

[66] Broadcom, “BCM43570 Advance Data Sheet, Revision 43570-DS108-R”, San Jose, CA, Mar. 2016.

[67] Nordic Semiconductor, “nRF51822 Product Specification v3.2”, Trondheim, Norway.

[68] Renata SA, “CR2477N Data Sheet, Rev. CR2477N.06/12.06”, Itingen, Switzerland.

[69] Renata SA, “ICP621333PA Data Sheet, Rev. Li Ion ICP621333- 11.09”, Itingen, Switzerland.

[70] Digi-key Electronics, http://www.digikey.se.

Printed by Tryckeriet i E-huset, Lund 2017

LUND
UNIVERSITY

Series of Master's theses
Department of Electrical and Information Technology
LU/LTH-EIT 2017-565

http://www.eit.lth.se